

Miltenyi Biotec B.V. & CO. KG

Inhaber: Stefan Miltenyi



Sensing of soluble molecules with adapter chimeric antigen receptors for the controllable activation of T cells in an immunosuppressive subcutaneous solid tumor model

Dissertation

zum Erwerb des Doktorgrades der Naturwissenschaften
an der Medizinischen Fakultät der
Ludwig-Maximilians-Universität zu München

vorgelegt von

Niels Werchau

aus

Chemnitz

Jahr

2022

Mit Genehmigung der Medizinischen Fakultät

der Universität München

Betreuer: Prof. Dr. Dr. Michael von Bergwelt-Baildon

Zweitgutachter: Prof. Dr. rer. nat. Ludger Klein

Dekan: Prof. Dr. med. Thomas Gudermann

Tag der mündlichen Prüfung: 12. Mai 2023

Table of content

Table of content	3
Zusammenfassung	6
Abstract	7
1. Introduction	8
1.1 Development of cancer and immunosurveillance	8
1.2 New perspectives of cancer therapy	10
1.2.1 Cancer immunotherapy	10
1.2.2 CAR T cells in cancer therapy	11
1.2.3 AdCAR T cells for cancer therapy	15
1.3 Tumor microenvironment of solid cancer	17
1.4 The role of TGF- β in the TME	19
1.4.1 Structure and secretion of TGF- β	19
1.4.2 TGF- β activation and downstream signaling	20
1.4.3 TGF- β and its role in tumor biology	21
1.4.4 Targeting TGF- β in cancer therapy	22
2. Materials	24
2.1 Kits	24
2.1.1 Buffers and reagents	24
2.1.2 Cell culture media and supplements for eukaryotic cells	26
2.1.3 Cell culture media and supplements for prokaryotic cells	27
2.1.4 Cell lines	27
2.1.5 Plasmids	28
2.1.6 Antibody-conjugates used for cyclic fluorescent imaging and flow cytometry	29
2.1.7 Consumables	32
2.1.8 Instruments	33
2.1.9 Software	34
3. Methods	35
3.1 Molecular biology methods	35
3.1.1 Transformation of <i>E. coli</i> with plasmid DNA	35
3.1.2 Cultivation of <i>E. coli</i> and isolation of plasmid DNA	35
3.1.3 Biochemical modification of immunoglobulins	35
3.2 Cell culture methods	36
3.2.1 Cell lines and culture conditions	36
3.2.2 Lentiviral vector production	36
3.2.3 Titration of lentiviral vectors	38
3.2.4 Lentiviral transduction of cell lines	38
3.2.5 Isolation of human peripheral blood mononuclear cells	38
3.2.6 Isolation of primary human T cells	39
3.2.7 Lentiviral transduction of primary human T cells	39
3.2.8 Enrichment of transduced primary human T cells	39
3.2.9 Automated isolation, transduction and cultivation of human T cells	40
3.2.10 Cryopreservation and thawing of cell lines	41

Table of content

3.2.11	Cryopreservation and thawing of leukaphereses	41
3.2.12	Immunofluorescent staining and flow cytometry.....	42
3.3	Functional analysis of AdCAR T cells	42
3.3.1	Co-culture of AdCAR T cells with soluble antigens	42
3.3.2	Analysis of cytokines.....	43
3.3.3	AdCAR T cell reporter assay.....	43
3.3.4	Transwell assay.....	43
3.3.5	<i>In vitro</i> cytotoxicity assay.....	44
3.4	<i>In vivo</i> studies	44
3.4.1	Animal models	44
3.4.2	Tumor cell inoculation	45
3.4.3	Injection of T cells.....	45
3.4.4	Injection of adapter molecules and immunoglobulins	45
3.4.5	Bioluminescent <i>in vivo</i> imaging of tumor cells	45
3.4.6	Preparation of blood plasma	46
3.4.7	Preparation of blood for <i>ex vivo</i> analysis.....	46
3.4.8	Preparation of spleens for <i>ex vivo</i> analysis.....	46
3.4.9	Preparation of tumors for <i>ex vivo</i> analysis.....	46
3.4.10	Preparation of tumors for immunohistochemistry.....	46
3.4.11	Cyclic fluorescent imaging of human tumor tissue.....	47
3.4.12	Statistical analysis	49
4.	Scope.....	50
5.	Results.....	52
5.1	TME composition of ovarian tumor tissue.....	52
5.2	Soluble antigen-induced activation of AdCAR T cells.....	55
5.2.1	AdCAR T cells sense soluble human LAP in presence of adapter.....	55
5.2.2	Soluble antigen-induced AdCAR T cell activation can be modulated by both adapter and antigen concentration <i>in vitro</i>	56
5.2.3	Sensing of soluble antigens induces transgene expression in AdCAR T cells.....	58
5.2.4	Secretion of soluble latent TGF- β by human tumor cell lines <i>in vitro</i>	59
5.2.5	Tumor cell line-secreted latent TGF- β induced AdCAR T cell activation.....	60
5.2.6	AdCAR T cells sense soluble latent TGF- β in presence of tumor cells	62
5.2.7	Combinatorial targeting of soluble latent TGF- β and CD66c with AdCAR T cells <i>in vitro</i>	64
5.3	Sensing soluble antigens with AdCAR T cells <i>in vivo</i>	68
5.3.1	Establishment of a latent TGF- β -secreting tumor model in NSG mice	68
5.3.2	Targeting human latent TGF- β with AdCAR T cells is tolerated by NSG mice.....	71
5.3.3	Sensing of latent TGF- β with AdCAR T cells induces rapid stimulation of pro-inflammatory cytokine secretion <i>in vivo</i>	75
5.3.4	Sensing of latent TGF- β with AdCAR T cells induces systemic activation of CAR T cells <i>in vivo</i>	77
5.3.5	Combined sensing of latent TGF- β with AdCAR T cells and targeting a TAA with CAR T cells <i>in trans</i> does not interfere with anti-tumor efficacy.....	79
5.3.6	Endogenous immune cells enhance sensing of latent TGF- β and anti-tumor efficacy of AdCAR T cells in an immunosuppressive tumor model.....	82
5.3.7	Endogenous immune cells enhance proliferation and tumor infiltration of AdCAR T cells in an immunosuppressive tumor model	84

Table of content

5.3.8 Cytotoxic T cells show adapter-dependent accumulation in the peritumor	87
6. Discussion.....	88
6.1 Latent TGF- β is localized in the TME of ovarian tumors	88
6.2 AdCAR T cells are activated by soluble antigens and effector responses are tunable by both adapter and antigen dose	91
6.3 AdCAR T cells can target a soluble antigen and a TAA simultaneously.....	93
6.4 In the subcutaneous AsPC-1-TGF mouse model latent TGF- β is present both in serum and the TME	96
6.5 Sensing of soluble latent TGF- β <i>in vivo</i> induces systemic AdCAR T cell activation characterized by an early induction of pro-inflammatory cytokine secretion.....	99
6.6 The anti-tumor effect of AdCAR T cells is enhanced in NSG mice reconstituted with autologous PBMCs.....	101
6.7 AdCAR T cells show deficits to infiltrate solid tumor tissue.....	104
6.8 Outlook	105
7. References.....	107
8. Table of figures	130
9. Abbreviation	132
10. Publications	135
10.1 Manuscripts	135
10.2 Poster presentations	135
10.3 Patent applications	135
Affidavit.....	136
Danksagung.....	137

Zusammenfassung

Auf Grund des Erfolgs von chimären Antigen Rezeptor (CAR) T-Zellen in der Behandlung von hämatologischen Tumoren wird eine Ausweitung der Behandlung auf solide Tumore untersucht. Die klinische Übertragbarkeit auf solide Tumore wird allerdings durch das Fehlen tumorspezifischer Antigene und durch ein komplexes Tumormilieu (TME) erschwert. Zur Identifikation neuer tumorspezifischer Antigene fokussieren sich die meisten Ansätze auf membranständige Proteine. Zahlreich im TME vorkommende lösliche immunmodulatorische Signalmoleküle werden dabei größtenteils nicht adressiert. Ein solches lösliches Molekül, das eine Vielzahl von Immunzellen im TME supprimiert, ist TGF- β .

Im Rahmen dieser Arbeit wurde latentes TGF- β im TME von primären Ovarialkarzinomen nachgewiesen. Eine Korrelation mit Fibroblasten-assoziierten Oberflächenmarkern und mit Integrinen, die beide mit Tumor-Invasivität und Immunsuppression in Zusammenhang stehen, wurde gezeigt. Latentes TGF- β kann membrangebunden oder löslich vorliegen und wurde daher in dieser Arbeit ausgewählt, um die Sensitivität von Adapter-CAR (AdCAR) T Zellen gegenüber löslichen Antigenen zu zeigen. Es wurde anhand von Aktivierungsmarkern und Zytokin-Sekretion nachgewiesen, dass die Adapter-vermittelte Bindung eines löslichen Antigens an AdCARs zu einer funktionellen Aktivierung von AdCAR T-Zellen führt. Die Aktivierung der AdCAR T-Zellen war sowohl abhängig von der Adapterkonzentration als auch von der Antigenkonzentration. Die Aktivierung durch lösliches Antigen konnte weiterhin in einem immunsuppressiven Umfeld bei direktem Zellkontakt mit Tumorzellen und bei räumlicher Trennung der Zelltypen gezeigt werden. In drei verschiedenen duktalem Pankreaskarzinom (PDAC) Xenograft Modellen führte eine Adapter-vermittelte Bindung von latentem TGF- β durch AdCAR T-Zellen zu einer schnelleren IFN- γ Sekretion verglichen mit CAR T-Zellen, die direkt ein Tumor-assoziiertes Antigen (TAA) erkennen. Zytotoxische CD8⁺ AdCAR T Zellen reicherteten sich in der Milz an, was auf eine Stimulation dieser Zellen durch lösliches latentes TGF- β hindeutete. In einem immunkompetenten Mausmodell konnte die Flexibilität des AdCAR gezeigt werden. Durch die Applikation zweier verschiedener Adapter konnte ein TAA und gleichzeitig immunsuppressives latentes TGF- β adressiert werden. Eine gegenseitige funktionelle Blockade konnte nicht ermittelt werden. Sowohl die Zytokin-Sekretion als auch die Kontrolle des Tumorwachstums konnten in Gegenwart von autologen Immunzellen verbessert werden. Dadurch konnte eine transiente Kontrolle des Tumorwachstums im immunsuppressiven PDAC Tumormodell erreicht werden. Zusammengefasst zeigen diese Daten, dass AdCARs durch lösliche Antigene auch *in vivo* stimuliert werden können. Dies ermöglicht, das Spektrum potentieller Antigene für die CAR Therapie solider Tumor auf lösliche Antigene zu erweitern. Weiterhin bietet das neu entwickelte Konzept die Möglichkeit, membranständige und lösliche Antigene bei der Behandlung von Krebs mit CAR T-Zellen zu kombinieren.

Abstract

Due to the tremendous success of chimeric antigen receptor (CAR) T cell therapy in the treatment of hematologic malignancies, the clinical translation of this therapeutic concept to solid tumors is currently under investigation. The lack of tumor specific antigens and a complex tumor microenvironment (TME) are hurdles for the translation of CAR T cell therapy to solid tumors. To identify novel tumor specific antigens most approaches are focusing on membrane-bound targets. Thus, neglecting the huge repertoire of soluble immunomodulatory signaling molecules present in the TME. A soluble molecule present in the TME suppressing a variety of immune cells is TGF- β .

In the presented work here, latent TGF- β was found in the TME of ovarian cancer tissue. A correlation of latent TGF- β with surface markers expressed on fibroblasts and with integrins was shown. Both are linked to tumor invasiveness and immunosuppression. Latent TGF- β can be found membrane-bound as well as in soluble form. Therefore, latent TGF- β was selected in this study to investigate sensing of soluble antigens with AdCAR T cells. It could be demonstrated that an adapter-mediated binding of soluble antigens to AdCAR T cells induces effector functions in T cells. This was indicated by the expression of activation markers and cytokine secretion. The activation of AdCAR T cells was dependent on the adapter as well as on the antigen concentration. In addition, soluble antigen sensing was shown under immunosuppressive conditions in direct cell-to-cell contact of AdCAR T cells with tumor cells and with spatial separation of both cell types. In three different pancreatic ductal adenocarcinoma (PDAC) xenograft mouse models the targeting of latent TGF- β with AdCAR T cells induced a rapid stimulation of IFN- γ secretion, when compared to CAR T cells directly targeting a tumor associated antigen (TAA). The enrichment of cytotoxic CD8⁺ T cells in spleens was indicative for soluble latent TGF- β -mediated stimulation of AdCAR T cells. The versatility of the AdCAR system was demonstrated in an immunocompetent mouse model. The combined administration of two different adapter specificities was feasible to target a TAA and immunosuppressive latent TGF- β simultaneously. Neither cytotoxicity nor the sensing of the soluble ligand was blocked by a second adapter specificity. Furthermore, it was demonstrated that cytokine secretion and control of tumor growth were improved in presence of autologous immune cells. Thus, transient tumor control of the immunosuppressive PDCA tumor model was achieved.

Overall, these data demonstrate sensing of soluble antigens with AdCAR T cells *in vivo*. This expands the spectrum of possible antigens by soluble ligands to target solid tumors with AdCAR T cells. Furthermore, the novel developed concept allows to combine targeting of a TAA and a soluble antigen in the treatment of cancer with CAR T cells.

1. Introduction

1.1 Development of cancer and immunosurveillance

More than 100 years ago changes in the structure of chromosomes of tumor cells were observed and described^{1,2}. The events causing these genetic abnormalities are just as diverse as tumors themselves. Probably one of the biggest risk factors to trigger malignant transformation is our way of life. Tobacco consumption, alcohol and obesity all contribute to the development of cancer³. In addition to our own behavior pathogens like viruses are reported to cause cancer, e.g. Epstein-Barr virus and the human papillomavirus^{4,5}. Environmental factors like UV exposure are linked to transformation of normal cells as well⁶. All of these external and internal influences can cause lesions of the DNA more than 10,000 times per day in the genome of a single cell⁷. Most commonly only one strand of the DNA helix is showing defective or mismatched base pairing termed as single-strand DNA breaks. However, in more severe cases even double-strand breaks can happen. Despite the manifold threats exerted on genome integrity, various repair strategies have evolved to guarantee the genetic stability before cancer develops. Single strand DNA breaks are repaired throughout the excision of incorrect base pairs mostly by three mechanisms: base excision repair, mismatch repair and nucleotide excision repair⁸⁻¹⁰. The more severe double strand DNA breaks are either repaired by homologous recombination, using the non-damaged homologous chromosome as a template, or the more error prone non-homologous end-joining, which ligates the broken DNA strand in absence of a template¹¹. In case repair mechanisms are overwhelmed or not sufficient anymore, e.g. as associated with age, genetic lesions may indeed result in tumor formation. Tumor cells can arise from normal tissue by genetic lesions, e.g. acquired from inherited germline mutations or somatic mutations. Point mutations and inter- and intrachromosomal relocations are frequently found in the genome of tumor cells causing the abnormality in cancer¹². The type and the extent of those mutations are numerous but commonly they drive uncontrolled cell cycle. For example, these mutations can result in silencing of tumor suppressor genes, e.g. p53, or generate constitutively active signaling molecules like the BCR-ABL fusion protein^{13,14}.

However, even if cells start to transform, both the innate and the adaptive immune response are able to protect against cancer formation, by a mechanism coined immunosurveillance¹⁵⁻¹⁷. Immunosurveillance is extremely important. This is especially evident when immunosurveillance is suppressed by, e.g. drugs. After organ transplantation, for instance, the long-lasting immunosuppression in those patients, originally induced to prevent graft rejection, is known to result in higher incidences of cancer, thus stressing the potential tumor suppressive role of our immune cells^{18,19}. In addition, the importance of anti-cancer immune responses was illustrated in cancer patients who were suffering from a viral or bacterial infection and cancer at the same

time^{20,21}. One patient diagnosed with Hodgkin lymphoma got infected with the SARS-CoV-2 virus and after four months the patient went into remission although no corticosteroid or immunotherapy was administered. It is assumed that the pneumonia caused by viral infection triggered the patient's immune system and induced the anti-tumor response²⁰. Although our immune system does in principle provide an effective protection against the occurrence of tumors non-immunocompromised individuals are frequently diagnosed with cancer. In 2020 alone, according to estimations of the global cancer statistics, 19.3 million new cases of cancer were diagnosed²². The processes by which cancer escapes control by the immune system were described by Schreiber *et al*²³. The so called tumor immunoediting is divided into three phases: elimination, equilibrium and escape. In the elimination phase the innate immune response is alarmed by tumor cell-mediated inflammation due to tumor invasiveness and cytokine production. A diverse set of immune cells including $\gamma\delta$ T cells, NK-cells and macrophages are recruited and recognize tumor-related antigens, e.g. MICA or Rae1 via the NKG2D receptor followed by IFN- γ secretion²³⁻²⁶. IFN- γ is counteracting tumor progression by its antiproliferative, pro-apoptotic or angiostatic effect on malignant cells²⁷⁻²⁹. Finally, adoptive CD4⁺ and CD8⁺ T cells infiltrate the tumor and induce tumor cell killing, thus amplifying the innate anti-tumor response leading to tumor clearance²³. In case of an incomplete tumor clearance, malignant cells can enter the equilibrium phase. In the equilibrium phase tumor cells that were not eradicated are under constant selection pressure by the immune system. Due to the selective pressure exerted by the TME cancer cells acquire mutations to evade the immune response. This leads first to clonal expansion of malignant cells and later on to intratumoral heterogeneity. Subsequently, transformed cells escape from the tumor suppression³⁰⁻³². In the last phase, tumors evade the control of the immune system and show continuous growth. This is achieved by lowering the immunogenicity of the tumor due to an accumulation of further mutations in addition to the ones that initially drove cancer development, e.g. a loss of MHC I expression, induced expression of immune checkpoint molecules like PD-L1 or acquisition of mutations in the transforming growth factor- β (TGF- β) signaling pathway³³⁻³⁵. However, this observation that the immune system has the potential to control tumor development *per se* resulted in several therapeutic strategies aiming to induce or restore immunosurveillance.

1.2 New perspectives of cancer therapy

Over the past years our understanding of cancer improved fundamentally, especially the knowledge of the molecular mechanisms leading to its formation, progression and resistance to immune control. Based on this increasing knowledge cancer therapy has evolved dramatically. From first chemotherapeutic approaches treating lymphoma with nitrogen mustard to personalized patient specific treatment options that combine several layers of immunotherapy to elicit a broad immune reaction against cancer, treatment options for patients are constantly increasing^{36,37}. The access to better treatment options is reflected in a continuous decrease of cancer mortality over the past years³⁸.

1.2.1 Cancer immunotherapy

The starting point of today's immunotherapy was marked by studies of William B. Coley in 1891 who demonstrated that extracts of bacteria boost the immune response against cancer³⁹. Subsequently, Lewis Thomas and Sir Frank Macfarlane Burnet postulated the hypothesis of cancer immunosurveillance^{40,41}. In 1997 the US Food and Drug Administration (FDA) approved the first monoclonal antibody for the treatment of malignant B cells, named Rituximab⁴². The use of monoclonal antibodies (mAbs) for targeting cancer by re-directing the patient's own immune system marked the start for a new era of cancer therapeutics. As a next step, the therapeutic concept using mAbs was translated to the field of solid cancer. The blocking of the immune checkpoint molecule CTLA-4 with Ipilimumab achieved FDA approval in 2011. Ipilimumab administration improved long term survival of patients suffering from unresectable or metastatic melanoma^{43,44}. In 2014, two additional checkpoint blocking antibodies, pembrolizumab and nivolumab both targeting PD-1, were approved for the treatment of melanoma patients^{45,46}. The use of both therapeutic agents was continuously expanded to other malignancies, e.g. non-small-cell lung cancer or head and neck squamous cell carcinoma^{47,48}. Furthermore, it turned out that simultaneous targeting of more than one checkpoint pathway was even more beneficial in treating cancer. A combination of CTLA-4 and PD-1 blocking showed promising results in several phase III clinical trials and led to FDA approval, e.g. for the treatment of unresectable malignant pleural mesothelioma⁴⁹⁻⁵¹. Here, a combination of these antibodies led to prolonged overall survival rates compared to the standard of care⁴⁹. In addition to mAbs, cytotoxic T cells were shown to be a promising treatment option for cancer by Chester M. Southam in 1966⁵². Leukocytes derived from cancer patients and administered together with their own tumor cells were found to induce tumor rejection in his studies⁵². This adoptive cell therapy (ATC) was developed further by Rosenberg and colleagues. In particular, tumor infiltrating lymphocytes (TILs) were isolated from tumor biopsies and expanded *ex vivo* in the presence of IL-2 and injected back into the patient's body. In previously lymphodepleted patients this approach

showed a remarkably complete tumor remission in 22 % of metastatic melanoma patients⁵³. The lymphodepletion was essential in this therapeutic setting as it led to an increased level of IL-7 and IL-15, which promotes the homeostatic proliferation of transferred cells⁵⁴. However, this approach is limited, as it depends on the presence of tumor reactive TILs at sufficient numbers for isolation and expansion. To overcome this bottleneck autologous T cells were genetically modified to express recombinant T cell receptors (TCRs) specific for a cancer antigen, e.g. NY-ESO-1. Subsequently, the modified T cells are expanded and re-injected into cancer patients. NY-ESO-1 TCR expressing T cells demonstrated clinical response in patients with melanoma and synovial cell sarcoma emphasizing the potential of this method⁵⁵.

TILs and TCR transgenic T cell approaches build on the establishment of a highly specific TCR-MHC-peptide complex as prerequisite for T cell activation. However, one mechanism of tumor cells to evade T cell mediated elimination is the silencing of MHC expression. To counteract the limitations of TCR based cellular therapy a new class of antibodies was developed. Novel antibody generation methods and the use of “knobs-into holes mutations” allowed the production of recombinant antibody fragments with two different specificities⁵⁶. Subsequently, antibodies were developed to cross-link cytotoxic T cells with cancer antigens expressed on the cell surface, independent of the T cell’s TCR specificity. The new class of molecules was called bispecific T cell engagers (BiTEs). With blinatumomab the FDA approved the first BiTE against B-cell lymphoblastic leukemia in 2014, after blinatumomab treatment resulted in event-free survival in 31 % of treated patients⁵⁷. A potential disadvantage of BiTEs is that the molecule needs to be constantly re-injected to elicit anti-tumor T cell responses and thus, long term protection against recurrent malignant cells may be impaired⁵⁸. However, this bottleneck was overcome by a new class of genetically engineered immune cells not occurring in nature. The concept of so called chimeric antigen receptor (CAR) expressing T cells and its study in clinical trials led to groundbreaking results in cancer therapy.

1.2.2 CAR T cells in cancer therapy

Since its first description by Eshhar *et al.* in 1993 CAR T cell therapy underwent an enormous evolution⁵⁹. Constant improvements in CAR design and CAR manufacturing has led to the FDA approval of six CAR T cell therapies so far: Kymriah™, Yescarta™, Tecartus™, Breyanzi®, Abecma® and CARVYKTI™⁶⁰. All currently approved CAR T cell therapies focus on hematological malignancies with four of them targeting CD19, whereas Abecma® and CARVYKTI™ are targeting BCMA in patients with relapsed or refractory multiple myeloma⁶⁰. Currently more than 650 CAR T cell trials are registered as recruiting or active, indicating that the CAR T cell therapy will possibly be available to more indications in the future (as registered at clinicaltrials.gov, 28.01.2022). In contrast to previous cancer therapies, CAR T cells provide an option to heavily pre-treated patients for which other standard-of-care therapies have already failed. In relapsed

and refractory multiple myeloma patients, who have undergone at least three other treatments before, Abecma® demonstrated an overall response rate of 73 % with a median progression free survival of 8.8 months⁶¹. This impressively shows how CAR T cells can give hope to patients who previously had no treatment options left and may explain why CAR T cells have gained such an enormous attention in the field of immunotherapy.

To build a CAR, four structural elements are essential: (1) antigen binding domain, (2) hinge-region, (3) transmembrane domain and (4) intracellular signaling (**Figure 1**).

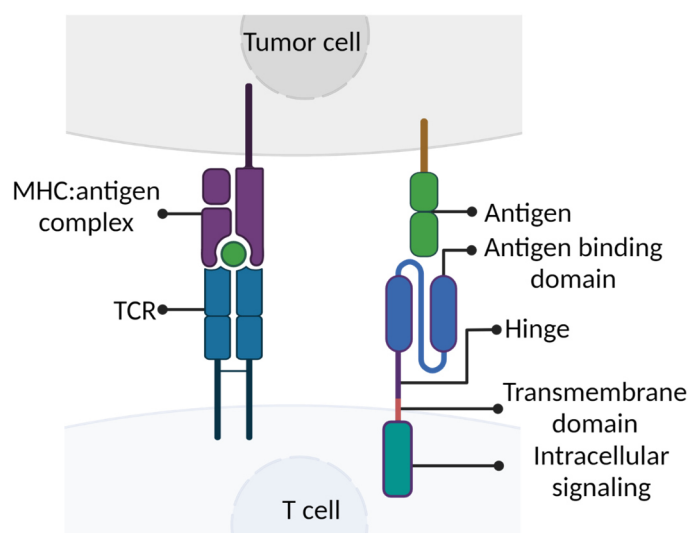


Figure 1: Structural differences of TCRs and CARs.

Processed peptides are presented by MHC molecules expressed on, e.g. tumor cells. The TCR binding of native T cells is restricted to the MHC:peptide complex, therefore tumor cells downregulate MHC expression to evade anti-tumor immune response. The CAR is MHC independent due to its architecture. The CAR contains four essential elements: (1) antigen binding domain, (2) hinge, (3) transmembrane domain and (4) intracellular signaling. Adapted from Lee, YH. *et al.* Evolution of chimeric antigen receptor (CAR) T cell therapy: current status and future perspectives. Arch. Pharm. Res. (2019). Illustration created with BioRender.com.

In most cases the antigen binding domain is a single chain variable fragment (scFv). The scFv allows CAR T cells binding to tumor antigens independent of the peptide-MHC complex and defines the specificity of the CAR. The scFv does not simply crosslink the CAR with its cellular target. Parameters like the position of the epitope, e.g. more proximal or more distal from the tumor cell membrane, and binding affinity impact the cytolytic activity as well as persistence of CAR T cells. Furthermore, the binding properties of the scFv can be used to discriminate between healthy and malignant cells^{62–64}. Although scFvs are frequently used many other binding domains, e.g. nanobodies, receptor ligands or darpins have been evaluated in CAR format^{65–67}. The binding moiety is followed C-terminally by the hinge region. The hinge domain regulates the distance between the CAR T cell and the target cell. The hinge sequence is often derived from IgG domains or from endogenous T cell co-receptors, like CD28 or CD8. The composition of the hinge region, as well as length and flexibility, were shown to modulate efficacy and persistence of the CAR T cells *in vivo*^{68,69}. Therefore, the optimal hinge needs to be determined

empirically, for each CAR and the corresponding target antigen. The CAR complex is anchored to the T cell membrane by a transmembrane domain (TM) commonly derived from the native CD8 α or CD28 TM receptor sequence. In addition to the anchoring of the CAR the TM can improve CAR T cell responses by incorporating native TCR signaling molecules into the CAR synapse or induce activation independently of intracellular signaling domains⁷⁰⁻⁷².

The endodomain is essential to convert the binding of a tumor cell into CAR T cell activation. This structural element of CAR T cells plays a crucial role in CAR T cell functionality as demonstrated early in the development of CARs. The first generation of CAR T cells was composed of CD3 γ or CD3 ζ endodomains⁵⁹. However, those cells showed limited proliferation *in vitro* and limited anti-tumor efficacy in a clinical proof of concept study in patients^{73,74}. This changed with the introduction of second generation CAR T cells in which CD3 ζ and CD28 signaling were combined. Those constructs with co-stimulation mediated long term persistence and robust cytokine secretion of CAR T cells⁷⁵. In third generation CARs different co-stimulatory domains, e.g. CD28, 4-1BB, OX-40 or ICOS, were combined to further improve activation⁷⁶⁻⁷⁸. In order to harness CAR T cell therapy in solid tumors, additional domains for cytokine production were included into the endodomain of CARs to generate fourth generation CARs. The local triggering of the CAR induces deposition of, e.g. IL-12 or IL-18, and stimulates the innate anti-tumor response in addition to the antigen dependent CAR T cytotoxicity⁷⁹⁻⁸¹. In contrast to previous CAR designs, complete activation of native T cells includes cytokine-derived stimulation in addition to TCR activation and co-stimulation. The limitation of the missing cytokine engagement by CAR T cells was overcome in fifth generation CARs. In the fifth generation of CARs co-stimulatory signaling elements have been extended by endodomains of cytokine receptors like IL-21R or IL-2R to induce JAK-STAT signaling in dependency of CAR engagement. By this architecture CARs recapitulate cytokine-derived stimulation and therefore were found to improve the efficacy in solid tumors^{82,83} (**Figure 2**).

All of these CAR designs have in common that for any CAR T cell product, once injected into a patient, the pharmacological control is limited. Importantly, in contrast to previous cancer drugs CAR T cells are living agents capable to proliferate and persist. This makes CAR T cell therapy difficult to control in case of severe side effects or after tumor eradication. Therefore, adapter CARs (AdCARs) have been developed which combine the features of CAR T cells with properties of mAbs.

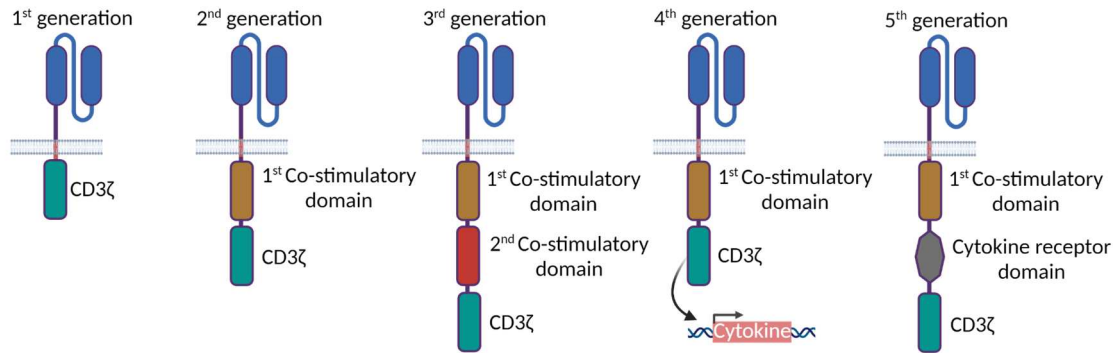


Figure 2: Evolution of CAR design.

First generation CARs contained only one intracellular signaling motif. In second generation CARs one co-stimulatory domain and in third generation CARs two co-stimulatory domains were added to the design of first generation CARs. Fourth generation CARs built on the framework of second generation CARs and contained a signaling motif to induced cytokine secretion. The fifth generation of CARs was also derived from the second generation design and included the intracellular signaling moieties of cytokine receptors to trigger the JAK-STAT signaling pathway. Adapted from Tokarew, N., Ogonek, J., Endres, S. *et al.* Teaching an old dog new tricks: next-generation CAR T cells. *Br J Cancer* (2019). Illustration created with BioRender.com.

1.2.3 AdCAR T cells for cancer therapy

In AdCARs the tumor binding domain and the signaling domains are not covalently linked. AdCAR T cells bind to the tumor cell via an additional adapter molecule which is designed to allow tumor cell and AdCAR T cell cross-linking. The adapter controls the specificity of the AdCAR T cells and adds an additional layer of control to the therapy as no anti-tumor response is elicited in absence of adapter. This principle is comparable with Fc-receptor induced antibody-dependent cell-mediated cytotoxicity (ADCC) of macrophages or NK cells. In the context of immunotherapy, ADCC was observed to eradicate patient-derived lymphoma cells with rituximab or in breast cancer patients treated with trastuzumab^{84,85}. Indeed, this ADCC principle has been translated to CAR T cells in which Fc receptors, instead of scFvs, were combined with the signaling architecture of 1st generation CARs. This modification allowed to induce ADCC with genetically modified T cells in presence of mAbs⁸⁶. In additional concepts, AdCARs binding to tagged biomolecules and AdCARs binding bispecific molecules were developed. Especially the field of tag-specific CARs is extremely diverse. Biotin, FITC, peptide motifs, leucine zipper or spy tags have been successfully applied as tag structures coupled to antibodies or fragments thereof⁸⁷⁻⁹¹ (Figure 3).

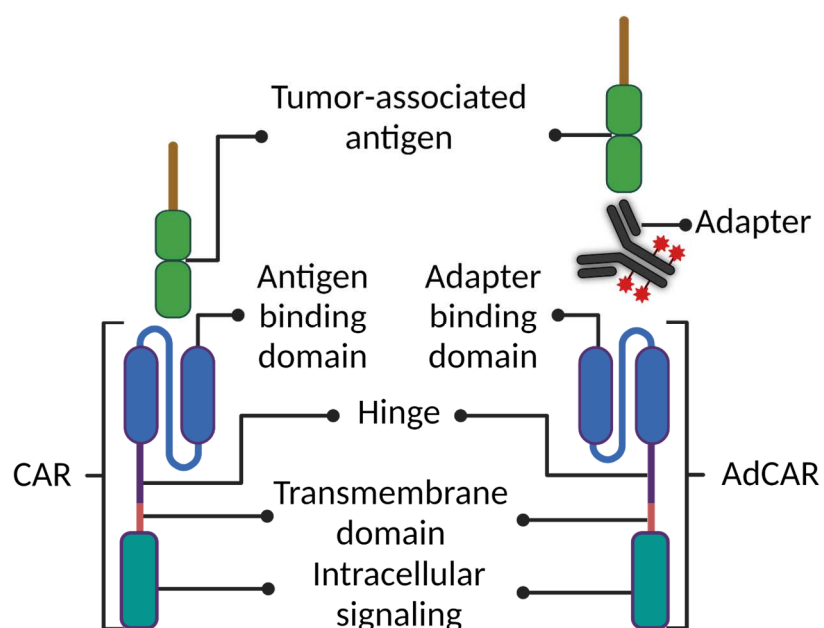


Figure 3: Structural differences of CARs and AdCARs.

CARs and AdCARs share most of their basic structural elements. The major difference is the binding of the target antigen. In contrast to CARs, AdCARs do not bind directly to the tumor cell, since the adapter binding domain of the AdCAR is specific for a tagged adapter molecule, rather than for a TAA. The adapter cross-links the AdCAR and the tumor cell. Thus, AdCARs show no effector function in absence of adapter, offering a better pharmacologic control after AdCAR T cells administration. Adapted from Seitz *et al.* Novel adapter CAR-T cell technology for precisely controllable multiplex cancer targeting. *Oncolmmunology* (2021). Illustration created with BioRender.com.

All AdCAR systems have in common that they offer a safety mechanism in case of severe side effect, like CRS or neurotoxicity. The cytolytic activity of AdCAR T cells is dependent on the

adapter concentration, which is in contrast to CAR T cells. Therefore, also side effects are manageable via the dosing of the adapter. A gradual increase of adapter dosing over time starting at suboptimal doses of adapter, discontinuation of the adapter injections or withdrawal of the adapter injections were demonstrated to limit CRS like symptoms in mice^{92,93}. The improved safety profile of AdCARs is a major advantage in comparison to CARs. However, the controllability of AdCAR T cells significantly depends on the pharmacokinetics of the adapter molecule which, e.g. can be modulated by the molecular size of the adapter. Whereas small adapters, e.g. nanobodies or scFvs, were shown to be cleared from the blood of mice within minutes larger biomolecules like IgGs were found to circulate for days in the blood stream^{94–96}. A potential drawback of adapter molecules with a small molecular weight is the need for continuous re-dosing to ensure a constant supply of AdCAR T cells with adapter. An additional advantage of AdCARs is the option to consecutively target multiple cancer antigens and/or apply Boolean logics via mixtures of adapters. This is helpful in solid tumors with heterogenous target antigen expression or to antagonize healthy tissue damage when AdCAR-mediated on target-off tumor cytotoxicity is observed^{87,90}.

Since AdCAR T cells are a promising new CAR technology this concept has been already evaluated in clinical trials. CAR T cells using the FcγRIII as binding moiety have been evaluated in a phase I clinical trial in combination with Rituximab as adapter moiety. In this trial an overall response rate of 64 % was reported⁹⁷. Unfortunately, the trial was later on stopped due to grade three serious adverse events in one patient⁹⁸. Nevertheless, clinical trials with other AdCAR systems, e.g. tag specific AdCAR CARs, are planned or currently ongoing^{99,100}. Promising intermediated results were reported for three patients suffering from relapsed/refractory acute myeloid leukemia treated with UniCAR-T-CD123 cells. The patients received AdCAR T cells in combination with a tagged CD123 specific scFv. The investigators reported no dose limiting toxicities and only mild side effects. Most importantly, all the patients showed either complete or partial remission¹⁰¹.

As described initially, CAR T cell therapy achieved remarkable success in hematological malignancies. Although numerous improvements in CAR architecture were made and promising response rates in clinical trials were observed with CAR T cells in hematologic malignancies such results currently have not been achieved in solid tumor settings¹⁰². The cellular composition, the antigen distribution and accessibility of solid tumors differs substantially from liquid tumors. Especially the microenvironment of solid tumors is highly immunosuppressive and represent a major obstacle for CAR T cell therapy necessitating novel concepts to advance CAR T cell therapies into the field of solid tumor therapy.

1.3 Tumor microenvironment of solid cancer

The tumor mass is made of a heterogenous composition of tumor cells, non-malignant cells, structural proteins and soluble molecules. Together, all of these components form the so-called TME^{103,104}. All classes of immune cells but also non-immune cells like stromal cells and endothelial cells form a complex and dynamic network around the tumor. The TME and tumor cells are in constant exchange via cell-to-cell contacts, the extracellular matrix as well as chemokines and cytokines¹⁰⁵. The impact of the TME on the tumor has been reported to be manifold and can be either anti- or pro-tumorigenic. For instance, infiltrating T cells and dendritic cells (DCs) are able to form tertiary lymphoid structures (TLSs) as part of the TME. The organization of such structures, which were shown to even contain high endothelial venules, closely resembles a lymph node like architecture. Within the TME, a TLS provides space for activation of cytotoxic T cells and B cell maturation as proinflammatory cytokines are enriched and cancer immunosuppression is absent^{106,107}. In patients, the presence of TLSs was positively correlated with survival and was predictive for higher responsiveness to immunotherapy^{108,109}. Besides these proinflammatory “hot” TMEs non-tumor reactive “cold” TMEs have been reported, and especially glioblastomas stand out as an example¹¹⁰. A non-tumor reactive TME promotes the accumulation of a diverse set of immunosuppressive immune cells including regulatory T cells (T_{regs}), myeloid-derived suppressor cells, tumor-associated macrophages or tumor-associated neutrophils¹⁰⁶. In addition, a central element of the TME are cancer-associated fibroblasts (CAFs). CAFs can represent the majority of cells within the TME. For example, in PDAC up to 90 % of the solid tumor can consist of CAFs¹¹¹. Multiple progenitor cells like quiescent fibroblasts, bone marrow-derived mesenchymal cells, adipocytes and endothelial cells are able to develop into CAFs^{112–114}. CAFs are in constant cross-talk with almost all immune cells within the TME and contribute to shape the environment as a favorable niche for tumor progression. In particular, CAFs produce a variety of immunosuppressive signaling molecules, e.g. TGF- β and IL-6^{115,116}. In this way, CAFs contribute essentially to tumor immune evasion by inducing M2 polarization of macrophages, suppressing cytotoxic T cells or by promoting the generation of regulatory dendritic cells^{116–118}. Furthermore, CAFs are responsible for the deposition of extracellular matrix (ECM) molecules and thereby contribute to the remodeling of the ECM. Furthermore, CAFs shape a pre-existing ECM by secretion of ECM degrading enzymes, e.g. matrix metalloproteinases (MMPs)^{119,120}. As a result, CAFs form a dense and rigid desmoplastic stroma as it can be found in PDAC¹²¹.

The ECM is a central structure within the TME made of numerous proteins, e.g. collagen, hyaluronic acid or heparan sulfate¹⁰³. Exactly like the TME, the ECM is a dynamic and patient specific structure that has been shown to even allow prediction of the disease outcome of breast cancer patients¹²². The ECM, as a component of the TME, provides proliferative signaling to malignant cells, helps to avoid immune destruction and is involved in tumor vascularization. All

of these characteristics belong to a group of central properties Hanahan and Weinberg classified as hallmarks of cancer that need to be acquired by malignant cells to enable tumor formation. This underlines further the importance of the ECM, and the TME in general, for tumor formation^{123–125}. The ECM protects the tumor from cytotoxic immune cell infiltration. Dense and aligned collagen fibers have been shown to reject lymphocytes from entering encapsulated tumor cells by determining the trajectory migration of T cells¹²⁶. However, due to its composition the ECM does not only restrict the access of T cells to the tumor, in addition it recruits immunosuppressive cell types. Tumor associated macrophages (TAMs), for instance, are attracted by ECM areas rich in hyaluronic acid and then modulate neovascularization to promote tumor growth¹²⁷. The example of hyaluronic acid shows that the ECM is also providing survival stimuli directly to malignant cells, since tumor cells bind hyaluronic acid via CD44 to activate downstream signaling of several kinases. This interaction actively contributes to tumor proliferation and invasion^{128,129}. A similar mechanistic relation is described for cancer cell-expressed integrins engaging the ECM, as the ECM does provide stimulatory ligands for integrins. Integrins are an inevitable class of receptors of malignant cells to interact with the ECM. An integrin is assembled by pairing of an α and β chain. Through the combination of the 18 α and 8 β subunits, 24 different receptors can be made, binding to different ECM components like fibronectin, vitronectin or collagen^{130,131}.

Integrins support tumor progression and survival by, e.g. contributing to chemo- and immunotherapy resistance or by providing immunosuppressive cytokines within the TME. The integrin $\beta 1$ expressed on small cell lung carcinoma cells and PDAC, e.g. induces activation of tyrosine kinases, thus mitigating the cytotoxic effect of chemotherapeutics^{132,133}. Furthermore, integrin $\beta 1$ is linked to counteract the therapeutic effect of the Her-2 targeting monoclonal antibody Trastuzumab¹³⁴. Integrins are also involved in the localization and concentration of growth factors within the TME. One important example in this context is TGF- β which is anchored to the ECM in its inactive form. However, this immunosuppressive molecule can be activated via an interaction of, e.g. integrin $\alpha\beta 6$ or $\alpha\beta 8$ binding to an RGD motif of TGF- β resulting in soluble active TGF- β ^{135,136}.

Overall, the TME is an essential element of solid tumors with multiple cellular and molecular components, and one prominent example is TGF- β .

1.4 The role of TGF- β in the TME

A tight regulation of cellular processes like proliferation, differentiation or apoptosis is required for an organism to maintain functional integrity. One regulatory element that is involved in orchestrating these processes is TGF- β . Almost all classes of immune cells as well as stromal cells are susceptible to TGF- β . Depending on the context, TGF- β is able to both stimulate certain cell types and inhibit functions of others. This dual role was described by Anita B. Roberts in the 1980s as TGF- β was found to induce collagen secretion by fibroblasts but also to suppress growth of human tumor cells^{137,138}. Because of this bi-functionality and the fact that TGF- β and its signaling pathways are prone to mutations in cancer TGF- β is of high interest in cancer immunotherapy.

1.4.1 Structure and secretion of TGF- β

As first step TGF- β is synthesized as a pre-pro-peptide located in the endoplasmic reticulum, consisting of the N-terminal latency associated peptide (LAP) and the C-terminal TGF- β . LAP and TGF- β are subsequently cleaved by furin proteases and re-assemble non-covalently to form the small latent complex (SLC). The SLC consists of the dimeric LAP non-covalently linked to the also dimeric mature TGF- β . LAP is required for correct folding of TGF- β , as in absence of LAP no active TGF- β is formed¹³⁹⁻¹⁴¹. In addition, LAP wraps around TGF- β and blocks the receptor binding sites to keep TGF- β in its latent form¹⁴². The SLC can further associate with ECM anchoring proteins during the secretion process in the endoplasmic reticulum¹⁴³. Most frequently the SLC is bound covalently to latent TGF- β binding proteins (LTBPs) via disulfide bonds between LAP and LTBP. The formed complex is termed large latent complex (LLC). The LLC is subsequently secreted and can be tethered to the ECM by, e.g. fibronectin or collagen. This anchoring to the ECM is crucial for later activation and release of active TGF- β (**Figure 4**)^{139,144,145}. In addition to LTBP a few specialized SLC binding partners exist, e.g. for T_{regs} or macrophages. On T_{regs} the SLC is bound and presented on the cell surface by glycoprotein A repetitions predominant protein (GARP) which is furthermore predictive for the degree of immunosuppression of these cells^{146,147}. Another specialized SLC binding partner is the Leucine-Rich Repeat-Containing Protein 33 (LRRC33). LRRC33 is essential for activation of TGF- β presented on macrophages or microglia. The different binding partners are assumed to allow differential spatial activation of TGF- β ^{148,149}.

Three different isoforms of TGF- β exist. However, the secretion and maturation process is shared between all isoforms of the beta-type subfamily members. The beta-type subfamily of mammals is composed of the isoforms TGF- β 1, TGF- β 2 and TGF- β 3, which share 71-79 % of sequence homology within the active part of TGF- β ¹⁵⁰. In contrast to the active part, the inactive part of TGF- β is less conserved between the isoforms, showing only 36-51 % sequence

identity¹⁵⁰. Despite this high sequence similarity the different isoforms exert specific functions *in vivo* which is associated with differences in the LAP sequence¹⁵¹. For example during keratinocyte differentiation isoforms two and three are more related to the proliferation of keratinocytes, whereas isoform one is upregulated during differentiation¹⁵². Isoform specific functionality was also described during wound healing. An excess of isoform three compared to isoforms one and two was described to induce scar free wound healing¹⁵³. In the context of cancer, it was described that tumors of different origin display a unique TGF- β isoform signature, further highlighting the isoform specific functionality *in vivo*¹⁵⁴.

Besides cancer cells themselves, a broad spectrum of cells is described to secrete TGF- β ¹⁵⁵. This includes immune cells like T cells, B cells, DCs, TAMs and granulocytes^{156–160}. In addition, stromal cells as CAFs and platelets were reported to be major sources of TGF- β in the context of cancer^{161,162}. Finally, to carry out its biological function, TGF- β needs to be released from LLC by removing it from LAP.

1.4.2 TGF- β activation and downstream signaling

The conversion of latent TGF- β into its active form can be mediated by an acidic pH, an enzymatic reaction or an interaction of the LLC with integrins^{135,163,164}. For the later, the RGD motif of LAP plays an important role to convert inactive latent TGF- β into active TGF- β . This motif serves as a binding site for integrins, e.g. $\alpha\beta6$ and $\alpha\beta8$. Upon binding to LAP integrin $\alpha\beta6$ applies a physical force to the LLC as the integrin β -chain interacts with the contracting actin cytoskeleton. Since the LLC is covalently attached to the ECM by, e.g. LTBP the integrin-mediated force induces a deformation of the latent complex and a subsequent release of active TGF- β ^{165,166}. In contrast to the physical force needed for integrin $\alpha\beta6$ -dependent TGF- β activation, it is postulated that $\alpha\beta8$ in contrast acts with MMP14 to release active TGF- β , representing an interplay between enzymatical and non-enzymatical activation processes¹⁶⁷. Upon release from the LLC active TGF- β initiates intracellular signaling by binding to four receptors: TGF- β receptor I (T β RI or ALK-5), activin receptor-like kinase 1 (ALK-1), TGF- β receptor II (T β RII) and TGF- β receptor III (T β RIII). Whereas T β RI, T β RII and T β RIII are widely expressed, ALK-1 expression is more restricted to, e.g. endothelial cells, skin fibroblasts or microglia^{168–173}. In general, intracellular signaling is mediated via T β RI and T β RII. In detail, active TGF- β binds and multimerizes T β RII and induces a phosphorylation of T β RI^{174,175}. T β RIII is described to act as a co-receptor with contrary mechanistic outcomes. T β RIII is described to improve the binding of TGF- β 2 to the T β RII, thus enhancing the signaling¹⁷⁶. However in MDA-MB231 cells T β RIII was found to compete with T β RI/II complex formation, thus lowering TGF- β induced signaling¹⁷⁷. In general, the multimeric receptor signaling complex consisting of homodimeric T β RII and homodimeric T β RI can either induce the canonical signaling pathway or the non-canonical signaling pathway¹⁷⁸. For canonical pathway activation the receptor complex induces the phosphorylation of

Smad proteins leading to translocation of the Smad complex to the nucleus to induce gene expression¹⁷⁹. In addition to Smad dependent signaling TGF- β interacts with several other non-canonical pathways related to growth and survival, e.g. NF- κ B or the AKT/PKB pathway^{180,181}. Since TGF- β can trigger a large portfolio of signaling pathways it can also exert a broad spectrum of biological functions within the TME (**Figure 4**).

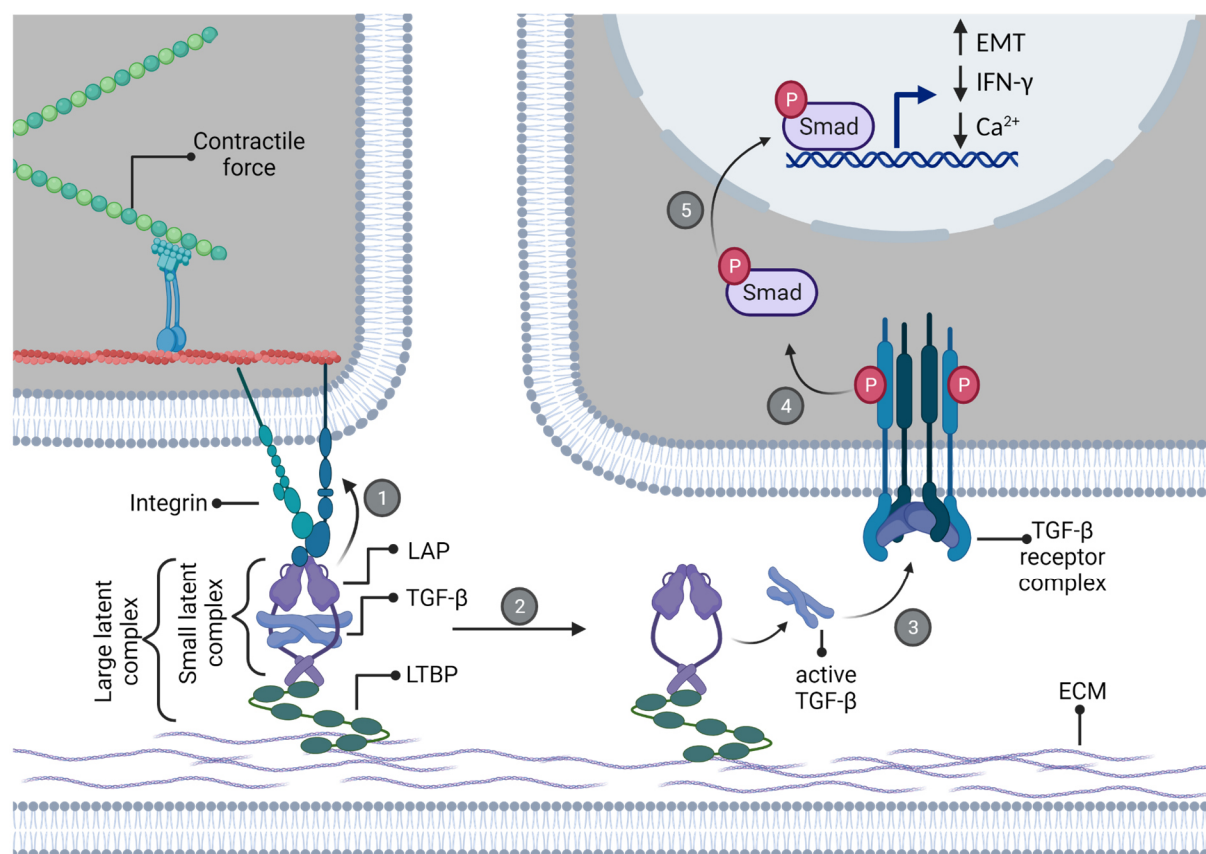


Figure 4: Secretion and activation of latent TGF- β .

TGF- β is secreted non-covalently attached to LAP forming the SLC. LAP keeps TGF- β in an inactive latent form and anchors the SLC to ECM binding proteins like LTBP building the LLC. The LLC tethers the complex to the ECM for subsequent activation of TGF- β : (1) Integrins like α v β 6 bind the RGD motif of LAP. (2) By applying physical force to the LLC active TGF- β is released. (3) Active TGF- β binds T β RII causing dimerization of the receptor. (4) This induces phosphorylation and multimerization of T β RI forming a larger T β RI/T β RII signaling complex. Next, the receptor complex phosphorylates Smad proteins. (5) Finally, the phosphorylated Smad proteins translocate into the nucleus and exerting gene expression. Adapted from Robertson *et al.* Latent TGF- β -binding proteins. *Matrix Biology* (2015) and Kubiczkova *et al.* TGF- β – an excellent servant but a bad master. *Journal of Translational Medicine* (2012). Illustration created with BioRender.com.

1.4.3 TGF- β and its role in tumor biology

In tumor biology, TGF- β has been described to act as a tumor suppressor at onset but may convert later into a tumor promoter enhancing immune evasion. Under physiological conditions, TGF- β acts as a negative regulator of cell cycle progression by inhibiting cyclin-dependent kinases via p15^{INK4B} and p21^{CIP1} and thus preventing uncontrolled proliferation^{182,183}. In the course of cancer progression, tumor cells can accumulate mutations within the TGF- β signaling

pathway, which make the malignant cells resistant to cell cycle regulation by TGF- β . A frequently found mutation in the TGF- β signaling pathway of PDAC causing TGF- β resistance is resulting in inactivation of Smad4 or loss of Smad4 expression. In addition, mutations of T β RI and T β RII are described as well^{184,185}. TGF- β is also involved in the epidermal-to-mesenchymal transition (EMT)¹⁸⁶. During EMT cells lose the expression of epithelial markers but upregulate e.g. fibronectin expression which is a classical mesenchymal marker¹⁸⁶. Furthermore, cells reduce cell-to-cell contacts and lose the typical apical-basal polarity. This enhances the motility of cancer cells and the potential to form metastases¹⁸⁷. Furthermore, in PDAC EMT is linked to chemoresistance, whereas in other cancers like endometrial carcinomas an increased invasiveness is related to EMT^{188,189}.

Importantly, TGF- β not only acts directly on cancer cells as TGF- β also orchestrates immune evasion by modulating almost all immune cell subsets involved in anti-tumor immunology. NK cells, for example, show reduced activity in presence of TGF- β due to a variety of inhibited processes mediated by TGF- β , e.g. suppression of IFN- γ secretion, blockade of IL-15 downstream signaling crucial for proliferation, or by downregulation of expression of NK cell receptors that mediate sensing of malignant cells^{190–192}. As already described, DCs are key to elicit T cell mediated anti-tumor response as those cells are responsible for presenting cancer antigens to cytotoxic T cells. In presence of TGF- β , however, this central function of DCs is impaired. In addition, TGF- β drives the development of immature immunosuppressive DCs^{193,194}. Besides dampening the innate immune response, TGF- β is highly suppressive to cells of the adaptive immune response as well. In T cells TGF- β lowers the calcium influx upon T cell receptor (TCR) stimulation, thus impairing the Th1 and Th2 differentiation. Calcium influx is occurring early in the signaling cascade following TCR or CAR activation. As a result, TGF- β signaling in T cells suppresses key effector functions like IFN- γ , IL-2 or granzyme production^{195–197}. Furthermore, and dependent on its local concentration within the TME, TGF- β and IL-2 can induce the differentiation of T cells into immunosuppressive T_{regs}^{198,199}. T_{regs}, in turn, are a central source of TGF- β , and the presence of this cell type after chemotherapy is negatively correlated with the overall survival of patients suffering from PDAC²⁰⁰. In sum, TGF- β is fundamentally involved in cancer development and progression, which makes this multi-faceted molecule and its underlying signaling pathways attractive targets in cancer therapy.

1.4.4 Targeting TGF- β in cancer therapy

Since TGF- β is involved in many processes promoting cancer progression several therapeutic approaches were investigated in clinical trials, e.g. neutralizing antibodies, ligand traps, siRNAs, small molecules or vaccines^{201–205}.

Bintrafusp alfa is a chimeric fusion protein composed of the T β RII and a monoclonal PD-L1 antibody. This bifunctional molecule has been reported to combine TGF- β neutralization with

prevention of checkpoint inhibition²⁰⁶. For instance, Bintrafusp alfa showed promising results in a phase I clinical trial with patients suffering from NSCLC with an overall response rate of approx. 21 %. Nevertheless, the future of this drug is unclear due to setbacks observed in recent clinical trials. The defined primary objective of overall survival was not reached which led to a discontinuation of the study²⁰⁷. Belagenpumatucel-L belongs to the group of cancer vaccines. This therapeutic agent is made of four engineered human NSCLC cell lines. The human cancer cells were irradiated and express the TGF- β 2 antisense gene to shut down TGF- β expression and prevent immunosuppression²⁰⁸. In a phase II study with patients suffering from NSCLC, Belagenpumatucel-L treated cohorts showed an improved survival. Moreover, in responding patients enhanced secretion of proinflammatory cytokines was observed²⁰⁵. Efficacy of Belagenpumatucel-L was already tested as a maintenance therapy in a phase III clinical study, including stage IV NSCLC patients. Unfortunately, no differences in the overall survival were observed with regard to the total patient cohort in comparison to the placebo-treated control cohort. However, in patients receiving the vaccine not later than twelve weeks after initial chemotherapy or in patients who underwent radiation before, the vaccine led to prolonged patient survival. This clinical trial stresses the potential of TGF- β in cancer therapy²⁰⁹.

In the development of an effective TGF- β targeting drug neutralizing antibodies appear to be an alternative and promising approach. One example is NIS793 which binds and neutralizes TGF- β and received orphan drug designation by the FDA for the treatment of PDAC. Future phase III clinical trials may show whether this treatment strategy can result into regular market authorization of NIS793 for treating PDAC^{210,211}.

In addition, the inhibition of TGF- β signaling in combination with adoptive cellular therapy was shown to be an interesting emerging therapeutic concept in the treatment of cancer^{212,213}. In a phase I clinical trial, T cells specific for Epstein-Barr virus related proteins were modified to express a dominant negative T β RII and used to treat relapsed Hodgkin lymphoma. The modified T cells induced a clinical response in four out of seven patients enrolled to the study. Interestingly, modified T cells showed expansion in blood even without a lymphodepletion prior to infusion²¹⁴. Overall, these data demonstrate that TGF- β and its signaling pathways are interesting targets to improve cancer therapy and targeting TGF- β may even enhance the efficacy of adoptive cellular therapies in solid cancers. Nevertheless, the clinical translation appears challenging and necessitates further investigation in the future.

2. Materials

2.1 Kits

Table 1: Ready to use kits

Kit	Application	Supplier
NucleoSpin Plasmid (NoLid), Mini kit	DNA preparation	Macherey-Nagel, Düren, GER
ZymoPURE II Plasmid Midiprep Kit	DNA preparation	Zymo Research Corporation, Irvine, US
NucleoBond Xtra Maxi EF, Maxi kit for endotoxin-free plasmid DNA	DNA preparation	Macherey-Nagel, Düren, GER
Pan T cell isolation kit	T cell isolation	Miltenyi Biotec, Bergisch Gladbach, GER
MACSelect™ LNGFR system	T cell enrichment	Miltenyi Biotec, Bergisch Gladbach, GER
LEGEND MAX™ Human Latent TGF-β ELISA Kit	ELISA	BioLegend, San Diego, US
MACSPlex Cytokine 12 Kit, human	Cytokine multiplex assay	Miltenyi Biotec, Bergisch Gladbach, GER
Tumor Dissociation Kit human	Dissociation of s.c. tumor xenografts	Miltenyi Biotec, Bergisch Gladbach, GER

2.1.1 Buffers and reagents

Table 2: Reaction buffers and reagents

Buffer/Reagent	Application	Supplier
MACS® BSA Stock Solution	Flow cytometry/Cell separation	Miltenyi Biotec, Bergisch Gladbach, GER
CliniMACS PBS/EDTA Buffer	Flow cytometry/Cell separation	Miltenyi Biotec, Bergisch Gladbach, GER
Dimethyl sulfoxide (DMSO)	Cryopreservation	Sigma-Aldrich, St. Louis, US
InsideFix solution	Flow cytometry	Miltenyi Biotec, Bergisch Gladbach, GER
MACSQuant bleach solution	Flow cytometry	Miltenyi Biotec, Bergisch Gladbach, GER
MACSQuant running buffer	Flow cytometry	Miltenyi Biotec, Bergisch Gladbach, GER
MACSQuant storage solution	Flow cytometry	Miltenyi Biotec, Bergisch Gladbach, GER
MACSQuant washing solution	Flow cytometry	Miltenyi Biotec, Bergisch Gladbach, GER

2 Materials

Buffer/Reagent	Application	Supplier
Pancoll	Cell separation	Pan-Biotech, Aidenbach, GER
NaHCO ₃	Conjugation	Sigma-Aldrich, St. Louis, US
EZ-Link™ NHS-LC-LC-Biotin	Conjugation	Thermo Fisher Scientific, Waltham, US
Gibco™ PBS, pH 7,2	Conjugation/Cell culture	Thermo Fisher Scientific, Waltham, US
Accutase® Cell Detachment Solution	Cell culture	BioLegend, San Diego, US
Polyethylenimine, MW 25,000 (PEI)	Lentivirus production	Polysciences, Warrington, US
Sodium butyrate	Lentivirus production	Sigma-Aldrich, St. Louis, US
CliniMACS® Formulation Solution	Cryopreservation	Miltenyi Biotec, Bergisch Gladbach, GER
Cryo Supplement 3x	Cryopreservation	Miltenyi Biotec, Bergisch Gladbach, GER
MACSQuant® calibration beads	Flow cytometry	Miltenyi Biotec Bergisch Gladbach, GER
Albumin (Human) 25 %	Flow cytometry/Cell separation	Octapharma, New York, US
Recombinant Human LAP (TGF-beta 1) Protein	Co-culture assay	R&D Systems, Minneapolis, US
Isoflurane	Anesthesia of mice	Zoetis, New Jersey, US
Human intravenous immunoglobulin (IVIG)	Fc-receptor blocking/ latent TGF-β	Takeda, Tokyo, JPN
D-Luciferin, Potassium Salt	<i>In vivo</i> imaging	GoldBio, St Louis, US
Red blood cell lysis buffer	<i>Ex vivo</i> analysis	Miltenyi Biotec Bergisch Gladbach, GER
autoMACS® Running Solution	<i>Ex vivo</i> analysis	Miltenyi Biotec Bergisch Gladbach, GER
OCT mounting medium	Immunohistochemistry	VWR, Radnor, US
Inside Fix	Immunohistochemistry	Miltenyi Biotec Bergisch Gladbach, GER
Permeabilization Solution	Immunohistochemistry	Miltenyi Biotec Bergisch Gladbach, GER
Antibody Staining Solution	Immunohistochemistry	Miltenyi Biotec Bergisch Gladbach, GER
DAPI	Immunohistochemistry	Sigma-Aldrich St. Louis, US
Fluoromount™ Aqueous Mounting Medium	Immunohistochemistry	Sigma-Aldrich St. Louis, US
Cover glasses for slipping equipment, Menzel Gläser	Immunohistochemistry	VWR, Radnor, US
Adhäsionsobjektträger, Super-Frost® Plus	Immunohistochemistry	VWR, Radnor, US

2 Materials

Buffer/Reagent	Application	Supplier
Hoechst	Cyclic fluorescent imaging	Sigma-Aldrich, St. Louis, US
7-AAD	Flow cytometry	Miltenyi Biotec Bergisch Gladbach, GER
Propidium Iodide	Flow cytometry	Miltenyi Biotec Bergisch Gladbach, GER

2.1.2 Cell culture media and supplements for eukaryotic cells

All cell culture media and supplements were purchased as sterile solutions. Reagents were stored according to manufacturer's protocol.

Table 3: Cell culture media for eukaryotic cells

Medium	Supplier
DMEM high glucose w/ L-glutamine w/ sodium pyruvate	Biowest Nuaille, FR
RPMI 1640 w/o L-glutamine	Biowest Nuaille, FR
TexMACS GMP Medium	Miltenyi Biotec Bergisch Gladbach, GER

Table 4: Cell culture supplements for eukaryotic cells

Supplement	Supplier
L-glutamine 200 mM	Lonza Basel, CHE
FBS-Maximus	Catus Biotech Tutzing, GER
MACS [®] GMP Recombinant Human IL-7	Miltenyi Biotec Bergisch Gladbach, GER
MACS [®] GMP Recombinant Human IL-15	Miltenyi Biotec Bergisch Gladbach, GER
T Cell TransAct [™] , human	Miltenyi Biotec Bergisch Gladbach, GER
MACS [®] GMP T Cell TransAct [™]	Miltenyi Biotec Bergisch Gladbach, GER

2.1.3 Cell culture media and supplements for prokaryotic cells

The ingredients were dissolved under constant steering in deionized water. Prior to sterilization, the pH was adjusted to 7.5 by adding 1 M NaOH (Roth, Karlsruhe, GER) to the solution.

Table 5: Culture medium for prokaryotic cells

Medium	Ingredient	Supplier
Lysogeny broth(LB) medium liquid	10 g/L NaCl	Roth, Karlsruhe, GER
	5 g/L Veggie Yeast Extract	Merck, Darmstadt, GER
	10 g/L Veggie Peptone	Merck, Darmstadt, GER
LB medium solid	10 g/L NaCl	Roth, Karlsruhe, GER
	5 g/L Veggie Yeast Extract	Merck, Darmstadt, GER
	10 g/L Veggie Peptone	Merck, Darmstadt, GER
	15 g/L LB Agar	Roth, Karlsruhe, GER
SOC medium	ready to use	NewEngland BioLabs, Ipswich, US

The ingredients were dissolved in ddH₂O and filtered through a PVDF-filter (Merck, Darmstadt, GER) with a pore size of 0.22 µm. The stock solution was stored at -20 °C.

Table 6: Cell culture supplements for prokaryotic cells

Supplement	Ingredient	Dilution	Supplier
Antibiotic ampicillin	Ampicillin 100 mg/mL	1:1000	Roth, Karlsruhe, GER
Antibiotic kanamycin	Kanamycin 50 mg/mL	1:1000	Sigma-Aldrich, St. Louis, US

2.1.4 Cell lines

Table 7: Cell lines and culture conditions

Cell line	Application	Culture medium	Reference
HEK293 T	Lentiviral vector production	DMEM, 10 % FCS	ATCC CRL-3216
SUP-T1	Titration of lentiviral vectors	RPMI, 10 % FCS, 2 mM L-glutamine,	ATCC CRL-1942
AsPC-1 WT	Target cell line <i>in vitro</i> and <i>in vivo</i>	RPMI, 10 % FCS, 2 mM L-glutamine,	Daniel Schaefer ²¹⁵
AsPC-1-TGF	Target cell line <i>in vitro</i> and <i>in vivo</i>	RPMI, 10 % FCS, 2 mM L-glutamine,	This work

2.1.5 Plasmids

Table 8: Plasmids

ID	Description	Reference
pMDG	CMV promotor, VSV-G	Addgene
pCMVdr8.74	CMV promotor, gag, pol, rev, RRE	Addgene
MB_TV_LPC_701_050 (AdCAR1)	RRE, 5'LTR, 3' sin LTR PGK promotor, IL22RA2 leader LLE-CAR (scFv: h Bio3-3.18E7), hlgG4hinge, CD8 TM, CD28 and 4-1BB, CD3 ζ , P2A, LNGFR	Miltenyi Biotec
MB_TV_LTG701_115 (AdCAR2)	RRE, 5'LTR, 3' sin LTR, EF-1 α IL22RA2 leader LLE-CAR (scFv: Bio2_4G10), hlgG4hinge, CD8 TM, CD28 and 4-1BB, CD3 ζ	Miltenyi Biotec
pGF-NFAT	RRE, 5'LTR, 3' sin LTR, 4xhNFAT-AP-1 binding site, CMV minimal promotor, cop GFP, T2A, Luciferase	System Bioscience

A schematic representation of the AdCAR constructs used in this thesis is shown (**Figure 5**).

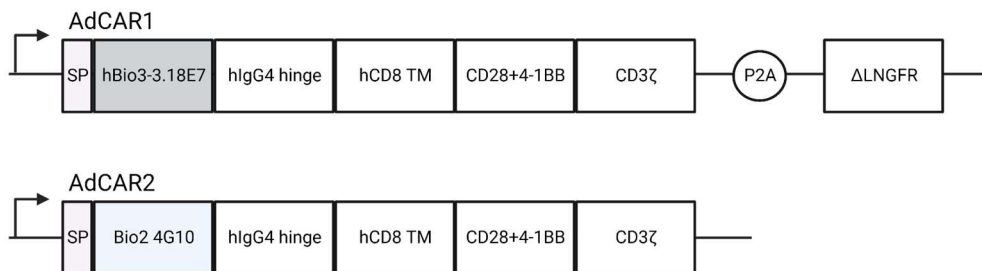


Figure 5: Illustration of AdCAR constructs.

Both AdCARs contained an IL22RA2 signal peptide (SP), a human IgG4 hinge and a human CD8 transmembrane region. The AdCARs were 3rd generation CARs, with a CD28 and a 4-1BB intracellular signaling domain. The biotin-specific scFv of AdCAR1 was derived from the antibody clone hBio3-3.18E7, whereas the biotin-specific scFv of AdCAR2 was derived from the antibody clone Bio2_4G10. As a transduction marker and as a tag for enrichment the AdCAR1 construct included a truncated LNGFR, separated via a P2A element downstream of the CAR sequence.

2.1.6 Antibody-conjugates used for cyclic fluorescent imaging and flow cytometry

Antibody conjugates were obtained from Miltenyi Biotec (Bergisch Gladbach, GER), with the exception of CD274, TCF1 (BioLegend, San Diego, US) and MECA79 (eBioscience, Waltham, US).

Table 9: Antibody conjugates used for cyclic fluorescent imaging

Specificity	Conjugate	Dilution factor	Clone	Specificity	Conjugate	Dilution factor	Clone
CD3	PE	50	BW264/56	CD163	PE	50	REA812
LAP	PE	50	CH6-17E5.1	CD22	PE	10	REA340
CD274	PE	50	29E.2A3	CD26	PE	10	FR10-11G9
TCF1	PE	50	7F11A10	CD21	PE	10	HB5
CD272	PE	50	REAL858	CD80	PE	50	REA661
CD4	PE	50	REA623	CD83	PE	50	REA714
CD8	PE	10	BW135/80	CD86	PE	50	REA968
CD69	PE	50	REA824	CD34	PE	50	REA1164
CD39	PE	10	REA739	CD40	PE	50	REA733
CD279	PE	50	PD1.3.1.3	CD64	PE	50	REA978
CD103	PE	50	REA803	CD31	PE	50	REA730
CD366	PE	50	REA635	CD11a	PE	50	REA378
Ki67	PE	50	REA183	CD150	PE	10	REA299
CD137	PE	10	REA756	CD11c	PE	10	REA618
CD101	PE	50	REA954	CD154	PE	10	REA238
CD25	PE	10	REA945	CD141	PE	10	REA674
CD278	PE	50	REA192	CD183	PE	10	REA232
CD161	PE	10	REA631	CD196	PE	10	REA190
CD244	PE	10	REA112	CD1c	PE	10	REA694
CD57	PE	10	REA769	CD235a	PE	10	REA175
CD38	PE	10	REA572	KLRG1	PE	10	REA261
HLADR	PE	10	REA805	IgM	PE	10	PJ2-22H3
CD152	PE	50	REA152	IgA	PE	10	IS11-8E10
CD9	PE	10	SN4 C3-3A2	IgD	PE	50	REA740
CD7	PE	10	CD7-6B7	CD79a	PE	50	REA1142
CD159a	PE	10	REA110	CCR10	PE	50	REA326
CD49a	PE	50	REA1106	CD53	PE	10	REA259
CD357	PE	10	REA1007	CD58	PE	10	TS2/9
CD134	PE	10	REA621	CD273	PE	10	REA985
CD162	PE	10	REA319	HLADQ	PE	50	REA303
CD45	PE	10	REA747	HLAABC	PE	10	REA230
CD20	PE	10	REA780	CD52	PE	10	REA164
CD19	PE	50	REA675	CD54	PE	10	REA266
CD56	PE	50	REA196	CXCL10	PE	10	REA334
CD15	PE	50	VIMC6	CD5	PE	10	UCHT2
CD68	PE	10	REA886	TNF α	PE	10	REA656
CD138	PE	10	REA929	CD102	PE	10	REA878
CD14	PE	10	REA599	CX3CR1	PE	50	REA385
CD62L	PE	10	REA615	CD107a	PE	10	REA792

2 Materials

Specificity	Conjugate	Dilution factor	Clone	Specificity	Conjugate	Dilution factor	Clone
CD45RO	PE	10	REA611	CD197	PE	10	REA108
CD45RA	PE	10	T6D11	Vimentin	PE	10	REA409
CD27	PE	10	M-T2T1	TSPAN8	PE	10	REA443
CD28	PE	50	REA612	FoxP3	FITC	10	REA1253
LIF	PE	10	REA350	MECA79	FITC	50	MECA-79
CD24	PE	10	REA832	CD66b	FITC	10	REA306
CD10	PE	50	REA877	CD11b	FITC	10	REA713
CD105	PE	50	43A4E1	CD103	FITC	50	REA803
CD90	PE	50	DG3	CD326	FITC	50	REA764

Antibodies for flow cytometry were obtained from Miltenyi Biotec (Bergisch Gladbach, GER), with the exception of Fibronectin and Goat anti-Rab-bit IgG (H+L) which were obtained from Thermo Fisher Scientific (Waltham, US).

Table 10: Antibody conjugates used for the characterization of cellular composition via flow cytometry

Specificity	Conjugate	Clone	Dilution factor	Application
CD45	VioBlue	REA747	50	Cellular composition
CD4	VioGreen	REA623	50	
CD3	FITC	REA613	50	
CD16	PE	REA423	50	
CD56	PE	REA196	50	
CD20	PE-Vio770	REA780	50	
CD14	APC	REA599	50	
CD8	APC-Vio770	REA734	50	

Table 11: Antibody conjugates used for the characterization of transduction efficacy via flow cytometry

Specificity	Conjugate	Clone	Dilution factor	Application
CD45	VioBlue	REA747	50	Transduction efficacy
CD4	VioGreen, APC	REA623	50	
CD3	FITC	REA613	50	
CD8	APC-Vio770, PE	REA734	50	
LNGFR	PE, APC	REA844	50	
Biotin	PE	in house	50	

2 Materials

Table 12: Antibody conjugates used for the characterization of T cell activation via flow cytometry

Specificity	Conjugate	Clone	Dilution factor	Application
CD45	VioBlue	REA747	50	
CD4	VioGreen	REA623	50	
CD8	APC-Vio770	REA734	50	
LNGFR	PE	REA844	50	<i>Ex vivo and in vitro</i> T cell activation
EpCAM	FITC	REA764	50	
CD25	PE-Vio770	REA570	50	
CD137	APC	REA765	50	
CD69	VioBlue	REA824	50	<i>In vitro</i> T cell activation

Table 13: Antibody conjugates used for immunohistochemistry

Specificity	Conjugate	Clone	Dilution factor	Application
CD4	APC	REA623	50	
CD8	PE	REA734	50	
LNGFR	PE, APC	REA844	50	
EpCAM	FITC	REA764	50	
Fibronectin	/	PA5-29578	200	Immunohistochemistry
CD31	PE	REA730	50	
LAP	APC	REA1214	50	
REA Isotype control	PE, APC, FITC	REA293	50	
Goat anti-Rabbit IgG (H+L)	Alexa Fluor Plus 488	A32731	200	

Table 14: Antibody conjugates used for the characterization of T cell exhaustion via flow cytometry

Specificity	Conjugate	Clone	Dilution factor	Application
CD45	VioBlue	REA747	50	
CD4	VioGreen	REA623	50	
CD8	APC-Vio770	REA734	50	
LNGFR	PE	REA844	50	<i>Ex vivo</i> T cell exhaustion
LAG3	FITC	REA351	50	
PD-1	PE-Vio770	REA1165	50	
TIM3	APC	REA635	50	

2.1.7 Consumables

Table 15: Consumables

Item	Supplier
Disposable PD-10 Desalting Column	GE Healthcare, Chicago, US
T75 culture flask	Corning, New York, US
T175 culture flask	Corning, New York, US
CellSTACK® Culture Chambers (CF2 or CF5)	Corning, New York, US
Filter unit 0.45 µm	Merck Millipore, Burlington, US
96-well U-bottom plate	Corning, New York, US
96-well flat-bottom plate	Corning, New York, US
24-well plate	Corning, New York, US
50 mL flacon tube	Corning, New York, US
LS-column	Miltenyi Biotec, Bergisch Gladbach, GER
Tubing set TS520	Miltenyi Biotec, Bergisch Gladbach, GER
CliniMACS® CD4 and CD8 reagent	Miltenyi Biotec, Bergisch Gladbach, GER
Transfer bag 20 mL	Miltenyi Biotec, Bergisch Gladbach, GER
Cryo vial 1.5 mL	Thermo Fisher Scientific, Waltham, US
Transferbag 600 mL	TERUMO CORPORATION, Tokyo, JPN
CryoMACS® Freezing Bag 500	Miltenyi Biotec, Bergisch Gladbach, GER
Syringe 50/5 mL	Becton Dickinson, New Jersey, US
6-well plate	Corning, New York, US
HTS Transwell-96 Permeable Support	Merck, Darmstadt, GER
SMUC IVIC CAGE	TECNIPLAST, Hohenpeißenberg, GER
Syringe BD Micro-Fine™+ 29G for s.c.	Becton Dickinson New Jersey, US
Syringe BD Plastipak 27G for i.v.	Becton Dickinson New Jersey, US
Heparin coated capillary tubes	Roche, Basel, CHE
Microvette EDTA coated	Sarstedt, Nürnbrecht, GER
gentleMACS™ C Tubes	Miltenyi Biotec, Bergisch Gladbach, GER
30 µm cell strainer	Miltenyi Biotec, Bergisch Gladbach, GER
Glass slide 24-well format	Zell-Kontakt, Nörten-Hardenberg, GER
24-well no-bottom plate	Zell-Kontakt, Nörten-Hardenberg, GER
96-well U-bottom plate	LVL technologies, Crailsheim, GER

Item	Supplier
MACSPlex filter plate	Miltenyi Biotec, Bergisch Gladbach, GER
Microcentrifuge tubes	STARLAB, Hamburg, GER
NALGENE Cryogenic vials	Thermo Fisher Scientific, Waltham, US

2.1.8 Instruments

Table 16: Devices

Device	Name	Supplier
Thermomixer	Eppendorf ThermoMixer® C	Eppendorf, Hamburg, GER
Incubator	Brutschrank IN75	Memmert, Schwabach, GER
Centrifuge	Centrifuge 5424 R	Eppendorf, Hamburg, GER
Centrifuge	Multifuge X3R	Heraeus Instruments, Hanau, GER
Incubator	ISF1-X	Adolf Kühner, Birsfelden, CHE
Incubator mammalian	HERACELL 240i	Thermo Fisher Scientific, Waltham, US
Photometer	NanoDrop ND-1000 Spectrophotometer	Thermo Fisher Scientific, Waltham, US
Hematology analyzer	Sysmex XP-300	Sysmex Deutschland, Norderstedt, GER
Cultivation device	CliniMACS Prodigy™	Miltenyi Biotec, Bergisch Gladbach, GER
Flow cytometer	MACSQuant® Analyzer 10	Miltenyi Biotec, Bergisch Gladbach, GER
Flow cytometer	MACSQuant® X	Miltenyi Biotec, Bergisch Gladbach, GER
Cell container	Mr. Frosty™	Thermo Fisher Scientific, Waltham, US
Water bath	SW22 Shaking water bath	JULABO, Seelbach, GER
Welding device	TSCD II	TERUMO CORPORATION, Tokyo, JPN
Plasma extractor	Plasma extractor	TERUMO CORPORATION, Tokyo, JPN
Control rate freezer	Consarctic BV-40	Consarctic, Westerngrund, GER
Microscope	Incucyte® S3 system	Sartorius, Göttingen, GER
<i>In vivo</i> imaging system	IVIS Lumina III imaging system	Perkin Elmer, Waltham, US
Tissue dissociator	gentleMACS™ Octo Dissociator	Miltenyi Biotec, Bergisch Gladbach, GER
Cryostat	CM3050 S cryostat	Leica, Chicago, US
Microscope	EVOS M5000	Thermo Fisher Scientific, Waltham, US

2 Materials

Device	Name	Supplier
Liquid handling system	TECAN liquid handling platform	TECAN Group, Männedorf, GER
Microscope	IN Cell Analyzer 2000	GE, Boston, US
Sterile hood	Cell culture hood, Hera Safe KS	Thermo Fisher Scientific, Waltham, US

2.1.9 Software

Table 17. Software

Software	Supplier
Flowlogic 8.4	Inivai Technologies Pty.Ltd., Mentone Victoria, AUS
MACSQuantify™ 2.13.0	Miltenyi Biotec, Bergisch Gladbach, GER
ImageJ 1.53e	National Institutes of Health, Bethesda, US

3. Methods

3.1 Molecular biology methods

3.1.1 Transformation of *E. coli* with plasmid DNA

Plasmids were transformed into *E. coli* DH5 α (New England Biolabs, Ipswich, US) according to manufacturer's instructions. The cells were thawed on ice and gently mixed with up to 100 ng plasmid DNA and incubated for 30 min on ice. Subsequently, a heat shock at 42 °C was performed for 30 sec, followed by 2 min incubation on ice. Next, 250 μ L pre-warmed SOC medium were added and cells were incubated at 37 °C for 45 min under constant shaking. Finally, 10 – 50 μ L cell suspension were plated on LB agar plates supplemented with antibiotics depending on the used resistance gene.

3.1.2 Cultivation of *E. coli* and isolation of plasmid DNA

E. coli DH5 α were transformed as described under 3.1.1. Next day, 5 mL of LB medium containing the required antibiotics were inoculated with a single colony of bacteria. The culture was incubated overnight at 37 °C and 220 rpm. Subsequently, the suspension was used for mini plasmid purification using the NucleoSpin Plasmid (NoLid) Mini kit. For preparation of larger amounts of plasmid DNA either 50 mL LB-medium (midi preparation) or 100 mL LB-medium (maxi preparation) were incubated over night at 37 °C and 220 rpm. For midi preparations the ZymoPURE II Plasmid Midiprep Kit and for maxi preparations the NucleoBond Xtra Maxi EF was used according to manufacturer's instructions.

3.1.3 Biochemical modification of immunoglobulins

First, IgGs were re-buffered in 0.1 M NaHCO₃ using a PD-10 column according to manufacturer's instructions. Protein concentration was determined by measuring the absorbance at 280 nm with the NanoDrop ND-1000 Spectro-photometer. Next, a 5 mM biotin solution was prepared in DMSO. Under constant steering the previously re-buffered antibody solution was mixed drop wise with a three-fold molar excess of biotin. The reaction mixture was incubated at RT for 1 h under constant steering. Afterwards, the reaction mixture was applied to a PD-10 column and re-buffered in PBS. Protein concentration was determined by measuring the absorbance at 280 nm with the NanoDrop ND-1000 Spectro-photometer. The degree of labeling was analyzed via LC-MS analysis at our inhouse core facility. Two different IgG₁ molecules specific for latent TGF- β (aLAP) recognizing the same epitope were used for adapter conjugation: (1) CH6-17E5.1 and (2) REA 1214. REA1214 based adapters were used for *in vivo* studies.

3.2 Cell culture methods

3.2.1 Cell lines and culture conditions

Human embryonic kidney cells 293T (HEK293T) was cultured in DMEM high glucose w/- L-glutamine supplemented with 10 % fetal bovine serum (FBS). HEK293T were cultivated in T75 or T175 flasks and subcultured twice a week at a ratio of 1:10. In order to subculture adherent cell lines the culture medium was removed and the cells were washed with PBS. Cells were detached by adding 1 mL accutase and incubated for 5 min at 37 °C. Next, 10 mL culture medium was added. Finally, the desired volume of detached cells was transferred into a new culture flask.

AsPC-1 cells expressing GFP and firefly luciferase (AsPC-1 WT) were used to generate AsPC-1 cells constitutively secreting latent TGF- β (AsPC-1-TGF). AsPC-1 WT and AsPC-1-TGF were cultured in RPMI 1640 supplemented with 2 mM L-glutamine and 10 % FBS. Both cell types were subcultured as described for HEK293T cells. SupT1 cells were cultivated in RPMI 1640 supplemented with 2 mM L-glutamine and 10 % FBS. SupT1 cells were subcultured twice a week at a ratio of 1:10. All cell lines and primary human cells were cultured at 37 °C, 5 % CO₂ and at constant humidity.

3.2.2 Lentiviral vector production

Lentiviral vectors (LVVs) pseudotyped with vesicular stomatitis virus glycoprotein (VSV-G) were produced in HEK293T via transient transfection using the polymeric cation PEI. Depending on the amount of LVV needed the production was done in T175 flasks or in Corning® CellSTACK® Culture Chambers with either two chambers (CF2) or five chambers (CF5). According to the production size HEK293T were seeded three days before transfection into the appropriate culture flask (Table 18). At the day of transfection cells should have reached a confluency of 70 – 90 %.

Table 18: Cell number and volume for transient transfection of HEK293T cells

Culture flask	T175	CF2	CF5
cell number [-]	4.5x10 ⁶	3x10 ⁷	7.4x10 ⁷
volume of culture medium [mL]	20	200	500

A fresh aliquot of PEI and the plasmid DNA were thawed and both solutions were vortexed for at least 1 min. Next, the DNA solution (Table 19) containing 51 % transfer plasmid (encoding the gene of interest), 10 % pMDG and 39 % pCMVdR8.74 as well as the PEI solution (Table 20) were prepared.

3 Methods

Table 19: Composition of the DNA solution for transient transfection of HEK293T cells

	T175	CF2	CF5
total DNA [μg]	35.1	252.4	631.8
volume DMEM [μL]	3464.9	24747.6	62368.2
total volume [μL]	3500	25000	63000

Table 20: Composition of the PEI solution for transient transfection of HEK293T cells

	T175	CF2	CF5
volume PEI (1 mg/mL) [μL]	140	1000	2500
volume DMEM [μL]	3360	24000	60500
total volume [μL]	3500	25000	63000

Both solutions were vortexed for at least 1 min and mixed, resulting in a DNA:PEI ratio of 1:4. The solution was incubated for 20 min at RT. Next, the culture medium was removed completely and replaced with DMEM either mixed with the DNA-PEI solution (CF2 and CF5) or with DMEM w/o additives (T175 flask) (Table 21). For T175 flasks the DNA-PEI solution was added to the cells dropwise afterwards.

Table 21: Volume of DMEM w/o additives added for transient transfection of HEK293T cells

	T175	CF2	CF5
volume DMEM [mL]	18	130	324

Afterwards, the cells were incubated at 37 °C for 4 – 6 h. Next, FBS was added in the same way as described for the PEI:DNA solution (Table 22).

Table 22: Volume of FCS added for transient transfection of HEK293T cells

	T175	CF2	CF5
volume FCS [mL]	2.5	20	50

The cells were supplemented with sodium butyrate in the same way as described for the PEI:DNA solution to enhance the production after 24 h of incubation (Table 23).

Table 23: Volume of sodium butyrate added for transient transfection of HEK293T cells

	T175	CF2	CF5
volume NaButyrat 500mM [mL]	0.52	4	10

After 24 h the supernatant containing the LVVs was harvested and centrifuged at 300 g to remove cell debris. Next, the supernatant was filtered through a 0.45 μm filter. Subsequently, the LVVs were concentrated via centrifugation at 4000 g at 4°C for 24 h. Finally, the supernatant was discarded and the LVVs were resuspended in ice-cold TexMACS™ medium to achieve a 100-fold concentration of LVVs. The LVVs were stored at -80 °C.

3.2.3 Titration of lentiviral vectors

The titer of LVVs was determined by transducing SupT1 with serial diluted LVVs. Therefore, 2×10^5 SupT1 were seeded in a 96-well U-bottom plate in 150 μL RPMI 1640 plus 2 mM L-glutamine. Next, 50 μL serial diluted LVVs were added to the cells. After 24 h the cells were fed with 90 μL RPMI 1640 supplemented with 2 mM L-glutamine and 10 % FBS. After 96 h, the titer of LVVs was calculated based on the transduction efficacy on SupT1 analyzed by flow cytometry and the corresponding volume of added LVVs. The result was given in units per volume (TU/mL).

3.2.4 Lentiviral transduction of cell lines

5×10^4 AsPC-1 WT per well were seeded in a 24-well plate in 1 mL RPMI 1640 supplemented with 2 mM L-glutamine and 10 % FBS. After 24 h the medium was removed completely and replaced with 1 mL RPMI 1640 and the according amount of LVVs. After 6 h 1 mL RPMI 1640 supplemented with 2 mM L-glutamine and 20% FBS was added to the cells. After three days the culture medium was removed completely and the cells were cultured as described in 3.2.1.

3.2.5 Isolation of human peripheral blood mononuclear cells

Anticoagulated blood samples (buffy coats) from healthy donors were obtained from *DRK Dortmund* after informed consent (Dortmund, GER). For isolation of peripheral blood mononuclear cells (PBMCs) 25 mL buffy coat were transferred to a 50 mL falcon tube and diluted with 10 mL CliniMACS® PBS/EDTA buffer plus 0.5 % MACS® BSA (PEB). The diluted buffy coats were layered on top of 15 mL Pancoll. The blood components were separated by density gradient centrifugation at 445 g for 35 min in a swing bucket rotor (acc:5, br:4). Due to their density, the PBMCs formed a layer between the erythrocytes and the plasma. The PBMCs were collected carefully by pipetting and washed. Therefore, the lymphocytes were resuspended in 50 mL PEB and centrifuged at 300 g for 15 min in a swinging bucket rotor. Next, the supernatant was discarded carefully and the sedimented cells were washed a second time as described previously. After a centrifugation at 200 g for 10 min the cells were resuspended in 10 mL PEB and the white blood cell (WBC) count was determined using the Sysmex XP-300. PBMC isolation for *in vivo* studies was kindly supported by Carolin Kolbe.

3.2.6 Isolation of primary human T cells

Primary human T cells were isolated with the Pan T cell isolation kit according to manufacturer's instructions. In brief, PBMCs isolated as described in 3.2.5 were resuspended in 40 μL PEB per 1×10^7 WBCs. Next, 10 μL of Pan T Cell Biotin-Antibody cocktail per 1×10^7 cells were added and the cell suspension was incubated for 5 min at 4 °C. Next, 30 μL PEB and 20 μL of Pan T Cell Microbead cocktail per 1×10^7 cells were added followed by an incubation for 5 min at 4 °C. T cells were isolated via a LS column. The column was washed twice with 3 mL PEB before the cells were applied. As this was an untouched T cell isolation the flowthrough was collected. The isolated cells were washed twice in TexMACS™ medium followed by a centrifugation at 300 g for 10 min. The pellet was resuspended in 10 mL TexMACS™ medium and the cell count was determined using the Sysmex XP-300.

3.2.7 Lentiviral transduction of primary human T cells

First, 2×10^6 T cells were seeded in a 24-well plate in 2 mL culture medium containing TexMACS™ medium supplemented with 12.5 ng/mL recombinant human IL-7 and 12.5 ng/mL recombinant human IL-15. T cells were activated with TransAct™ (diluted 1:100). After 24 h, the desired volume of LVVs corresponding to a multiplicity of integration (MOI) of five was added and the cells were resuspended. After three days, the culture medium was removed completely and replaced by fresh culture medium. T cells were passaged at a ratio of 1:2 every two days from day three on. T cells were expanded for at least ten days before they were used in functional assays.

3.2.8 Enrichment of transduced primary human T cells

Transduced T cells were enriched using truncated CD271 co-expressed with the CAR. Therefore, transduced T cells were enriched using the MACSelect™ LNGFR system according to manufacturer's instructions five to seven days after transduction. In brief, T cells were centrifuged at 300 g for 10 min and resuspended in 60 μL PEB and 20 μL CD271 microbeads per 1×10^7 cells. After an incubation time of 15 min at 4 °C the cells were washed in 2 mL PEB and centrifuged at 300 g for 10 min. The labeled T cells were resuspended in 500 μL PEB and magnetically separated via a LS column including two washing steps with 3 mL PEB. The positive fraction containing CD271⁺ T cells was eluted in absence of the magnetic field by adding 5 mL TexMACS™ medium onto the column and gently applying the plunger. Enriched T cells were washed twice in TexMACS™ medium and seeded as described previously (3.2.7). On day 10, the cellular product was characterized via flow cytometry as described in 3.2.12. Transduction efficacy and enrichment of CAR T cells was analyzed using the transduction efficacy panel (Table 11). Transduction efficacy of CD66c-specific CAR T cells was determined via staining of the transduction marker LNGFR. Transduction of biotin-specific AdCAR T cells was quantified using a biotinylated

PE conjugate. The transduction efficacy was defined as frequency of viable T cells expressing the transduction marker or the AdCAR.

3.2.9 Automated isolation, transduction and cultivation of human T cells

CAR T cells for *in vivo* studies were manufactured with the CliniMACS Prodigy™ using the TCT process version 8.4 and a single use tubing set TS520. As culture medium TexMACS™ GMP Medium supplemented with 12.5 ng/mL MACS® GMP Recombinant Human IL-7 and 12.5ng/mL MACS® GMP Recombinant Human IL-15 was used. For the priming of the tubing set and magnetic enrichment CliniMACS® PBS/EDTA supplemented with 0.5 % human serum albumin was used. The process of T cell isolation, transduction and cultivation was fully automated and was done according to manufacturer's instructions with the recommended activity matrix (Table 24). First, the LP was thawed as described in 3.2.11 and sterile welded onto the primed tubing set. Next, T cells were magnetically enriched using CliniMACS® CD4 and CliniMACS® CD8 reagents. The cellular composition and T cell concentration were analyzed by flow cytometry using the cellular composition panel (Table 10) in combination with the cellular composition express mode. Next, 1×10^8 T cells were seeded into the heated culture chamber and were activated in culture medium supplemented with MACS® GMP T Cell TransAct™. After 24 h a 20 mL transfer bag containing LVVs diluted in 10 mL culture medium was sterile welded to the tubing set to transduce T cells at an MOI of ten. On day three the cells were washed and continuously expanded until day ten. On day six transduction efficacy was analyzed via flow cytometry using the transduction efficacy panel (Table 11). On day 10, the cells were automatically harvested in TexMACS™ GMP Medium. Cell number and transduction efficacy were determined via flow cytometry using the transduction efficacy panel (Table 11).

Table 24: Activity matrix of the TCT process

Day	Activity	Volume [mL]
-1	Medium preparation and tubing set installation	/
0	CD4/CD8 enrichment	/
0	Seeding of T cells and shaker type 1	70
1	Transduction	100
3	Culture wash and shaker type 2	200
5	Media exchange	±50 (total:200)
6	Media exchange and shaker type 3	±130 (total:200)
7	Media exchange	±130 (total:200)
8	2x Media exchange	±130 (total:200)
9	Media exchange	±130 (total:200)
10	Harvest	/

3.2.10 Cryopreservation and thawing of cell lines

Cells were harvested and centrifuged at 300 g for 10 min. The cells were adjusted to a final concentration of 1×10^7 cells/mL in freezing solution containing 10 % DMSO and 90 % FBS. In total 1 mL cell suspension was transferred to cryovials and immediately placed in a Mr. Frosty™ pre-cooled at 4 °C. After 24 h at -80 °C the cells were transferred into liquid nitrogen for long term storage.

Cells were thawed in a SW22 Shaking water bath at 37 °C until the frozen sample was nearly completely melted. Subsequently, the cell suspension was transferred into 10 mL of the cell line specific culture medium. The cells were centrifuged at 300 g for 10 min and resuspended in culture medium. Finally, the cells were seeded as described in 3.2.1.

3.2.11 Cryopreservation and thawing of leukaphereses

Unstimulated leukaphereses (LPs) of healthy donors were obtained from “*Institut für klinische Transfusionsmedizin und Immunogenetik Ulm*”. The LPs were transferred into a 600 mL transfer bag. The final volume in the transfer bag was adjusted to 600 mL with CliniMACS® Formulation Solution. Next, the transfer bag was sterilely welded to a second transfer bag and centrifuged at 200 g for 15 min (br:0). Afterwards the plasma was removed using the Plasma extractor. Next, the cells were diluted in 100 mL ice-cold CliniMACS® Formulation Solution and 100 µL of the diluted cells were used to determine cell concentration and cellular composition via flow

cytometry using the cellular composition panel (Table 10). In total 1×10^9 cells were transferred into a CryoMACS® Freezing Bag 500 and the final volume was adjusted to 60 mL with Clin-iMACS® Formulation Solution. Subsequently, 30 mL ice-cold Cryo Supplement 3x was added to reach a final volume of 90 mL. The remaining air was removed using a sterile syringe and the bag was closed by sterile welding. Cells were frozen with the Consarctic BV-40 using the in house developed freezing program CP11. The cells were transferred into liquid nitrogen for long term storage after finishing the freezing program.

Cells were thawed in a SW22 Shaking water bath at 37 °C. Next, the cell suspension was transferred into a 600 mL transfer bag prepared with 180 mL TexMACS™ medium. Diluted cells were further used for automated isolation, transduction and cultivation of primary human T cells.

3.2.12 Immunofluorescent staining and flow cytometry

Cells were harvested and up to 5×10^5 cells were transferred in a 96-well U-bottom plate. After centrifugation at 300 g for 10 min the cells were washed with 200 μ L PEB. Next, antibody conjugates diluted in 50 μ L PEB were added according to manufacturer's instructions. For the analysis of cell viability either 7-AAD or PI was used according to manufacturer's instructions. The staining was performed at 4 °C for 10 min. Afterwards, the cells were washed in 150 μ L PEB and centrifuged at 300 g for 10 min. Finally, the cell pellet was resuspended in up to 200 μ L PEB.

Samples were analyzed either on a MACSQuant® Analyzer 10 or MACSQuant® X. In both devices three laser lines (405 nm, 488 nm and 640 nm) and ten emission detectors were available. Before the samples were acquired the machines were calibrated using MACSQuant® calibration beads. Data analysis was done with Flowlogic 8.4 or MACSQuantify™ 2.13.0. In general the target cell population was identified in the forward (FCS) and sideward scatter (SSC) and dead cells (7AAD or PI negative) were excluded. Subsequent gates were defined based on either negative controls or fluorescent minus one (FMOs) controls.

3.3 Functional analysis of AdCAR T cells

3.3.1 Co-culture of AdCAR T cells with soluble antigens

As soluble target molecules either recombinant human LAP (hLAP) or AsPC-1-TGF tumor cell-derived latent TGF- β was used. The hLAP was reconstituted according to manufacturer's instructions and stored at -20 °C. Tumor-derived latent TGF- β was obtained from the supernatant of AsPC-1-TGF. Therefore, the supernatant was centrifuged at 300 g for 10 min to remove the cell debris. Concentration of latent TGF- β was determined via ELISA and supernatant was stored at -20 °C or used freshly. AdCAR1 T cells were prepared as described in 3.2.7. T cells were harvested and resuspended in TexMACS™ medium and 5×10^4 LNGFR⁺ cells in 50 μ L were seeded

in a 96-well flat bottom plate. The concentration of hLAP and tumor-derived latent TGF- β was adjusted in TexMACS™ medium or if no concentration is indicated 50 μ L of tumor cell-derived supernatant were used. Afterwards, 50 μ L of the prepared antigen solution were added to the T cells. Next, all adapter molecules were adjusted to the desired concentration in TexMACS™ medium and subsequently 50 μ L of the prepared adapter solution were added. TexMACS™ medium was added to reach a final volume of 200 μ L. Cells were incubated for 24 h at 37 °C. Afterwards, the cells were centrifuged at 300 g for 10 min. Next, the supernatant was removed for cytokine analysis (3.3.2) and cells were analyzed via flow cytometry as described in 3.2.12 using the T cell activation panel (Table 12).

3.3.2 Analysis of cytokines

Cytokine secretion of T cells either after *in vitro* or *in vivo* co-culture was analyzed by MACSPlex Cytokine 12 Kit according to manufacturer's instructions. Supernatants of *in vitro* assays were used undiluted whereas serum samples of *in vivo* studies were diluted 1:8 in MACSQuant® Running Buffer. Concentration of latent TGF- β was determined via ELISA according to manufacturer's instructions. To determine latent TGF- β concentration in supernatant of tumor cell lines *in vitro*, cells were cultured in 6-well plates until they reached confluence. Supernatants of AsPC-1-TGF were serial diluted up to 10,000-fold whereas all other supernatants were used undiluted. Serum samples from *in vivo* studies were diluted 1:16 to 1:100.

3.3.3 AdCAR T cell reporter assay

AdCAR T cells were prepared as described in 3.2.7. Primary human T cells were co-transduced with LVVs encoding AdCAR1 at an MOI of ten and 50 μ L LVV encoding the pGF-NFAT reporter construct. The co-culture was prepared as described in 3.3.1. In brief, AdCAR T cells were co-cultured with 125 ng/mL hLAP and 10 ng/mL aLAP for 90 h. The expression of GFP was analyzed by live cell imaging using the Incucyte® S3 system. Total integrated GFP intensity was normalized to start values.

3.3.4 Transwell assay

Transwell assay was performed in HTS Transwell-96 Permeable Support with 0.4 μ m pore size. AsPC-1-TGF were harvested as described in 3.2.1 and 2×10^4 cells were seeded to the lower chamber of the transwell plate and cultured for 24 h. The culture medium was removed and replaced with 160 μ L TexMACS™ medium 24 h later. Next, 5×10^4 LNGFR⁺ cells were re-suspended in 75 μ L TexMACS™ medium and were added to the desired transwell chamber. Adapters were diluted in TexMACS™ medium and 75 μ L were added to the lower transwell chamber to reach a final adapter concentration of 100 ng/mL. Wells were filled with TexMACS™ medium

to a final volume of 310 μ L. After 24 h of incubation at 37 °C the supernatant was removed for cytokine analysis (3.3.2) and cells were analyzed via flow cytometry as described in 3.2.12 using the T cell activation panel (Table 12).

3.3.5 *In vitro* cytotoxicity assay

Primary human T cells were transduced (3.2.7) to express AdCAR1 or AdCAR2. AsPC-1 WT and AsPC-1-TGF were seeded in a 96-well flat bottom plate. After 24 h the medium was removed and 2.5×10^4 CAR positive T cells in 50 μ L TexMACS™ medium were added. The indicated adapters were diluted in TexMACS™ medium and 50 μ L of the adapter solution were added. All wells were filled up to 200 μ L with TexMACS™ medium. The cells were incubated at 37°C and the cytotoxicity was measured by live cell imaging using the Incucyte® S3 system. The acquisition time for the brightfield and the fluorescent imaging channel was set to 300 ms. Fluorescent intensity of GFP⁺ target cells was analyzed every two 2 h using the standard scan type. At each time point four pictures per well were taken. The quantification of GFP⁺ target cells was done using the Incucyte® S3 system analysis software. The analysis mask was trained to differentiate between GFP⁺ target cells and GFP⁻ cells by using in total six representative pictures at different time points. Top-Hat segmentation (radius:100 μ m) and a threshold (GCU) of 1 were used for the analysis. The area of the wells covered by GFP⁺ target cells was used as a metric for cytotoxicity. All values were normalized to the start values.

3.4 *In vivo* studies

All *in vivo* studies were performed according to the European and German guidelines for the care and use of laboratory animals. All experiments were approved by the ethical committee on animal care and use in North Rhine-Westphalia (approval numbers: 81-02.04.2018.A096, 81-02.04.2020.A255, 84-02.04.2017.A021). The data acquisition was kindly supported by Dr. Dominik Lock, Dr. Nicole Cordes, Simon Lennartz and Karin Teppert.

3.4.1 Animal models

In this work four to six weeks old female immunodeficient NOD.Cg-Prkdc^{scid} Il2rg^{tm1Wjl}/SzJ (NSG) mice (Charles River Laboratories, Wilmington, US) were used. Upon arrival animals were kept in IVIC SMUC cages in groups of up to six animals per cage for two weeks in order to adapt to the housing conditions before any experiments were performed. The wellbeing of all animals was monitored regularly as it was described in the individual approved permit.

3.4.2 Tumor cell inoculation

Tumor cells, e.g. AsPC-1 WT or AsPC-1-TGF were detached as described in 3.2.1 and 1×10^6 – 1×10^7 cells per 100 μ L were resuspended in PBS. The cells were kept on ice until injection. Before injection the mice were anesthetized by the inhalation of 2.0 % (v/v) isoflurane (Zoetis Schweiz, Zuerich, CHE). The right flank of the animals was shaved and 100 μ L of tumor cell suspension were subcutaneously (s.c.) injected. Tumors were engrafted for eight to nine days to form a palpable tumor mass. Tumor growth was monitored regularly by bioluminescent imaging (BLI). Mice were randomized two days before T cell injection according to the BLI measurement to achieve a homogenous distribution of tumor burden across the cohorts.

3.4.3 Injection of T cells

T cells were harvested as described in 3.2.9. T cells were resuspended in PBS at the desired concentration and kept on ice until injection. The number of total T cells injected was kept constant among all cohorts and was adjusted with untransduced T cells. If necessary T cells were co-injected with autologous PBMCs. Therefore, PBMCs were isolated as described in 3.2.5 and mixed with AdCAR T cells. The cells were kept on ice until injection. Human immune cells were injected intravenously (i.v.) in a volume of 100 μ L into the tail vein.

3.4.4 Injection of adapter molecules and immunoglobulins

Biotinylated adapter molecules were prepared as described in 3.1.3. Adapters were thawed and the concentration was adjusted to the indicated concentrations in PBS. IVIG (Takeda, Tokyo, JPN) was dissolved according to manufacturer's instructions. The final concentration was adjusted to 108.7 mg/mL. The solution was stored at -80 °C. Prior to injection IVIG was thawed and diluted in PBS to reach a final concentration of 100 mg/mL. Both IVIG and adapter molecules were injected intraperitoneally (i.p.) in a volume of 100 μ L. Mice were injected with adapter and IVIG one day before T cell injection and were re-injected twice a week as not mentioned different.

3.4.5 Bioluminescent *in vivo* imaging of tumor cells

D-Luciferin potassium was dissolved in PBS to reach a final concentration of 30 mg/mL. Mice were i.p. injected with 100 μ L D-Luciferin potassium salt. Images were acquired 10 min after injection using the IVIS Lumina III imaging system. Aperture and exposure time were adjusted automatically by the device. The bioluminescent signaling was quantified within the manually drawn region of interest covering the whole body of the animal. BLI was expressed as photons per second per cm^2 per steradian. The animals were anesthetized during the measurement as previously described in 3.4.2.

3.4.6 Preparation of blood plasma

Blood sampling was done by a puncture of the *vena facialis*. Blood was immediately collected in heparin coated capillary tubes (Roche, Basel, CHE). The blood was transferred into an EDTA containing microvette. The samples were centrifuged at 13000 rpm for 15 min at 4 °C to separate the plasma from cells. The supernatant was collected and stored at -20 °C.

3.4.7 Preparation of blood for *ex vivo* analysis

Blood was collected and separated from plasma as described in 3.4.6. The remaining cell pellet was resuspended in 1 mL red blood cell lysis buffer according to manufacturer's recommendation. After 5 min of incubation cells were centrifuged at 300 g and subsequently resuspended in 100 µL PEB. Cells were analyzed via flow cytometry using the T cell activation and the T cell exhaustion panel (Table 12 and Table 14).

3.4.8 Preparation of spleens for *ex vivo* analysis

Spleens were transferred into gentleMACS™ C Tubes filled with 3 mL autoMACS® Running Solution supplemented with 0.5 % BSA. Spleens were dissociated using the gentleMACS™ Octo Dissociator with the predefined program: m_spleen_01. The cell suspension was filtered with a 30 µm cell strainer. The red blood cell lysis was done as described in 3.4.7. The cells were finally resuspended in 1 mL PEB. Cells were analyzed via flow cytometry using the T cell activation panel, the T cell exhaustion panel and cellular composition panel (Table 10, Table 12, Table 14).

3.4.9 Preparation of tumors for *ex vivo* analysis

Tumors were dissociated using the Tumor Dissociation Kit human according to manufacturer's instructions. Tumors were dissociated using the gentleMACS™ Octo Dissociator with heater. The predefined program 37C_h_TDK_2 was used. The cell suspension was further processed as described in 3.4.8. Cells were analyzed via flow cytometry using the T cell activation panel, the T cell exhaustion panel and cellular composition panel (Table 10, Table 12, Table 14).

3.4.10 Preparation of tumors for immunohistochemistry

Tumors were isolated and embedded into OCT mounting medium. Afterwards, the tumors were frozen at -80 °C. Tissue slices with a thickness of 8 µm were cut on a CM3050 S cryostat and stored on object carriers at -80 °C for further processing. After thawing, the tissue slices were washed once with PBS and fixed with Inside Fix for 10 min. Next, the slices were washed twice with PBS and afterwards incubated with permeabilization solution for 10 min. All antibodies used for immunohistochemistry (Table 13) were diluted in antibody staining solution

according to manufacturer's instructions. Nuclei were stained with DAPI diluted 1:4000 (stock concentration: 10 µmg/mL). DAPI was added to the tissue slices together with the diluted antibody conjugates. Tissue slices were stained overnight at 4 °C. Prior to image acquisition the slices were washed three times with PBS. Finally coverslips were mounted with aqueous mounting medium. Images were acquired using the EVOS M5000 and analyzed with ImageJ 1.53e.

3.4.11 Cyclic fluorescent imaging of human tumor tissue

The ovarian cancer tissue was obtained from the Department of Obstetrics and Gynecology at the University Hospital of Cologne. The tissue was embedded in OCT mounting medium and frozen in liquid nitrogen. Tissue sections were prepared as described in 3.4.10. Tissue slices were mounted on a glass slide and fixed in -20 °C cold acetone for 20 min. Afterwards, the glass slide was glued to a 24-well no-bottom plate. Antibody fluorochrome conjugates (Table 9) were diluted in autoMACS® Running Solution and FcR blocking reagent according to the manufacturer's instructions. The different antibody conjugates were pipetted separately in a 96-well U-bottom plate. In addition, every 4th well of the 96-well plate contained Hoechst diluted 1:100 for nuclei staining. Per tissue section, 300 µL of the staining cocktail were prepared. The cyclic fluorescent imaging was done on a TECAN liquid handling platform in combination with an IN Cell Analyzer 2000. The device was handled and maintained by our in house core facility. The staining procedure was done automatically (**Figure 6**) except for the first step (Table 25). The images were taken at 20x magnification. Cyclic fluorescent imaging was kindly supported by Elvira Criado-Moronati and Andre Gosselink. Elvira supported during sample preparation as well as during preparation of the antibody staining cocktail. Andre developed the algorithm to calculate the Pearson correlation coefficient of final images. The acquired images were processed by the core facility using an in house developed workflow containing dark-frame subtraction, flat field correction and aligning the individual pictures based on the nuclei staining. Further image analysis was done with ImageJ 1.53e.

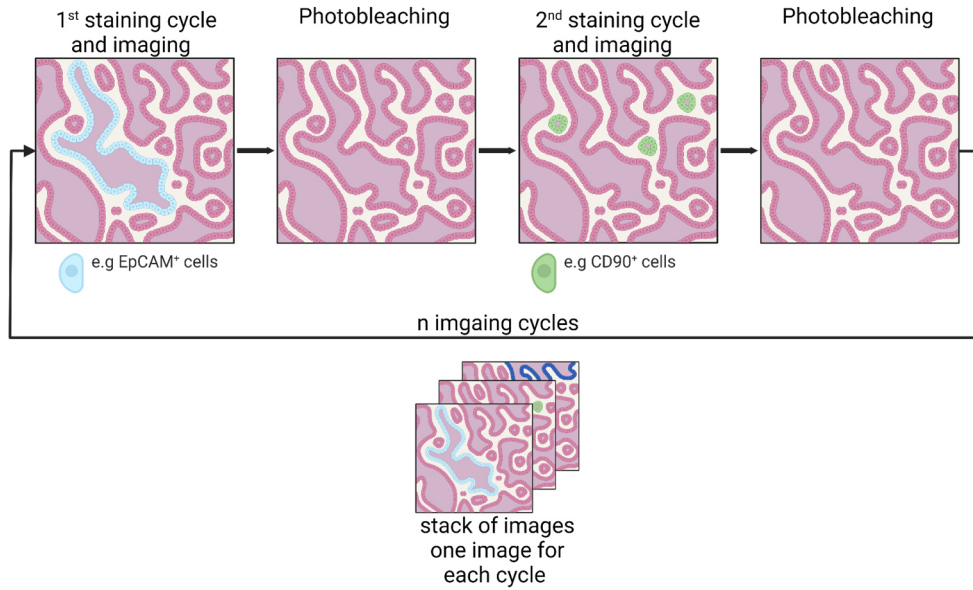


Figure 6: Illustration of the cyclic fluorescent imaging method.

Tumor tissue specimens are stained with an antibody fluorophore conjugate, e.g. an EpCAM specific antibody. Subsequently, a microscopic-image is acquired. Next, the fluorophore is bleached to prepare the tissue for the next cycle, e.g. with a CD90 specific fluorophore conjugate. This cycle can be repeated n-times, depending on the number of markers that are analyzed on the same tissue section. Adapted from Kinkhabwala, A., Herbel, C., Pankratz, J. et al. MACSima imaging cyclic staining (MICS) technology reveals combinatorial target pairs for CAR T cell treatment of solid tumors. *Sci Rep* (2022). Illustration created with BioRender.com.

Table 25: Cycles of cyclic fluorescent imaging.

Step-number	Task
1	region of interest selection
2	Image acquisition of autofluorescence
3	Photobleaching of autofluorescence
4	Transfer of the antibody conjugate to the tissue
5	Washing
6	10 min incubation
7	Image acquisition
8	Photobleaching of the antibody fluorophore
9	Image acquisition of remaining fluorophore signal

3.4.12 Statistical analysis

Data were analyzed with GraphPad Prism 8.1.2 software (GraphPad, USA). The method used for statistical data analysis of experimental groups, as well as the number of independent donors are mentioned in the corresponding figure legends. Correction for multiple comparisons was done by Holm-Sidak correction following ANOVA. Significance was defined by $p \leq 0.05$ ($p \leq 0.05$:*; $p \leq 0.01$:**; $p \leq 0.001$:***; $p \leq 0.0001$:****).

4. Scope

CAR T cell therapy demonstrated great potential in the treatment of hematologic tumors. However, the transferability to solid tumors is challenging. Therefore, new therapeutic CAR concepts are under investigation to improve the efficacy of CAR therapy in solid cancer, and one opportunity is to broaden the spectrum of target antigens.

Soluble molecules, either secreted by the tumor or TME-related cells, are essential to orchestrate immune evasion of solid tumors. Up to now, the majority of CARs is targeted to membrane bound antigens whereas only one example is described using the CAR to engage soluble ligands²¹⁶. A proof of concept study by Chang *et al.* demonstrated that a CAR can indeed be triggered by soluble TGF- β . The study described clustering of CARs inducing effector functions like cytokine secretion and T cell proliferation as function of soluble ligand binding. The strength of the response to soluble ligands was dependent on the ligand concentration as well as on the architecture of the CAR²¹⁶. This pioneering work demonstrated the opportunity to turn an immunosuppressive agent into a pro-inflammatory stimulus. However, targeting only soluble ligands will most likely not result in tumor eradication, therefore the co-expression of a second CAR specificity would be required. This mechanistic prerequisite would make a translation of soluble antigen sensing with CAR T cells into the clinics more complex. Moreover, targeting soluble ligands is challenging since those molecules are not tumor restricted. Thus, additional safety mechanisms have to be included to control CAR T cell responses in case of on-target off-tumor toxicities or after successful treatment.

On these grounds, the aim of this thesis is to sense soluble ligands by AdCAR T cells rather than by CAR T cells binding directly to the soluble antigen in order to improve the safety and to allow combined targeting of a soluble molecule and a TAA. Within this project, latent TGF- β , which is an immunosuppressive molecule present either ECM bound or soluble, has been evaluated as a possible target within the TME (**Figure 7**). The primary objective of this work was to prove soluble antigen sensing with AdCAR T cells by the example of latent TGF- β as a clinically relevant cue of the TME. First, the adapter-dependent activation of AdCAR T cells targeting a soluble ligand was examined *in vitro*. Furthermore, the responsiveness of AdCARs towards soluble ligands as well as the mechanistic outcome of targeting soluble antigens was characterized. Subsequently, sensing of tumor cell-secreted latent TGF- β and simultaneous targeting of CD66c as a TAA by combining different adapter molecules was studied. Finally, the concept of sensing soluble antigens with AdCAR T cells was validated *in vivo* using PDAC xenograft mouse models. The response of AdCAR T cells targeting latent TGF- β was compared to CAR T cells targeting the TAA CD66c. In addition, the anti-tumor treatment effects of targeting a TAA and a soluble antigen with two different CARs as well as the simultaneous targeting using two different adapters but only one AdCAR were examined. Finally, synergies between endogenous immune cells and AdCAR T cells were investigated in a reconstituted mouse model.

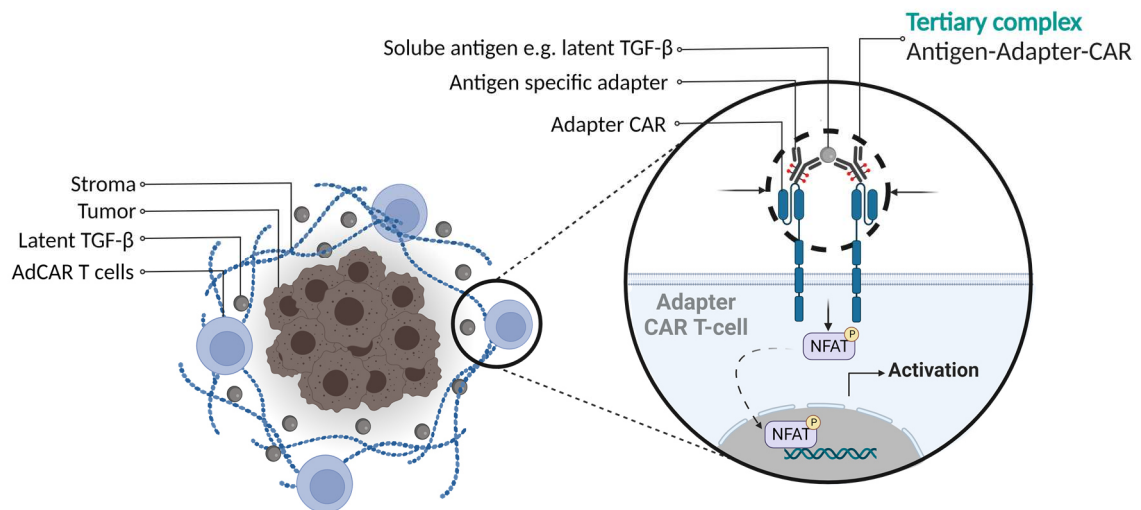


Figure 7: Overcoming the immunosuppressive TME with AdCAR T cells.

Schematic visualization of how a soluble protein complex serves as an activation trigger for AdCAR T cells within the otherwise suppressive stroma. In general, the TME consists of tumor cells, stromal components, e.g. fibroblasts or fibronectin, and a wide range of chemokines and cytokines, for instance latent TGF- β . Due to its pronounced expression in the TME of human cancer tissues, latent TGF- β is an interesting target for CAR T cell therapy of solid tumors. Importantly, latent TGF- β can be present in a TME in a cell-anchored form, but also as a secreted soluble molecule. To serve as a stimulus for AdCAR T cells, it is hypothesized that the soluble cue is required to be sequestered by the tagged antibody. In presence of adapter, the soluble antigen is complexed via the adapter. Subsequently, a tertiary complex made of antigen, adapter and CAR is formed. This adapter-antigen complex induces dimerization of the CAR to trigger a signaling cascade resulting in cellular activation characterized by e.g. pro-inflammatory cytokine secretion. Adapted from Werchau *et al.* Combined targeting of soluble latent TGF- β and a solid tumor-associated antigen with adapter CAR T cells. *OncImmunology* (2022). Illustration created with BioRender.com.

5. Results

5.1 TME composition of ovarian tumor tissue

To evaluate the localization of the latent TGF- β complex and its co-localization with other markers within the TME, human ovarian cancer tissue was analyzed via cyclic fluorescent imaging. In addition, the purpose of this analysis was to determine which regions of the tumor would be recognized by AdCAR T cells when latent TGF- β is used as an antigen.

One imaging cycle was composed of the staining with a fluorophore-conjugated antibody as first step followed by a subsequent bleach process. Cycles were repeated multiple times and allowed to analyze the expression of multiple markers on the same tissue section.

With this technique tissue sections of two patients suffering from ovarian cancer were investigated. The difference between both sections was that they were either infiltrated by the EpCAM⁺ tumor cells (**Figure 8**) or free of EpCAM⁺ tumor cells (**Figure 9**). In total three regions of interest (ROIs) showing EpCAM expression and three ROIs showing no EpCAM expression were analyzed. To demonstrate the presence of latent TGF- β in the tumor area the expression of LAP was used as a surrogate. In total 95 surface markers were analyzed and assessed for co-localization with latent TGF- β (Table 9).

The exemplary human ovarian cancer tissue showing EpCAM⁺ tumor cells (**Figure 8**) presented as two parts: a tumor-invaded desmoplastic area and a clearly separated non-tumor invaded area.

In order to quantify the degree of co-localization of latent TGF- β with other markers within the TME, a Pearson correlation analysis was performed. Analysis was done separately for both tumor- and non-tumor-bearing tissue sections, to compare the degree of correlation between both tissue areas. In total, three regions showing EpCAM⁺ tumor cells and three regions containing no EpCAM⁺ tumor cells were analyzed in the described way.

PCC analysis showed the highest degree of correlation between CD90 and CD49a. Expression of CD90 (PCC: $0,32 \pm 0,08$) and CD49a (PCC: $0,35 \pm 0,04$) increased linearly with LAP expression in the tumor area. In the analyzed tissue showing no tumor, lower correlation coefficients for CD90 (PCC: $0,13 \pm 0,05$) and CD49a (PCC: $0,11 \pm 0,04$) with LAP were observed, indicating a reduced linear correlation of those markers.

The results of the PCC analysis were also confirmed visually by the microscope images.

The desmoplastic area showed as dense structure with islets of EpCAM⁺ tumor cells surrounded by e.g. connective tissue. Areas invaded by the tumor showed dense expression of CD49a in combination with CD90. Within this desmoplastic area the expression of LAP was strongly overlapping with CD49a and CD90 (**Figure 8**). This overlapping expression pattern of LAP, CD49a and CD90 was not observed in the tissue section without EpCAM⁺ tumor cells (**Figure 9**).

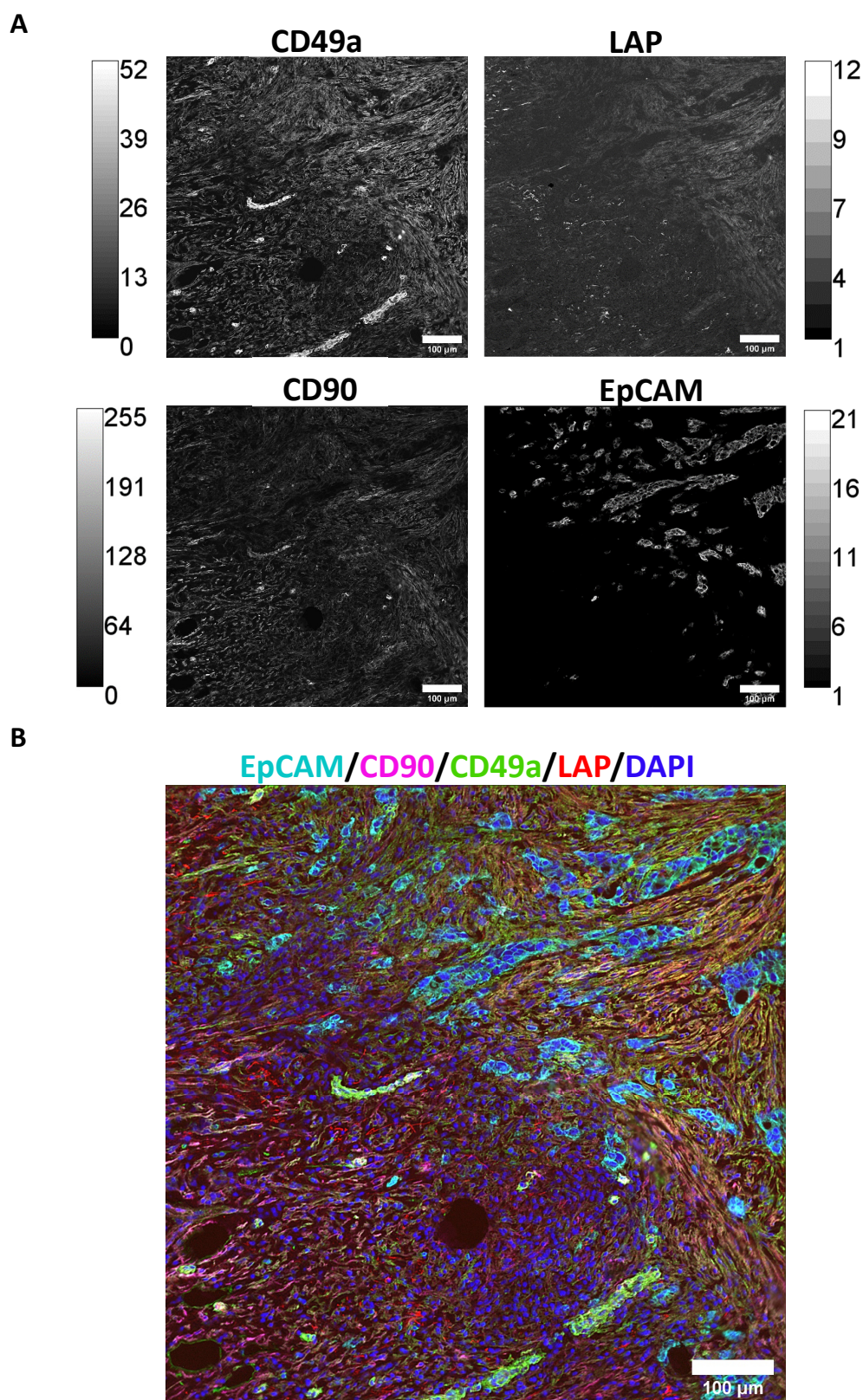


Figure 8: LAP expression in presence of tumor cells on human ovarian cancer tissue.

The expression pattern of human LAP was analyzed in human ovarian cancer tissue. (A) Single antibody staining with grey scale values for one exemplary ROI and (B) a merged image thereof are depicted (CD90: magenta, EpCAM: cyan, LAP: red, CD49a: green and DAPI: blue). Scale bar indicates 100 μm .

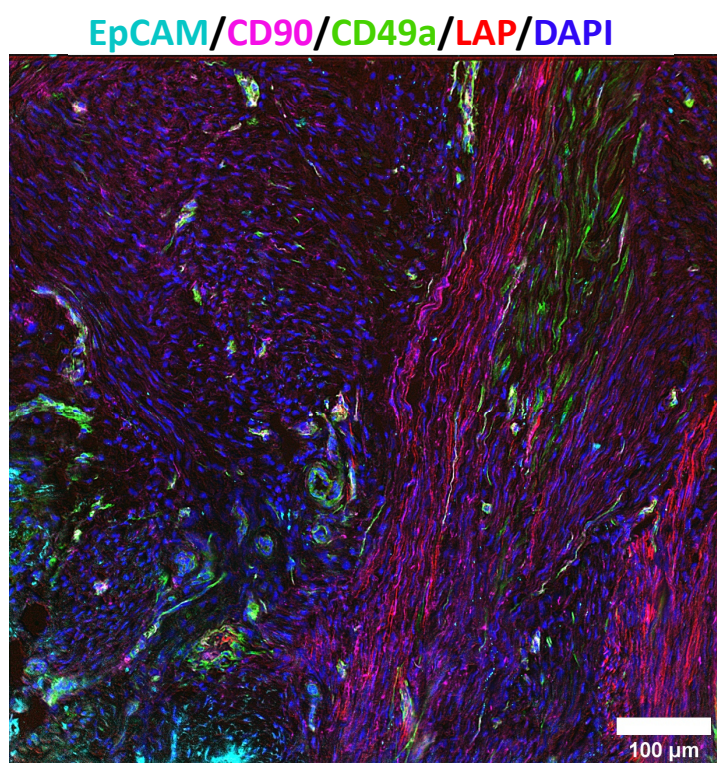


Figure 9: LAP expression in absence of tumor cells on human ovarian cancer tissue.

The expression pattern of human LAP was analyzed by cyclic immunofluorescent staining in a non-tumor bearing area of ovarian tissue isolated from a patient suffering from ovarian cancer. A merge picture thereof for one exemplary ROI (CD90: magenta, EpCAM: cyan, LAP: red, CD49a: green and DAPI: blue) is depicted. Scale bar indicates 100 μm.

5.2 Soluble antigen-induced activation of AdCAR T cells

5.2.1 AdCAR T cells sense soluble human LAP in presence of adapter

To validate the central hypothesis of this thesis, namely that AdCAR T cells can be activated by soluble ligands, primary human T cells were transduced to express a biotin specific CAR (AdCAR1). The antigen binding domain (scFv: h Bio3-3.18E7) of AdCAR 1 was specific for the linker-label-epitope (LLE) tag of LCLC-biotin. Transduction efficacy was 36 %, 38 % and 53 %. The AdCAR1 T cells were co-cultured in presence of soluble hLAP with or without LLE-conjugated IgG₁, specific for hLAP. Soluble antigen-induced activation of AdCAR T cells was quantified via flow cytometric analysis of CD69 and CD25. The frequency of cells co-expressing both activation markers when aLAP was available was normalized to background expression on T cells cultured in absence of hLAP and aLAP. The level of CD69 and CD25 was significantly increased in presence of both aLAP and hLAP (**Figure 10**) compared to hLAP only.

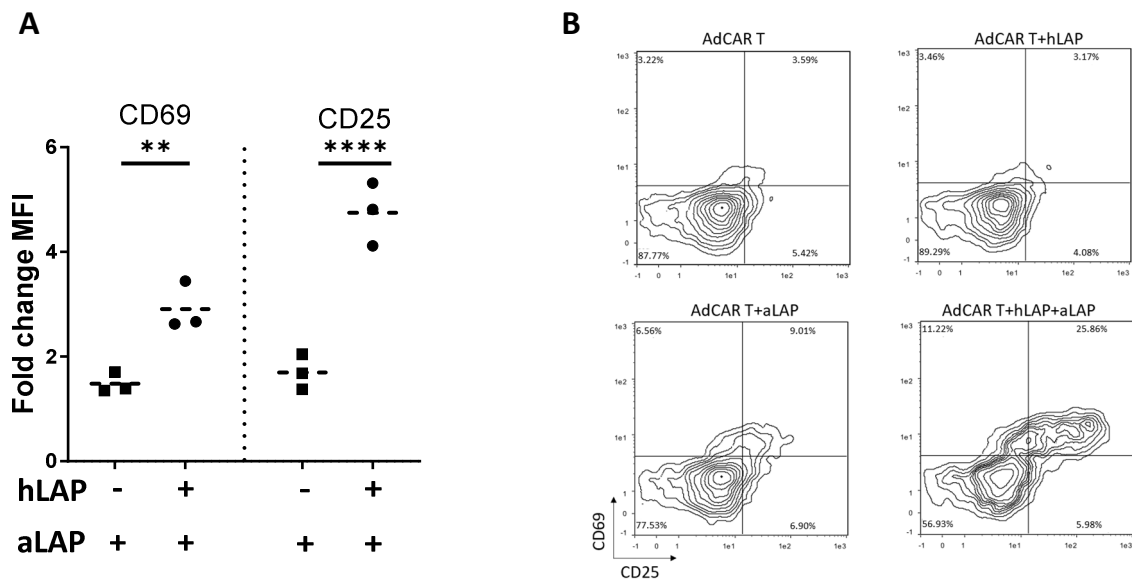


Figure 10: Activation marker expression of AdCAR1 T cells co-cultured in presence of hLAP and aLAP.

AdCAR1 T cells were incubated for 24h with 10 ng/mL aLAP with or without 125 ng/mL hLAP. (A) Activation of LNGFR⁺ AdCAR T cells was quantified by phenotyping, i.e. surface staining for CD69 and CD25 expression. Mean values were normalized to T cell activation in absence of soluble hLAP and aLAP. (B) CD69 and CD25 expression is shown for one exemplary donor. Data shown were obtained from n=3 healthy donors and plotted with mean (dashed lines). Statistical analysis was performed by Two-way ANOVA. Correction for multiple comparisons done with Holm-Sidak. Significance defined as: * p≤0.05; ** p≤0.01; *** p≤0.001; **** p≤0.0001.

The presence of only aLAP induced a slight expression of CD69 and CD25 which might have been caused by crosslinking of CAR molecules as the aLAP was conjugated to multiply LC-LC biotins. The soluble antigen on its own did not induce activation. In addition cytokine secretion of AdCAR1 T cells was analyzed after 24 h of co-culture (**Figure 11**). AdCAR T cells secreted pro-inflammatory cytokines only in presence of aLAP and hLAP (GM-CSF, IFN- γ , IL-2 and TNF- α). This cytokine secretion pattern further validated that AdCAR1 T cell activation observed was

dependent on presence of both adapter and soluble antigen. In summary, these data demonstrate that AdCAR T cells get activated by soluble antigens and do not require surface associated antigens.

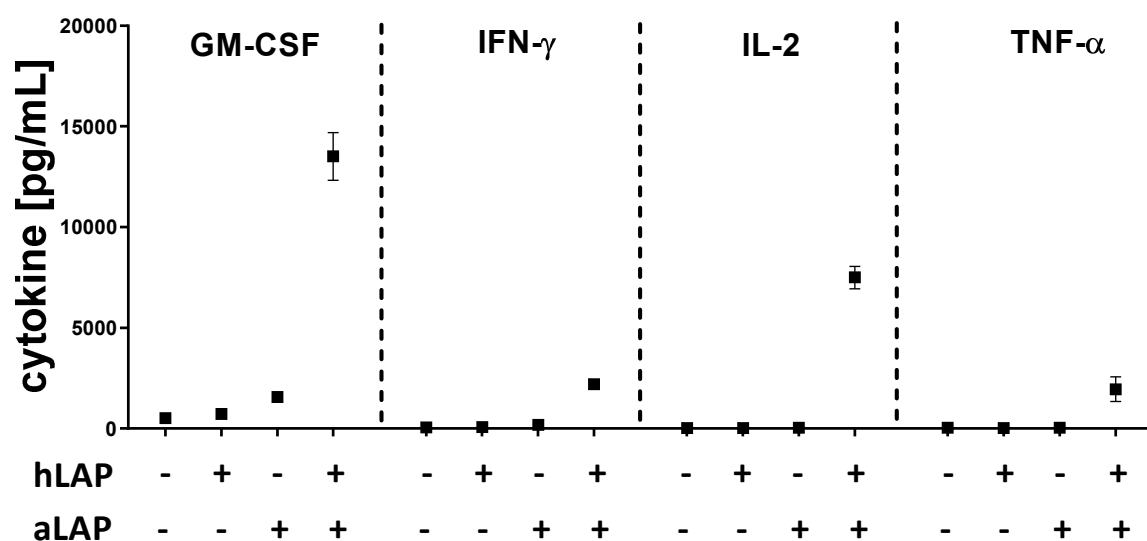


Figure 11: Cytokine secretion of AdCAR1 T cells co-cultured in presence of hLAP and aLAP.

AdCAR1 T cells were incubated for 24 h with 10 ng/mL aLAP with or without 125 ng/mL hLAP. As effector function cytokine secretion of activated AdCAR1 T cells was analyzed by cytokine multiplex assay. Data shown were obtained from n=2 healthy donors plotted with mean and ± 1 standard deviation (SD).

5.2.2 Soluble antigen-induced AdCAR T cell activation can be modulated by both adapter and antigen concentration *in vitro*.

After demonstrating successful sensing of hLAP with AdCAR1 T cells, the impact of antigen- or adapter concentration on cellular activation was analyzed. The influence of the adapter concentration was assessed by incubating AdCAR1 T cells with 250 ng of hLAP and varying concentrations of adapter. Transduction efficacy was 20 %, 18 % and 38 %. Activation-induced increase of CD69-MFI and CD25-MFI was observed from 10 ng/mL to 100 ng/mL of adapter (**Figure 12 A-B**). Similarly, activation dependency on target antigen concentration was studied. Here, the aLAP concentration was fixed to 100 ng/mL and the antigen concentration was varied. Transduction efficacy was 65 %, 52 % and 42 %. Clearly, CD69 and CD25 were expressed in an antigen concentration-dependent manner (**Figure 12 C**). In summary, these results strengthened the hypothesis that AdCAR T cells, indeed, can be re-directed towards soluble ligands. Their effector response appeared to be sensitively tunable by modulating the ligand- and the adapter concentrations. In accordance to previous results, the MFI of CD69 and CD25 was slightly increased in presence of aLAP compared to controls cultured without aLAP and hLAP. This as well pointed to minor background activation by the tagged adapter molecule. Overall, the data indicated that the strength of AdCAR1 T cell activation is adjustable. This is a property with potential relevance when targeting the TME of solid tumors considering antigen gradients as well as off-tumor effects that might require quick adapter withdrawal.

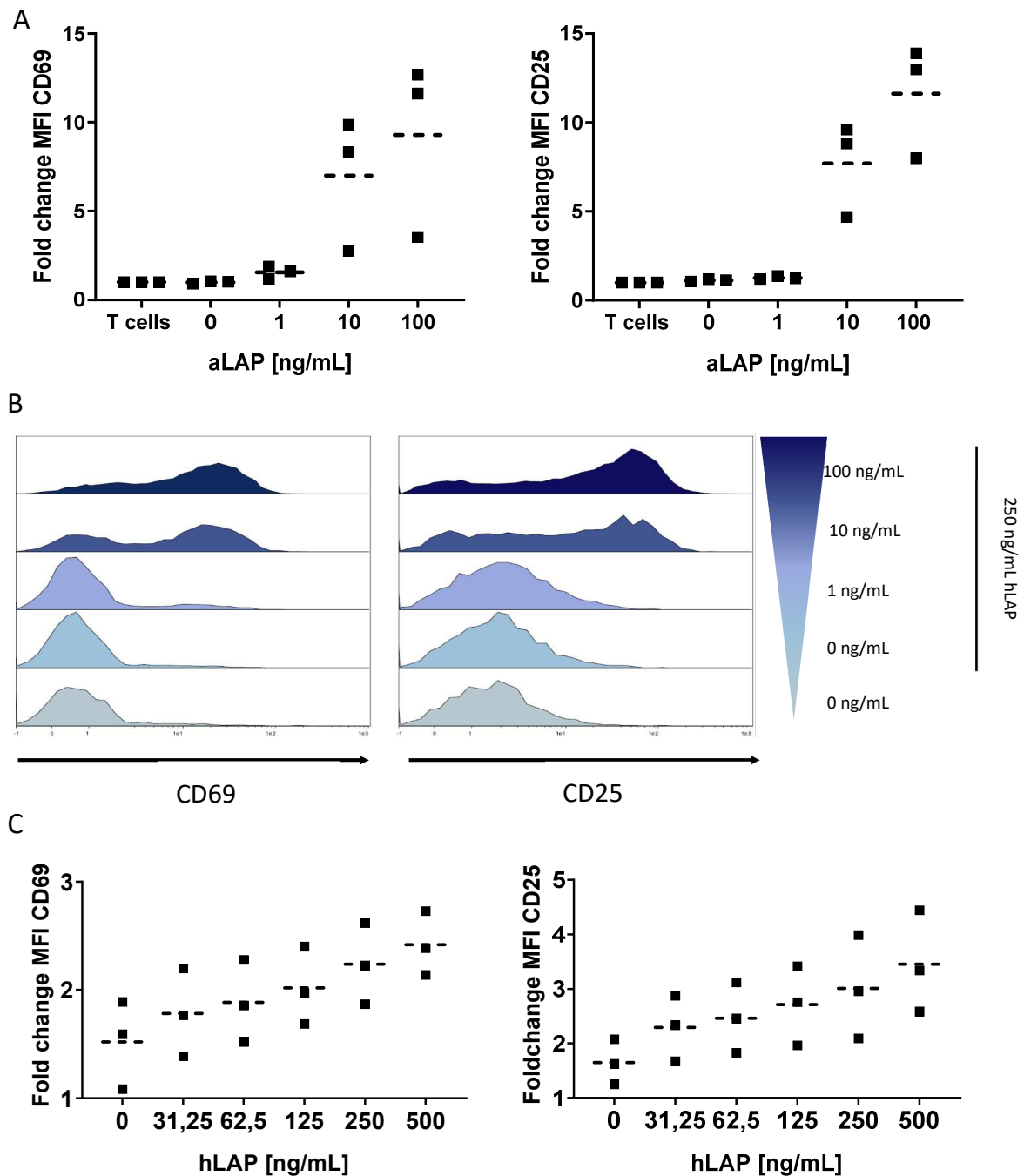


Figure 12: Activation marker expression of AdCAR1 T cells co-cultured in presence of varying concentrations of hLAP or adapter.

(A) AdCAR1 T cells were incubated for 24 h with 250 ng/mL of soluble recombinant hLAP and indicated concentrations of aLAP. Activation of LNGFR⁺ AdCAR1 T cells was quantified by phenotyping, i.e. expression of CD69 and CD25. (B) Histograms of one exemplary donor depicting CD69 and CD25 expression. (C) In addition, AdCAR1 T cells were incubated for 24 h with 100 ng/mL aLAP and varying concentrations of hLAP as indicated. Activation of LNGFR⁺ AdCAR1 T cells was quantified by gating on CD69⁺ or CD25⁺ events. MFI was normalized to T cell activation in absence of both hLAP and aLAP. Data shown were obtained from n=3 healthy donors and plotted with mean (dashed lines).

5.2.3 Sensing of soluble antigens induces transgene expression in AdCAR T cells

AdCAR1 T cells successfully converted soluble hLAP into an activating stimulus for T cells. This trigger was strong enough to induce expression of endogenous T cell genes related to T cell activation, e.g. surface markers and cytokines. Next, the stimulus-induced expression of a transgene upon AdCAR activation was investigated. Therefore, AdCAR1 T cells were transduced with a LVV encoding a reporter cassette. This cassette contained a repetitive sequence of the human NFAT-AP-1 binding site. In addition, to assess transgene expression, GFP was located 3' of the promoter sequence. In this way, GFP served as a reporter for activation-induced NFAT signaling in AdCAR1 T cells (**Figure 13 A**). GFP expression was quantified in AdCAR1 T cells co-cultured with hLAP, aLAP or both by fluorescent microscopy after 90 h. All values were normalized to background fluorescence of T cells measured at the beginning of the co-culture. In presence of both hLAP and aLAP AdCAR1 T cells showed three-fold increase of GFP intensity and thus, significantly higher integrated GFP intensity compared to controls cultured only with hLAP or aLAP (**Figure 13 B**).

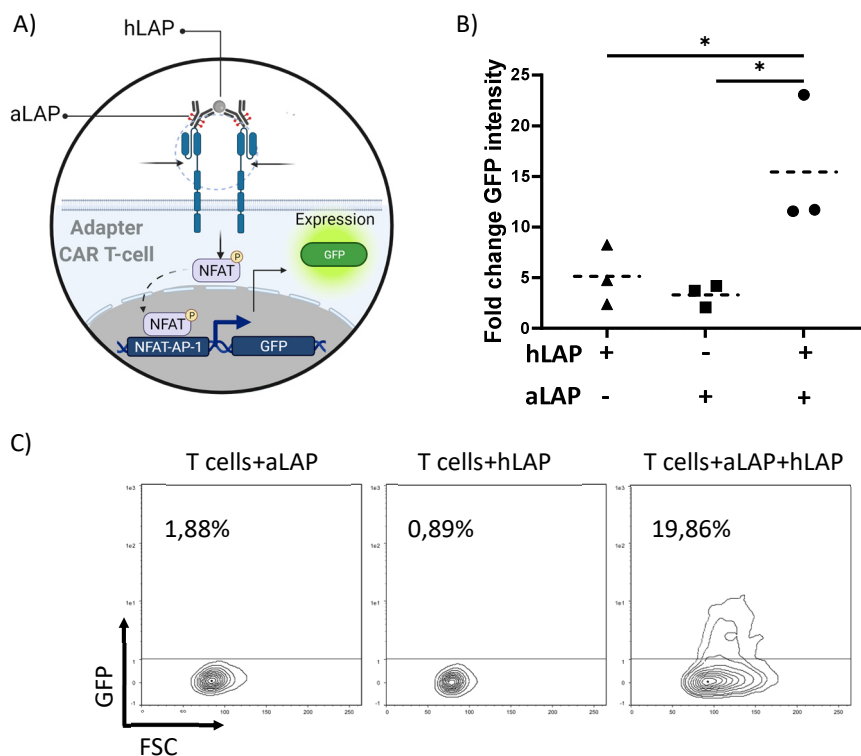


Figure 13: Transgene expression in AdCAR1 T cells co-cultured in presence of hLAP and aLAP.

(A) Schematic representation of the AdCAR1 T cell reporter assay using GFP expression as read-out for activation-induced signal transduction in dependency of AdCAR engaging hLAP. (B) Primary human T cells were transduced to express AdCAR1. In addition, cells were transduced with a LVV encoding a NFAT-AP1-GFP reporter construct to visualize downstream intracellular signaling upon CAR engagement by hLAP adapter complex. AdCAR1 T cells were incubated for 90 h with 10 ng/mL aLAP with or without 125 ng/mL hLAP. CAR signaling was analyzed by GFP expression with the Incucyte® S3 system. Integrated GFP intensity was normalized to start values. (C) Dot plots of one representative donor. GFP expression of viable total T cells was analyzed via flow cytometry after 90 h. Data shown were obtained from n=3 healthy donors plotted with mean (dashed lines). Statistical analysis was performed by One-way ANOVA. Correction for multiple comparisons done with Holm-Sidak. Significance defined as: * p<0.05; ** p<0.01; *** p<0.001; **** p<0.0001. Illustration created with BioRender.com.

This result confirmed the activation of the NFAT signaling pathway following soluble antigen-induced AdCAR1 T cell activation. The stimulus provided by soluble antigens was potent enough to induce the expression of a transgene, in this case GFP in AdCAR1 T cells.

5.2.4 Secretion of soluble latent TGF- β by human tumor cell lines *in vitro*

In order to assess soluble latent TGF- β as a soluble target antigen expressed by human tumor cell lines, supernatants of four human cancer cell lines were investigated by ELISA. Three pancreatic cancer cell lines (AsPC-1, BxPC-3 and AsPC-1-TGF), one neuroglioma cell line (H4) and one myeloma cell line (U266) were cultured in 6-well culture plates for 24 h (Figure 14 A). H4 cells secreted 168 ng/mL latent TGF- β , the highest amount amongst the tested cancer cell lines, whereas the pancreatic cancer cell lines secreted approx. 100-fold less latent TGF- β . U266 did not secrete latent TGF- β to detectable concentrations *in vitro*, since the measured values did not exceed the background level observed in this assay. In previous studies, our group developed CAR T cells for the treatment of pancreatic adenocarcinoma using an established AsPC-1 tumor model²¹⁵. To build on these previous experiments, and to allow inter-experimental comparisons, the AsPC-1 WT tumor model was selected for subsequent studies to integrate established conventional CAR constructs and to investigate differences of CAR T cells targeting a TAA or a soluble antigen. To achieve a constitutive secretion of the soluble target molecule by AsPC-1 WT, the secretion of human latent TGF- β was enforced via transduction of AsPC-1 WT with a LVV encoding human latent TGF- β (AsPC-1-TGF). The overexpression resulted in latent TGF- β concentrations of approx. 770 μ g/mL (Figure 14 B).

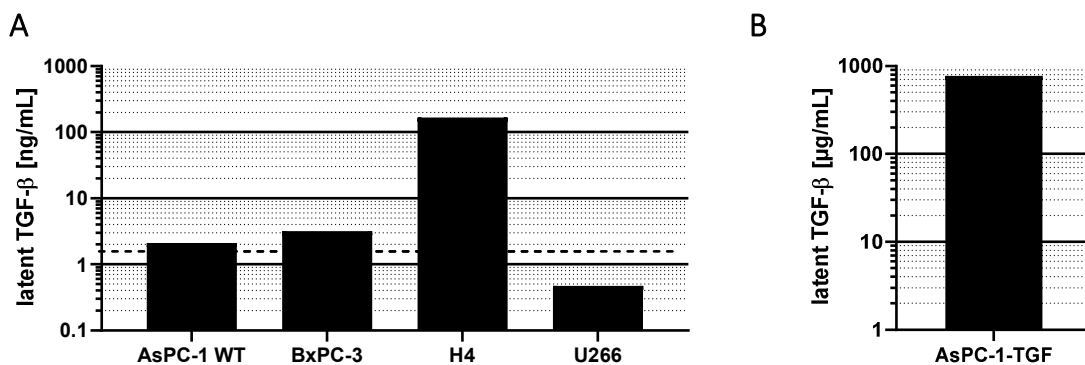


Figure 14: Latent TGF- β secretion of human tumor cell lines *in vitro*.

(A) Concentrations of latent TGF- β were quantified in supernatants of human tumor cell lines by ELISA. The dotted line indicates the limit of detection. (B) The AsPC-1 cell line was engineered to achieve constitutive secretion of latent TGF- β (AsPC-1-TGF) which was confirmed by ELISA.

5.2.5 Tumor cell line-secreted latent TGF- β induced AdCAR T cell activation

To assess the induction of activation and effector functions by AsPC-1-TGF-secreted soluble latent TGF- β , expression of surface markers and cytokine secretion of AdCAR1 T cells was analyzed. Transduction efficacy after enrichment was 90 %, 92 % and 88 %. First, AdCAR1 T cells were co-cultured with serial dilutions of soluble latent TGF- β derived from AsPC-1-TGF in presence or absence of aLAP for 24 h. Expression of activation markers was quantified by flow cytometry (**Figure 15 A**). Expression of CD69, CD25 and CD137 occurred only in presence of the adapter molecule and was dependent on the presence and concentration of the soluble ligand. The expression of all three markers reached a plateau between 193 $\mu\text{g}/\text{mL}$ and 10 $\mu\text{g}/\text{mL}$ soluble latent TGF- β . In the same experiment, the cytokine secretion of AdCAR1 T cells upon co-culture with tumor-derived soluble latent TGF- β was analyzed (**Figure 15 B**). In accordance with the activation marker expression, AdCAR1 T cells secreted pro-inflammatory cytokines in dependency of available soluble latent TGF- β when aLAP was added. In general, the highest concentration of target antigen induced the highest production of all four cytokines tested. Gradual reductions were observed with reduced concentrations of soluble latent TGF- β . With approx. 2000 pg/mL GM-CSF and IFN- γ were identified as most prominent cytokines. Although cytokines were detected for all three donors the intensity was highly donor dependent. These results showed that AdCAR1 T cells do respond to a tumor cell line-derived soluble factor *in vitro*. Sensing of soluble ligands by AdCAR1 T cells was not suppressed even in presence of the immunosuppressive latent TGF- β .

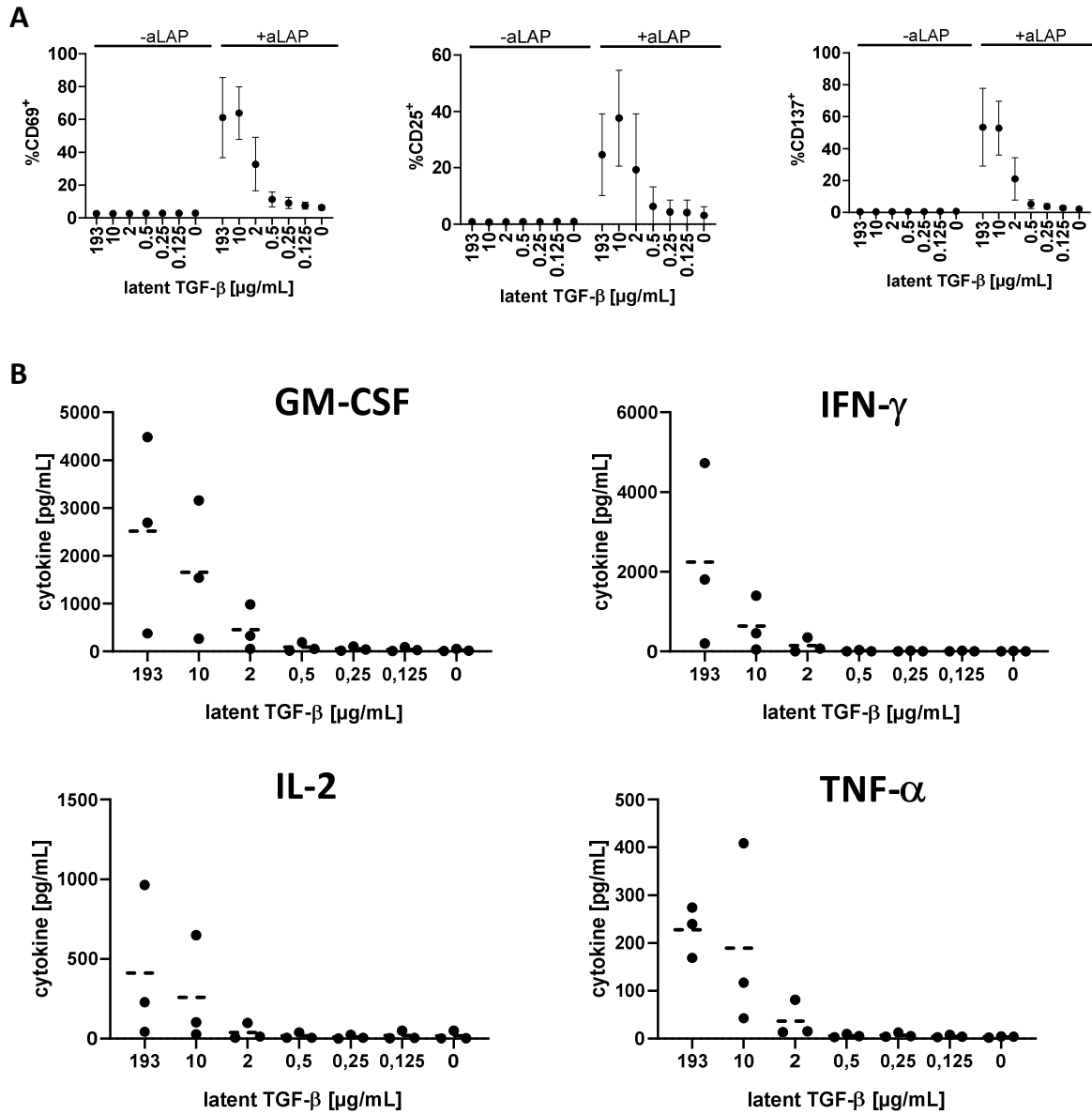


Figure 15: Activation marker expression and cytokine secretion of AdCAR1 T cells co-cultured in presence of AsPC-1-TGF-secreted latent TGF-β and aLAP.

(A) Tumor cell-secreted soluble latent TGF-β was titrated and activation markers of LNGFR⁺ AdCAR1 T cells were analyzed. (B) Quantification of GM-CSF, IFN-γ, IL-2 and TNF-α production by AdCAR1 T cells. Data shown were obtained from n=3 healthy donors plotted with mean (dashed lines) and ± 1 SD.

5.2.6 AdCAR T cells sense soluble latent TGF- β in presence of tumor cells

In previous experiments it was shown that AdCAR1 T cells are able to convert the presence of a soluble antigen into an activating stimulus. However, this was tested in absence of tumor cells. To mimic the situation in the TME more closely and to evaluate any additional immunosuppressive effects mediated by the tumor cells, soluble antigen sensing by AdCAR1 T cells was studied in co-cultures with AsPC-1-TGF. To dissect cell contact-independent and cell contact-dependent interactions between tumor cells and AdCAR1 T cells, as well as their impact on the sensing of latent TGF- β , a transwell experiment was performed (**Figure 16 A**). AsPC-1-TGF were cultured in the lower compartment with AdCAR1 T cells either in the same compartment or, separated by a membrane, in the upper compartment of the culture chamber. The membrane between the upper and the lower compartment had a pore size of 0.4 μm . The soluble latent TGF- β secreted by the tumor cells was able to diffuse through the membrane, whereas the AdCAR1 T cells were blocked from transwell migration. Transduction efficacy after enrichment was 97 %, 97 % and 98 %. The frequency and MFI of CD137⁺ cells were significantly increased in presence of AsPC-1-TGF and aLAP validating the activation of AdCAR1 T cells by a tumor-derived soluble ligand. Importantly, AdCAR1 T cell activation occurred without and with separation from AsPC-1-TGF. Both CD4⁺ and CD8⁺ AdCAR1 T cells showed activation induced expression of CD137, with CD8⁺ AdCAR1 T cells showing higher frequencies and MFI of CD137 compared to CD4⁺ AdCAR1 T cells. CD4⁺ AdCAR1 T cells that have been cultured in direct contact to tumor cells showed significantly higher frequencies of CD137⁺ cells and increased MFI of CD137⁺ cells compared to AdCAR1 T cells that had exclusive contact to the soluble antigen. In CD8⁺ AdCAR1 T cells these effects were less pronounced since a significant difference was only observed for the MFI of CD137⁺ whereas the frequency of CD137⁺ AdCAR1 T cells was not impacted by the well compartment the cells have been cultured in (**Figure 16 B-C**). These results provided additional evidence that the presence of tumor cells does not *per se* obviate the activation of AdCAR T cells induced by soluble ligands. Overall, it could be validated that both CD8⁺ and CD4⁺ AdCAR T cells were activated independently of target cell contact.

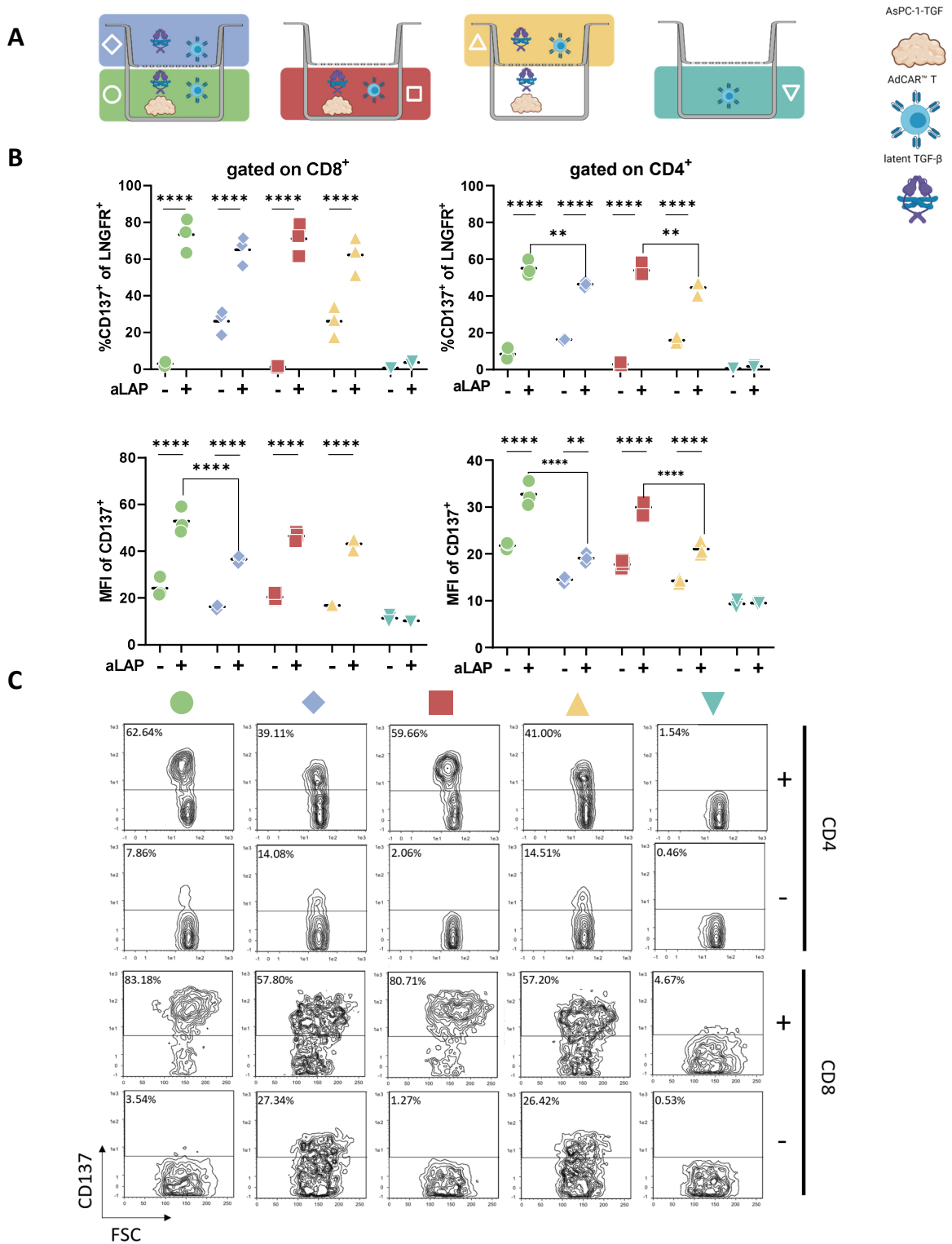


Figure 16: Activation marker expression of AdCAR1 T cells co-cultured in presence of AsPC-1-TGF and aLAP.

(A) An illustration of transwell conditions is shown. (B) Frequencies and MFI of LINGFR⁺ CD137⁺ AdCAR1 T cells were analyzed by flow cytometry. Activation markers were analyzed separately for CD4⁺ and CD8⁺ AdCAR1 T cells in presence (+) or absence (-) of aLAP. (C) CD137 expression of CD4⁺ or CD8⁺ AdCAR1 T cells after co-culture with AsPC-1-TGF in transwell assay depicted (for one donor). Normal well conditions (green circle, red square, cyan triangle) and transwell conditions (blue rhombus, yellow triangle). Data shown were obtained from n=3 healthy donors plotted with mean (dashed lines). Statistical analysis was performed by Two-way ANOVA. Correction for multiple comparisons done with Holm-Sidak. Significance defined as: * p<0.05; ** p<0.01; *** p<0.001; **** p<0.0001. Illustrations were created with BioRender.com.

5.2.7 Combinatorial targeting of soluble latent TGF- β and CD66c with AdCAR T cells *in vitro*

The flexibility to redirect AdCAR T cells by adapter choice is a major advantage compared to T cells expressing a CAR for direct targeting of a TAA. By combining different adapter molecules, AdCAR T cells can in principle be targeted towards multiple antigens at the same time, e.g. a soluble target and a TAA. To this end, AdCAR T cells were used to investigate combined sensing of soluble latent TGF- β and tumor cell killing via AsPC-1-TGF-expressed CD66c. CD66c was recently shown to be a potential antigen candidate for CAR T cells targeting pancreatic adenocarcinoma²¹⁵. First, CD66c expression was confirmed on AsPC-1 WT and AsPC-1-TGF. The expression level of CD66c was comparable in both cell lines (**Figure 17 A**). Therefore, CD66c was used as a model antigen for targeting a TAA with AdCAR T cells in this study. Next, the impact of a second adapter molecule specific for latent TGF- β on the killing efficacy of AdCAR T cells targeting CD66c was investigated. Apart from the concentration of adapters the affinity of the AdCAR for the LLE adapter-tag may also impact the combinatorial targeting. To address the impact of affinity, two adapter CARs with different LLE-specific scFvs were analyzed. AdCAR2 (scFv: Bio2 4G10) showed a higher affinity for LLE-tagged adapter molecules than AdCAR1 (scFv: h Bio3-3.18E7) in flow cytometry (data not published). For AdCAR1 transduction efficacy was 47 %, 52 % and 77 %. For AdCAR2 transduction efficacy was 52 %, 57 %, and 69 %. AdCAR T cells were co-cultured with AsPC-1 WT and AsPC-1-TGF and varying ratios of a CD66c-specific adapter (aCD66c) and aLAP. Both CAR constructs showed significant killing of AsPC-1 WT in presence of aCD66c (**Figure 17 B**). Killing efficacy was not significantly reduced at any of the tested ratios of aLAP and aCD66c compared to aCD66c alone. It should be noted that although not significant AdCAR1 showed a decrease in tumor killing at a ratio of 90 ng/mL aLAP plus 10 ng/mL aCD66c. This was not observed for AdCAR2. AdCAR2 T cells showed the same killing efficacy between 10 ng/mL to 100 ng/mL aCD66c irrespective of the amount of added aLAP. This may indicate that due to its higher affinity, AdCAR2 can induce target cell killing at lower concentrations of aCD66c. Surprisingly, AdCAR2 induced growth control of AsPC-1 WT in presence of 100 ng/mL aLAP but in absence of aCD66c. This was not observed for AdCAR1, and is possibly due to LAP expression on the surface of AsPC-1 WT or unspecific killing by AdCAR2. Killing of AsPC-1-TGF was found to be adapter-dependent as well, but less effective compared to AsPC-1 WT. Growth of AsPC-1-TGF was significantly reduced in presence of aCD66c (100 ng/mL) for both AdCARs compared to the control group without adapter. Importantly, killing efficacy was not significantly reduced in any of the tested mixtures of aLAP and aCD66c compared to aCD66c alone. However, in this experimental setting a concentration of 100 ng/mL aLAP led to a comparable anti-tumor effect as observed with 100 ng/mL aCD66c, indicating surface expression of LAP on AsPC-1-TGF. These results demonstrated that AdCAR T cells elicit tumor cell killing in presence of multiple adapter molecules, e.g. with one adapter being specific for a TAA and a second one being specific for a soluble antigen.

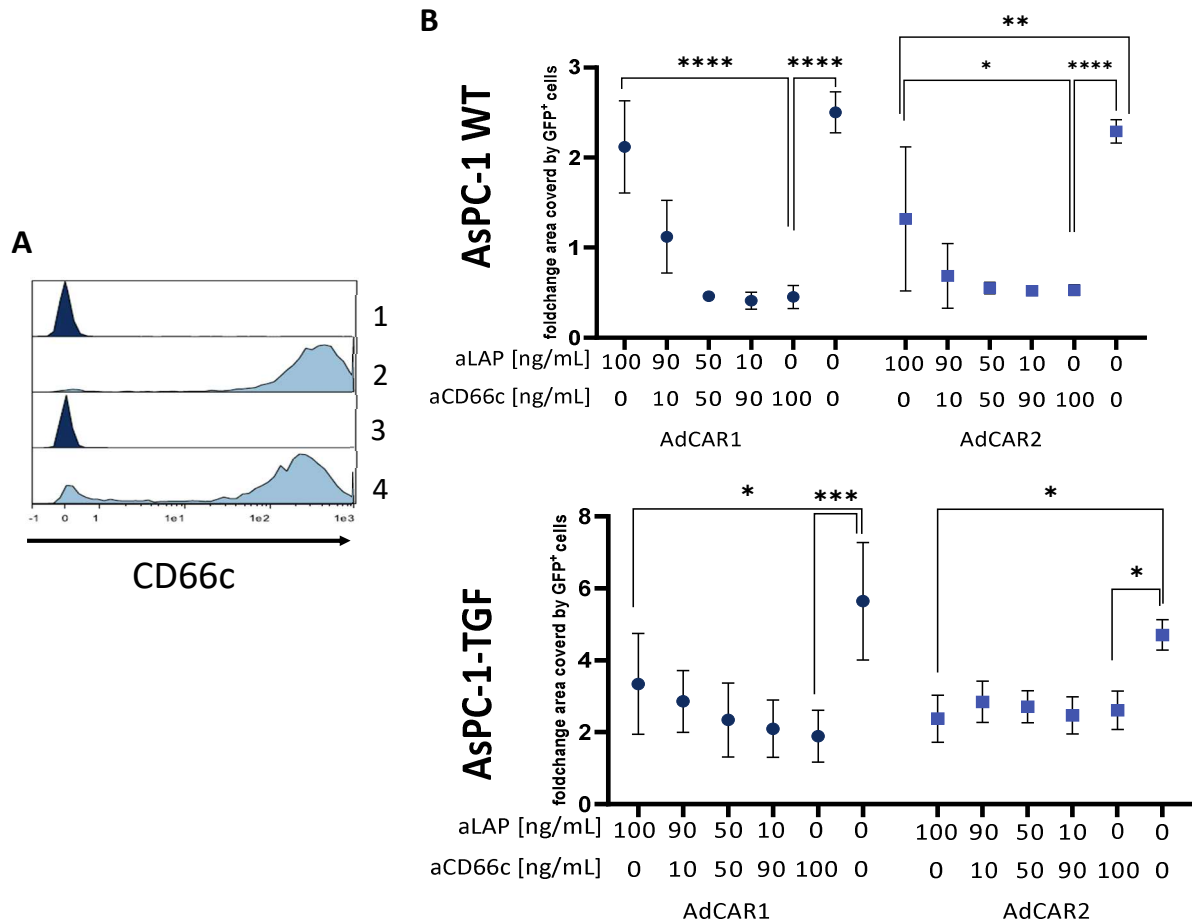


Figure 17: Killing of AsPC-1 WT or AsPC-1-TGF in presence of AdCAR T cells at varying ratios of multiple adapter specificities *in vitro*.

(A) AsPC-1-TGF (2) and AsPC-1 WT (4) were stained with anti-CD66c antibody for flow cytometric analysis. AsPC-1-TGF (1) and AsPC-1 WT (3) were stained with a PE-Isotype control. (B) Primary human T cells were transduced for expression of either AdCAR1 or AdCAR2. Subsequently, AdCAR T cells were either co-cultured with AsPC-1-TGF or AsPC-1 WT for 141 h in presence of indicated mixtures of aLAP and aCD66c. The surface area in wells covered by target cells was quantified with the Incucyte® S3 system. Data shown were obtained from n=3 healthy donors and plotted with mean \pm 1 SD. Data were normalized to the start values. Statistical analysis was performed by Two-way ANOVA. Correction for multiple comparisons done with Holm-Sidak. Significance defined as: * $p \leq 0.05$; ** $p \leq 0.01$; *** $p \leq 0.001$; **** $p \leq 0.0001$.

To evaluate the effect of aCD66c on the sensing of latent TGF- β via aLAP, AdCAR T cells were co-cultured with supernatant of AsPC-1 WT and AsPC-1-TGF plus aCD66c and aLAP at varying ratios. In contrast to previous studies, the MFI of CD137⁺ AdCAR T cells was used as metric for soluble antigen-induced activation instead of frequency. The lentiviral construct of AdCAR2 did not contain LNGFR as surrogate surface marker co-expressed with the AdCAR to identify AdCAR⁺ cells by flow cytometry. Thus, unlike for AdCAR1, the frequency of CD137⁺ AdCAR2 T cells could only be measured for total viable T cells. Hence, for comparability of both constructs the MFI of viable CD137⁺ cells was analyzed. After co-culture with supernatant of AsPC-1 WT, the MFI of CD137⁺ on AdCAR T cells increased as a function of aCD66c concentration irrespective of the used AdCAR construct. At a ratio of 100 ng/mL aCD66c plus 0 ng/mL aLAP, the activation was significantly increased compared to the 0 ng/mL aCD66c plus 100 ng/mL aLAP condition for both AdCAR constructs when co-cultured with supernatant of AsPC1 WT (**Figure 18 A**). This surprising finding may indicate the presence of soluble CD66c in supernatants of AsPC-1 WT acting as a soluble antigen for AdCAR T cells. The MFI of CD137⁺ T cells expressing AdCAR2 was slightly higher at lower concentration of aCD66c compared to AdCAR1. At a ratio of 50 ng/mL aCD66c plus 50 ng/mL aLAP the MFI of CD137⁺ was 2.08 for AdCAR1 compared to 2.5 for AdCAR2. As expected, in presence of supernatant derived from AsPC-1-TGF, cellular activation was observed in an aLAP concentration-dependent manner for both CAR constructs (**Figure 18 B**). The MFI of CD137⁺ T cells was higher compared to what was observed with supernatants of AsPC-1 WT. This points towards a stronger activation induced by soluble latent TGF- β compared to an unknown ligand, potentially soluble CD66c, secreted by AsPC-1 WT cells. The presence and the concentration of soluble CD66c needs to be further evaluated, e.g. by CD66c ELISA. Different concentrations of soluble CD66c and latent TGF- β may explain relative differences in activation when AdCAR T cells were co-cultured with supernatant of AsPC-1 WT and either aLAP or aCD66c.

Importantly, neither killing of tumor nor sensing of soluble ligands was blocked by the presence of a second non-related adapter. Taken together, these results demonstrated that AdCAR T cells can, in one approach, be directed towards two different target moieties *in vitro* and integrate antigenic simulation without detectable adverse inhibitory effects.

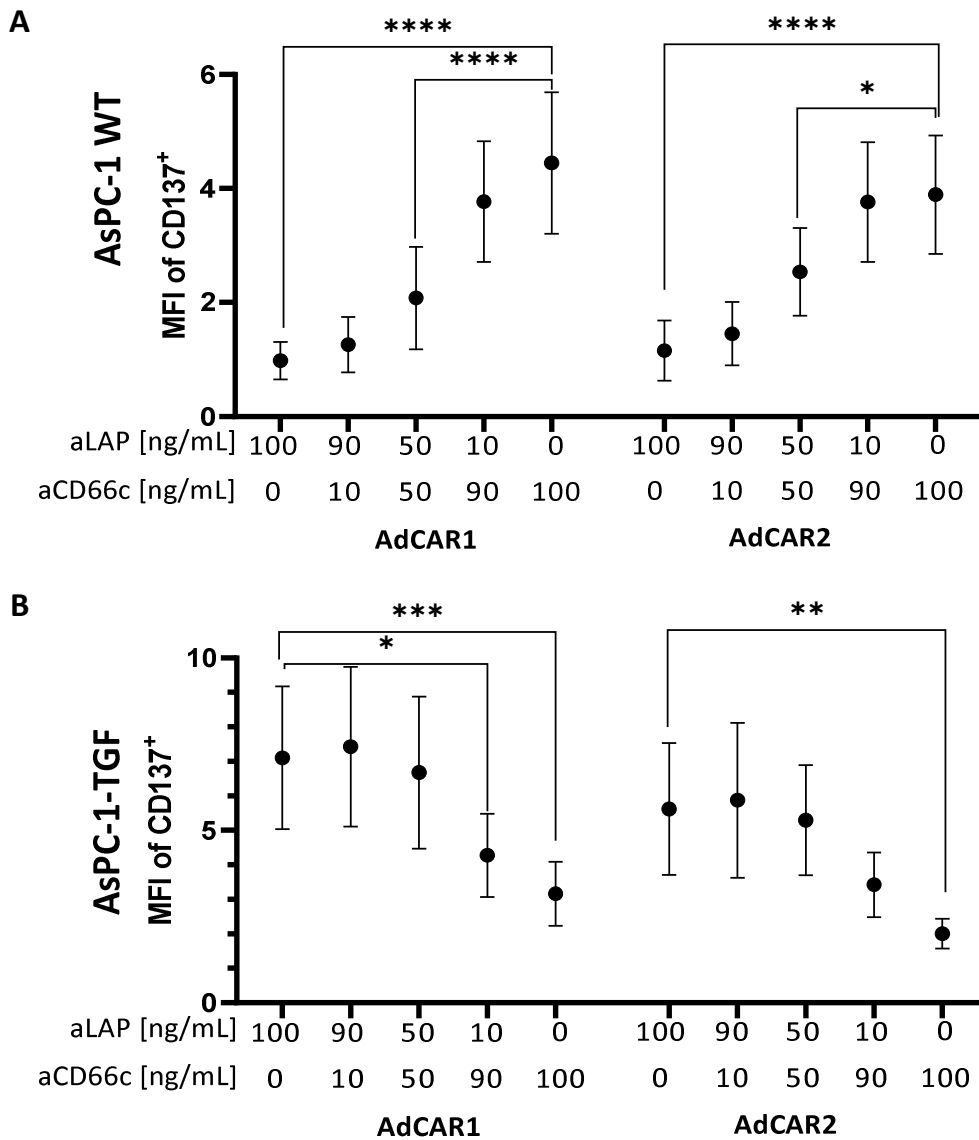


Figure 18: Activation of AdCAR T cells co-cultured in presence of supernatant of AsPC-1 WT or AsPC-1-TGF at varying ratios of multiple adapter specificities.

Primary human T cells were transduced for expression of AdCAR1 or AdCAR2. AdCAR T cells were either co-cultured with supernatant of AsPC-1 WT (A) or supernatant of AsPC-1-TGF (B) for 24 h in presence of indicated ratios of aLAP and aCD66c. MFI of CD137 on AdCAR T cells was analyzed. Data shown were obtained from n=3 healthy donors plotted with mean \pm 1 SD. Statistical analysis was performed by Two-way ANOVA. Correction for multiple comparisons done with Holm-Sidak. Significance defined as: * $p \leq 0.05$; ** $p \leq 0.01$; *** $p \leq 0.001$; **** $p \leq 0.0001$.

5.3 Sensing soluble antigens with AdCAR T cells *in vivo*

The previous results have shown that AdCAR T cells can be activated by soluble hLAP and latent TGF- β in an adapter and ligand-dependent manner. In order to confirm this novel mechanistic concept *in vivo*, a PDAC xenograft tumor model was used to build on TGF- β as soluble antigen as well as to ensure presence of an immunosuppressive TME by inoculating mice with TGF- β over-expressing tumor cells. In this way, the conversion of an otherwise inhibitory signal into a pro-inflammatory signal was investigated. Human latent TGF- β was chosen since this molecule can be present in soluble form and attached to the ECM. This makes it an ideal target to discriminate effector function of AdCAR T cells induced via a soluble antigen or locally within the TME.

5.3.1 Establishment of a latent TGF- β -secreting tumor model in NSG mice

NSG mice were s.c. inoculated with three different doses of AsPC-1-TGF. The tumor growth as well as animal welfare were monitored over 30 days. Tumor growth was quantified by BLI measurement and caliper (**Figure 19 A-B**). The genetically modified AsPC-1-TGF tumor engrafted similarly in all three cohorts. Animals showed palpable tumors in the flank at around day six. In the first two weeks after engraftment, tumors showed increase in size before reaching a plateau. Growth rate as well as total tumor sizes were comparable across all groups. Animals showed no signs of toxicity during tumor engraftment. Mice showed either weight gain when s.c. injected with 1×10^6 and 5×10^6 cells or stable body weight when s.c. injected with 1×10^7 cells (**Figure 19 C**). Any signs of toxicity were absent in the course of the study. On day 30, the amount of latent TGF- β was analyzed in sera as an indicator for the presence of the soluble target for subsequent *in vivo* studies (**Figure 20 A**). In all cohorts, latent TGF- β was detectable in soluble form by ELISA. The concentration of latent TGF- β in animal sera was approx. 10 $\mu\text{g}/\text{mL}$. In the context of this work, the characterization of the TME created by AsPC-1-TGF is of particular interest, especially the localization of latent TGF- β . The spatial distribution of latent TGF- β locally within the TME was assessed via immunofluorescent imaging of tumor tissue. As seen in human ovarian cancer tissue (**Figure 8**), latent TGF- β was present in the TME and associated with EpCAM⁺ AsPC-1-TGF tumors (**Figure 20 B-C**). The tumors formed a TME rich in fibronectin which showed to some extent an overlap in expression with latent TGF- β . The vascularization was assessed via staining for CD31 as an endothelial marker. Tumors showed low CD31 expression indicating a lack of functional vasculature within the solid tumor mass.

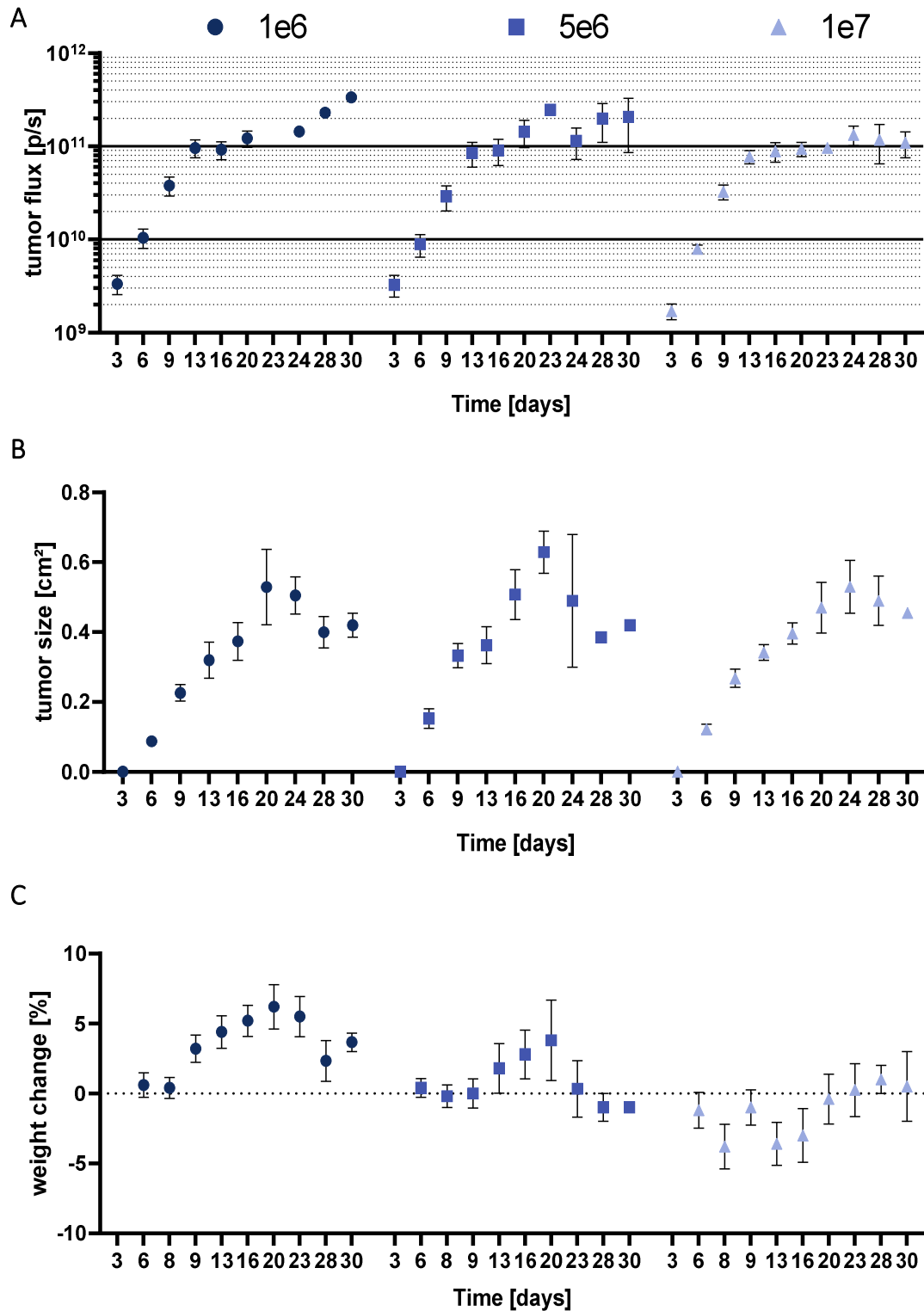


Figure 19: Tumor growth kinetic of AsPC-1-TGF in NSG mice.

AsPC-1-TGF were s.c injected into five NSG mice per cohort. Tumor formation of AsPC-1-TGF was analyzed by (A) BLI imaging and (B) caliper measurement. (C) Weight changes over time during tumor establishment. Data shown are plotted as mean with standard error of the mean (SEM).

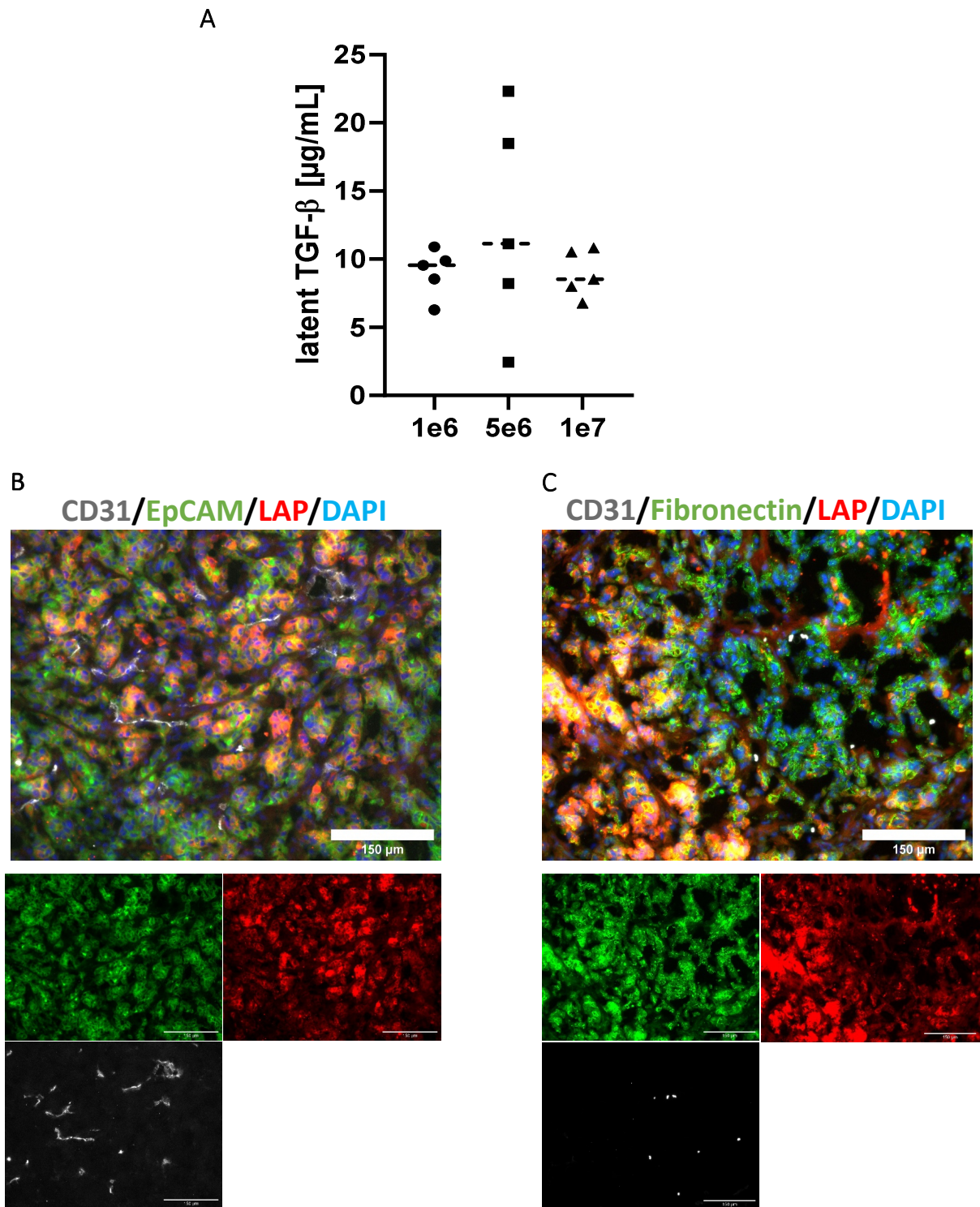


Figure 20: Localization of latent TGF- β in AsPC-1-TGF tumor-bearing mice.

(A) At day 30 after s.c. inoculation of NSG mice with three different doses of AsPC-1-TGF blood was collected from the *vena facialis* and presence of latent TGF- β was analyzed via ELISA. Data shown were obtained from n=5 NSG mice with median values plotted as dashed lines. The co-localization of LAP (red) with (B) EpCAM⁺ AsPC-1-TGF tumor cells (green) and (C) fibronectin (green) as a stroma marker was analyzed by immunofluorescence imaging. Scale bar indicates 150 μ m.

5.3.2 Targeting human latent TGF- β with AdCAR T cells is tolerated by NSG mice

Potential toxicities of AdCAR T cells targeting human latent TGF- β were investigated in NSG mice in absence of tumor cells but in presence of soluble latent TGF- β . Therefore, human T cells were transduced for AdCAR1 expression. The CAR expression was analyzed prior to injection by flow cytometry. AdCAR1 was expressed in 60.64 % of the cells. The functionality of the AdCAR1 T cells was confirmed *in vitro* at day ten before the cells were injected into mice. In presence of aLAP and AsPC-1-TGF, AdCAR1 T cells showed elevated CD137 expression and IFN- γ secretion confirming an adapter- and target-dependent activation *in vitro* (Figure 21 A-B).

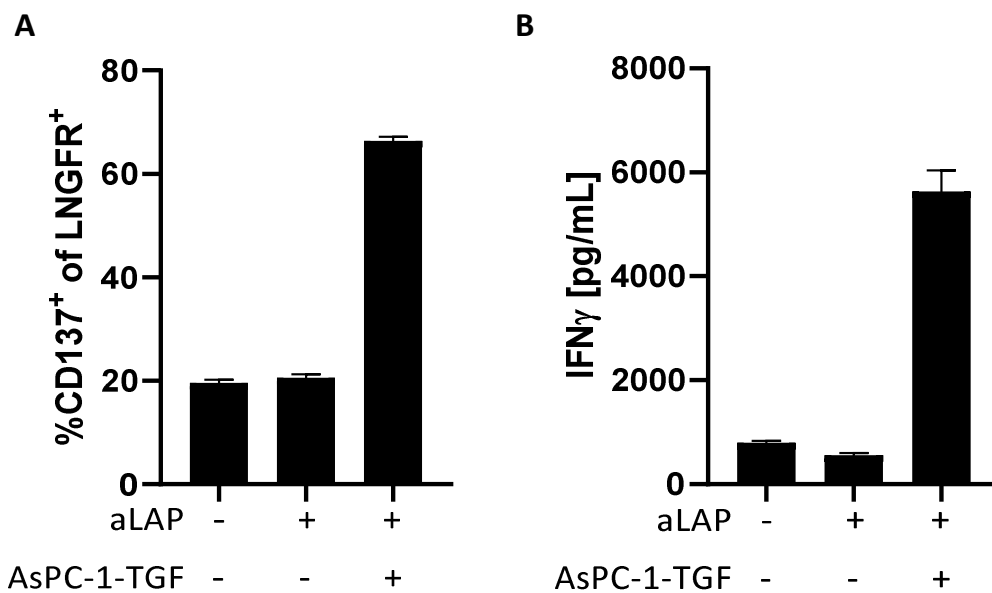


Figure 21: *In vitro* functionality of AdCAR1 T cells used for toxicity study.

AdCAR1 T cells and AsPC-1-TGF were co-cultured in presence or absence of 100 ng/mL aLAP. (A) Activation marker and (B) cytokine secretion were analyzed 24 h later and confirmed functionality of AdCAR1 T cells used for toxicity study. Values measured in duplicates. Mean is plotted with \pm 1SD.

Therefore, the functionality-controlled cellular product was considered as suitable for toxicity assessment. On day minus four, mice were i.p. injected with 10 mg human IVIG (LOT1). The human IVIG fulfilled two functions: (1) it saturated Fc-receptor binding sites that may function as a sink for the aLAP and (2) it contained soluble human latent TGF- β (Figure 22).

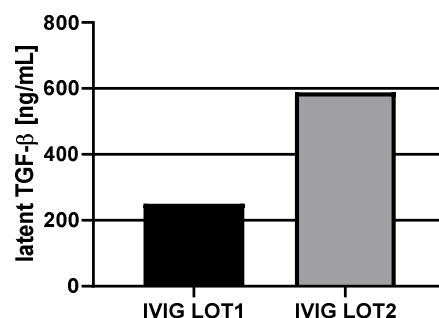


Figure 22: Concentration of soluble latent TGF- β in human IVIG.

Quantification of latent TGF- β in human IVIG was done via ELISA. Two different LOTs from the same supplier were tested. LOT1 was tested after freeze and thaw and LOT2 directly after reconstitution.

In case of any toxicities, the injection of both the adapter and the target could be withdrawn to distinguish between off target toxicity, e.g. due to unspecific AdCAR binding and toxicity caused by using latent TGF- β as a CAR antigen. On day minus one, animals were i.p. injected with either 230 $\mu\text{g}/\text{mL}$ or 25 $\mu\text{g}/\text{mL}$ aLAP. On day zero, 1×10^7 AdCAR1 T cells per mouse were i.v. injected. The weight change and animal score were monitored over 13 days as a metric for toxicity induced by AdCAR T cells in combination with aLAP (Figure 23 A-B).

In both cohorts, the mice' weight stayed mostly stable during the study. No indications of severe toxicities were observed as reflected by the animals' score. The highest score (5, weight loss 5 % to 10 %) was reached in the cohort treated with 230 $\mu\text{g}/\text{mL}$ aLAP between day one and six. The higher animal score in the cohort treated with 230 $\mu\text{g}/\text{mL}$ might indicate a latent TGF- β -triggered stimulation of AdCAR1 T cells. As for the *in vitro* studies, aLAP was tagged with multiple biotins and thus aLAP is possibly able to induce AdCAR cross-linking in absence of soluble antigen.

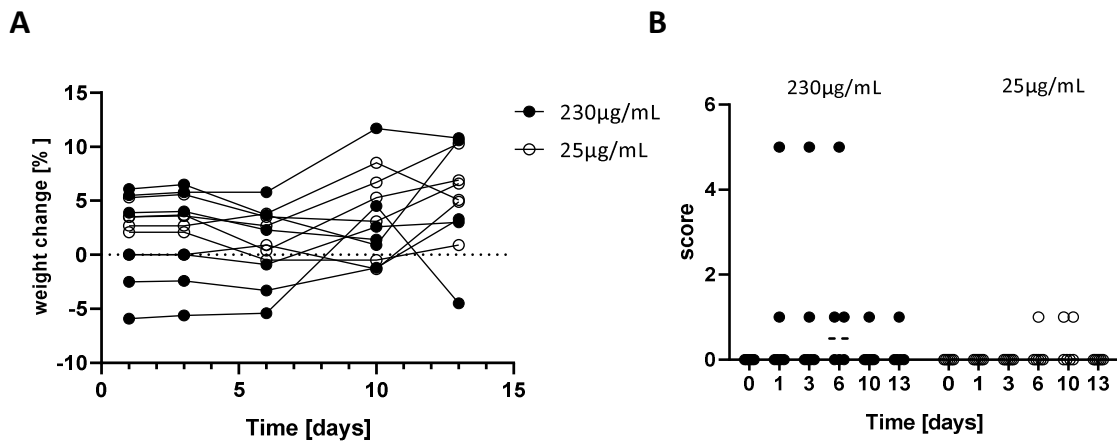


Figure 23: Assessment of aLAP-mediated toxicity in mice treated with AdCAR1 T cells in presence of soluble latent TGF- β .

(A) Weight change over time of NSG mice supplemented with latent TGF- β and treated with AdCAR1 T cells plus 230 $\mu\text{g}/\text{mL}$ or 25 $\mu\text{g}/\text{mL}$ aLAP. Each dot represents an individual animal. (B) Animal score over time for 230 $\mu\text{g}/\text{mL}$ or 25 $\mu\text{g}/\text{mL}$ aLAP-receiving cohorts as a metric for animal well-being. Animal score represents body condition, general condition, animal activity and study specific criteria. A score of 20 marks the abortion of the study. Each dot represents one animal. Median values shown as dashed lines.

For a more comprehensive understanding of potential aLAP-induced AdCAR1 T cell activation in absence of membrane-bound target, the IFN- γ level in sera was monitored throughout the course of the study (**Figure 24**). On day one and three, approx. 1200 pg/mL IFN- γ in sera were detected in the cohort that received the high aLAP dose (230 μ g/mL) compared to approx. 800 μ g/mL IFN- γ in the cohort that received the low aLAP dose (25 μ g/mL). On day three, the cytokine levels were significantly higher in the 230 μ g/mL aLAP cohort compared to the low aLAP dose. It should be noted that due to technical issues, only two animals were analyzed on day three in the 25 μ g/mL cohort which impacts the power of the statistical analysis. On day ten, almost no cytokines were detected in both groups.

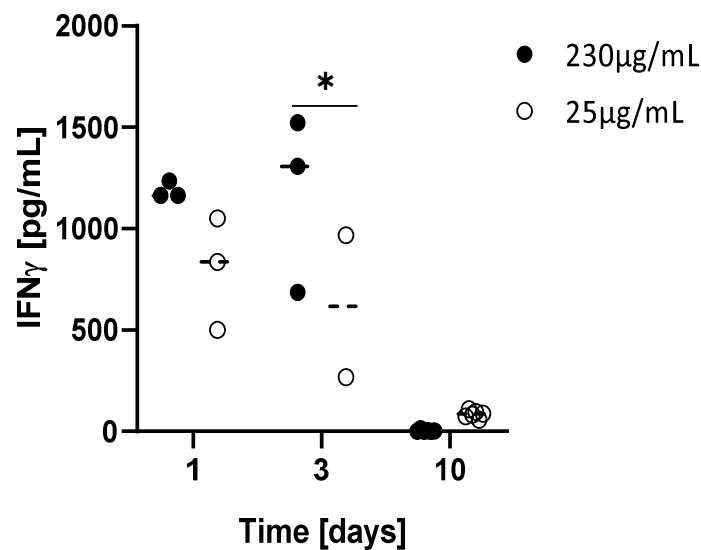


Figure 24: IFN- γ levels in mice treated with AdCAR1 T cells and aLAP in presence of soluble latent TGF- β .

Cytokine levels were determined at day one, day three and day ten after AdCAR1 T cell infusion. Each dot represents one animal. Median values are plotted as dashed lines. Statistical analysis was performed by Two-way ANOVA. Correction for multiple comparisons done with Holm-Sidak. Significance defined as: * $p \leq 0.05$; ** $p \leq 0.01$; *** $p \leq 0.001$; **** $p \leq 0.0001$.

Furthermore, the aLAP-induced activation of AdCAR1 T cells was quantified in different tissues by CD137 expression analysis *ex vivo* (**Figure 25**). To this end, AdCAR1 T cells were isolated from blood, bone marrow (BM) and spleen of recipient mice. The frequency of CD137⁺ cells was compared between mock T cells (LNGFR⁻) and CAR-expressing T cells (LNGFR⁺) to discriminate between activation induced by the environment and by aLAP. In none of the cohorts, a significant difference in CD137 expression was observed between LNGFR⁻ and LNGFR⁺ cells. However, although not significant, a higher frequency of CD137⁺ cells was detected in blood of animals that received 230 μ g/mL aLAP.

These results demonstrated that tumor-free NSG mice tolerated the infusion of AdCAR1 T cells and aLAP. No signs of toxicity were observed even at high doses of the adapter molecule. Cytokine secretion was observed at both adapter doses tested indicating adapter-induced signaling of the CAR construct in presence of soluble latent TGF- β . The activation could be either caused by crosslinking of CAR molecules via the tagged adapter or tonic signaling of the AdCARs. To exclude an activation that is triggered by tonic signaling control cohorts without adapter were included in next experiments.

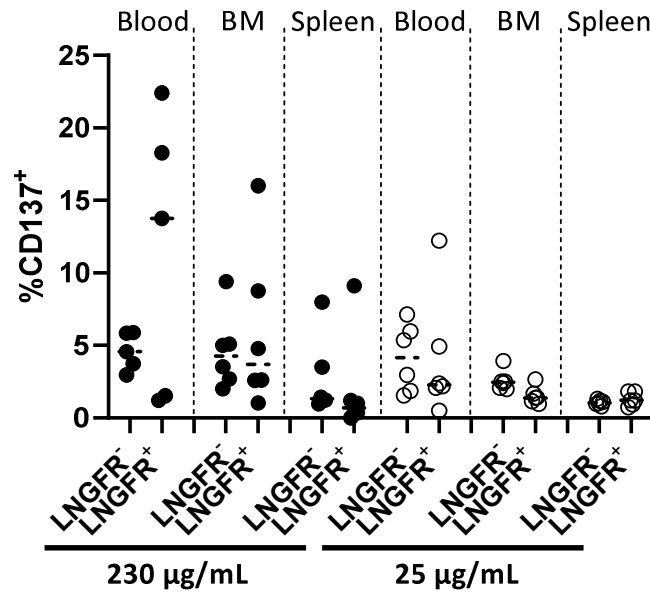


Figure 25: *Ex vivo* analysis of CD137 expression on mock T cells and AdCAR1 T cells in presence of latent TGF- β and aLAP.

CD137 expression was analyzed on day 13 in blood, bone marrow and spleen of NSG mice. Animals were supplemented with latent TGF- β and received AdCAR1 T cells at day zero plus aLAP at days minus one, three, six and nine. Each dot represents an individual animal and medians are represented as dashed lines.

5.3.3 Sensing of latent TGF- β with AdCAR T cells induces rapid stimulation of pro-inflammatory cytokine secretion *in vivo*

The main objectives of this study were to investigate whether AdCAR T cells can be stimulated by soluble TME-related antigens and to identify differentially induced effector functions when targeting a TAA compared to a soluble antigen *in vivo*. The previously established AsPC-1-TGF tumor model was used and combined with AdCAR1 CAR T cells for targeting tumor cell-secreted latent TGF- β by aLAP. NSG mice were s.c. inoculated with AsPC-1-TGF and randomized before AdCAR1 T cells were injected at day zero. Mice were i.p. injected with three different doses (200 μ g, 25 μ g or 0 μ g) of aLAP at day minus one and then injected twice a week with adapter. As a reference an established CD66c S CAR²¹⁵ was tested in the same tumor model (**Figure 26 A**). The CAR expression and CD4:CD8 ratio were analyzed prior to injection by flow cytometry. AdCAR1 was expressed in 64.22 % of the cells and CD66c S CAR was expressed in 70.04 % of the cells. The CD4:CD8 ratio was comparable between both cellular products (AdCAR1: 69.34 % CD4⁺, 21.42 % CD8⁺; CD66c S CAR: 67.45 % CD4⁺, 22.27 % CD8⁺). The CD66c S CAR showed transient reduction of tumor until day seven, indicating its functionality. However, the tumor reduction was followed by tumor outgrowth (**Figure 26 B**). BLI measurement revealed no tumor control in animals treated with AdCAR1 T cells and aLAP. Based on these observations, it was unclear whether AdCAR1 T cells were activated locally in the TME by ECM-attached latent TGF- β as no anti-tumor effect was observed. To analyze activation of AdCAR T cells via soluble latent TGF- β present in sera of tumor-bearing mice, cytokine levels were measured on day four (**Figure 26 C**). Animals treated with 200 μ g aLAP showed significantly higher IFN- γ secretion compared to cohorts treated with 25 μ g aLAP or no aLAP. Surprisingly, the CD66c S CAR T cells produced less IFN- γ in contrast to the AdCAR1 T cells in presence of 200 μ g aLAP, although CD66c S CAR T cells showed a transient anti-tumor effect. In accordance with the observations made in the AdCAR toxicity study, the AdCAR T cells secreted cytokines also in absence of adapter. The background cytokine level was higher than the cytokine level of the CAR. Taken together these results demonstrated a soluble tumor cell-derived antigen-induced rapid activation of AdCAR1 T cells. This activation was characterized by secretion of pro-inflammatory IFN- γ . The stimulation of cytokine secretion by AdCAR1 T cells was faster compared to a CAR pointing towards different sites of activation. AdCAR1 T cells may encounter the soluble target already in the peripheral blood, as the soluble form of latent TGF- β is present in sera of AsPC-1-TGF tumor inoculated mice. In contrast, the CD66c S CAR expressing T cells require migration to the tumor site to allow antigen-induced CAR activation.

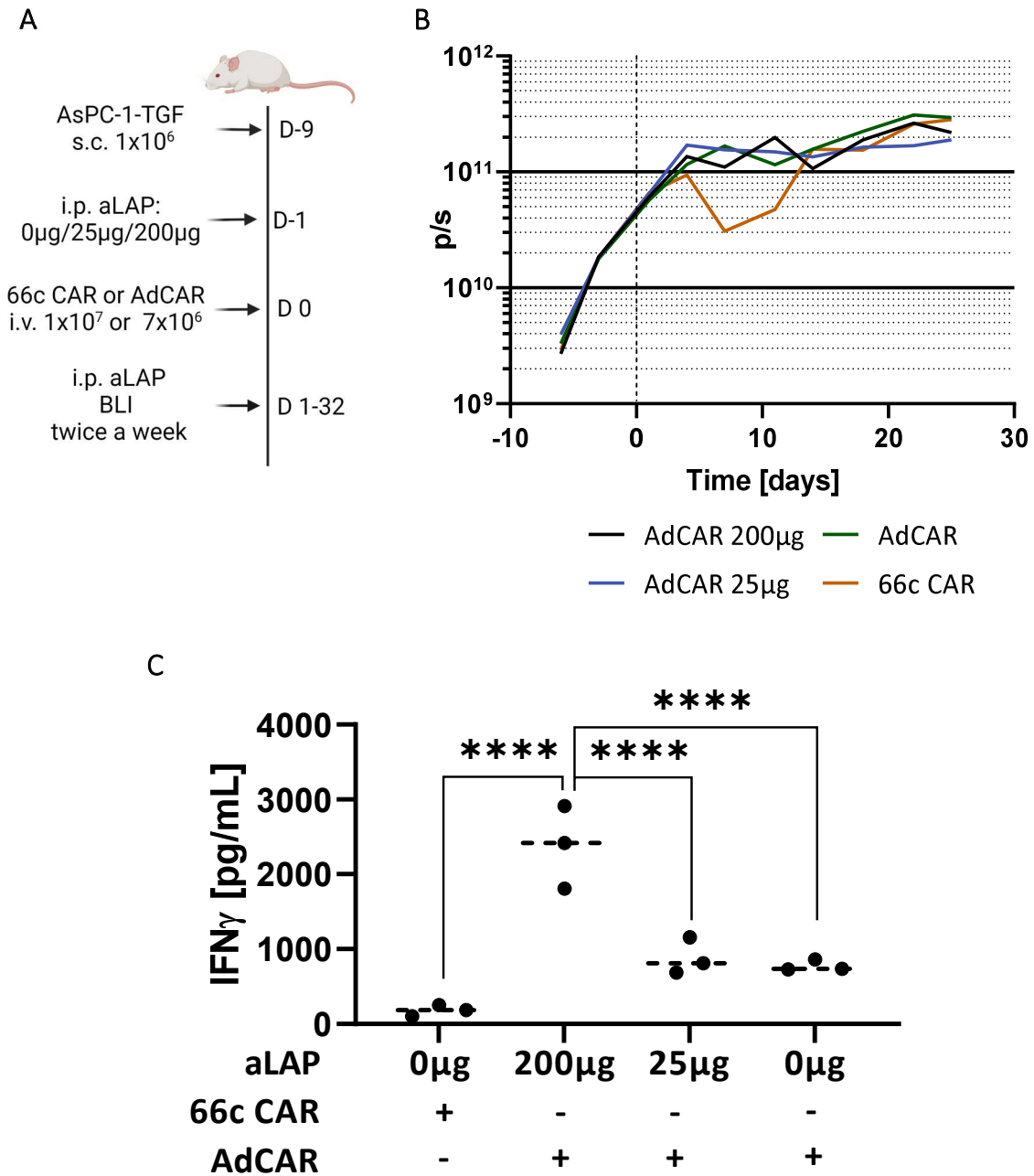


Figure 26: Treatment of AsPC-1-TGF tumor-bearing mice with AdCAR1 T cells and aLAP or CD66c S CAR T cells.

(A) Schematic representation of the study design to assess soluble antigen-induced AdCAR T cell activation in AsPC-1-TGF tumor-bearing NSG mice. (B) Tumor growth was analyzed by BLI imaging quantifying the median photon flux. Six mice were analyzed per cohort. (C) Cytokine levels in sera were determined at day four after AdCAR1 T cell infusion. At each time point the blood of at least three animals was analyzed. Median values are plotted as dashed lines. Statistical analysis was performed by One-way ANOVA. Correction for multiple comparisons done with Holm-Sidak. Significance defined as: * $p < 0.05$; ** $p < 0.01$; *** $p < 0.001$; **** $p < 0.0001$. Illustrations were created with BioRender.com.

5.3.4 Sensing of latent TGF- β with AdCAR T cells induces systemic activation of CAR T cells *in vivo*

To verify that AdCAR T cells were indeed systemically stimulated by soluble latent TGF- β *in vivo*, the expansion of CD8⁺ AdCAR T cells of the previously described *in vivo* study (5.3.3) was analyzed *ex vivo*. Spleens and tumor tissues were isolated and dissociated (**Figure 27 A**). The frequency of CD4⁺ and CD8⁺ AdCAR1 T cells was quantified by flow cytometry and the frequency of CD8⁺ CAR T cells was considered as being indicative for antigen-dependent stimulation of AdCAR1 T cells. In contrast to CAR T cells and AdCAR1 T cells without aLAP, a significant shift of the CD4:CD8 ratio towards CD8⁺ AdCAR1 T cells in spleens was observed for AdCAR1 T cells plus 200 μ g aLAP treated cohorts. In tumor tissue however, this shift was exclusively seen in cohorts treated with the CD66c S CAR.

Additionally, tumor tissue sections were analyzed by immunohistochemistry to further understand the spatial distribution of CAR T cells within the tumor (**Figure 27 B**). CD66c S CAR T cells were found to penetrate the EpCAM⁺ and LAP-expressing tumor areas. CD8⁺ CAR T cells were found to be more abundant in this cohort, which is in line with the flow cytometry data. In cohorts treated with 200 μ g aLAP, AdCAR1 T cells were found especially in the peritumor. In absence of aLAP only few AdCAR1 T cells were found in the tumor area. In any case, AdCAR1 T cells did not infiltrate the tumor as it was observed for the CAR T cells. These data supported the finding that AdCAR1 T cells targeting soluble latent TGF- β were already stimulated before reaching the tumor site due to the systemic availability of their target antigen. In contrast, the TAA-directed CAR T cells need to reach the tumor to become activated. This mechanistic difference between CD66c-directed CAR T cells and soluble antigen-directed AdCAR1 T cells may be responsible for their divergent migration pattern at the tumor site.

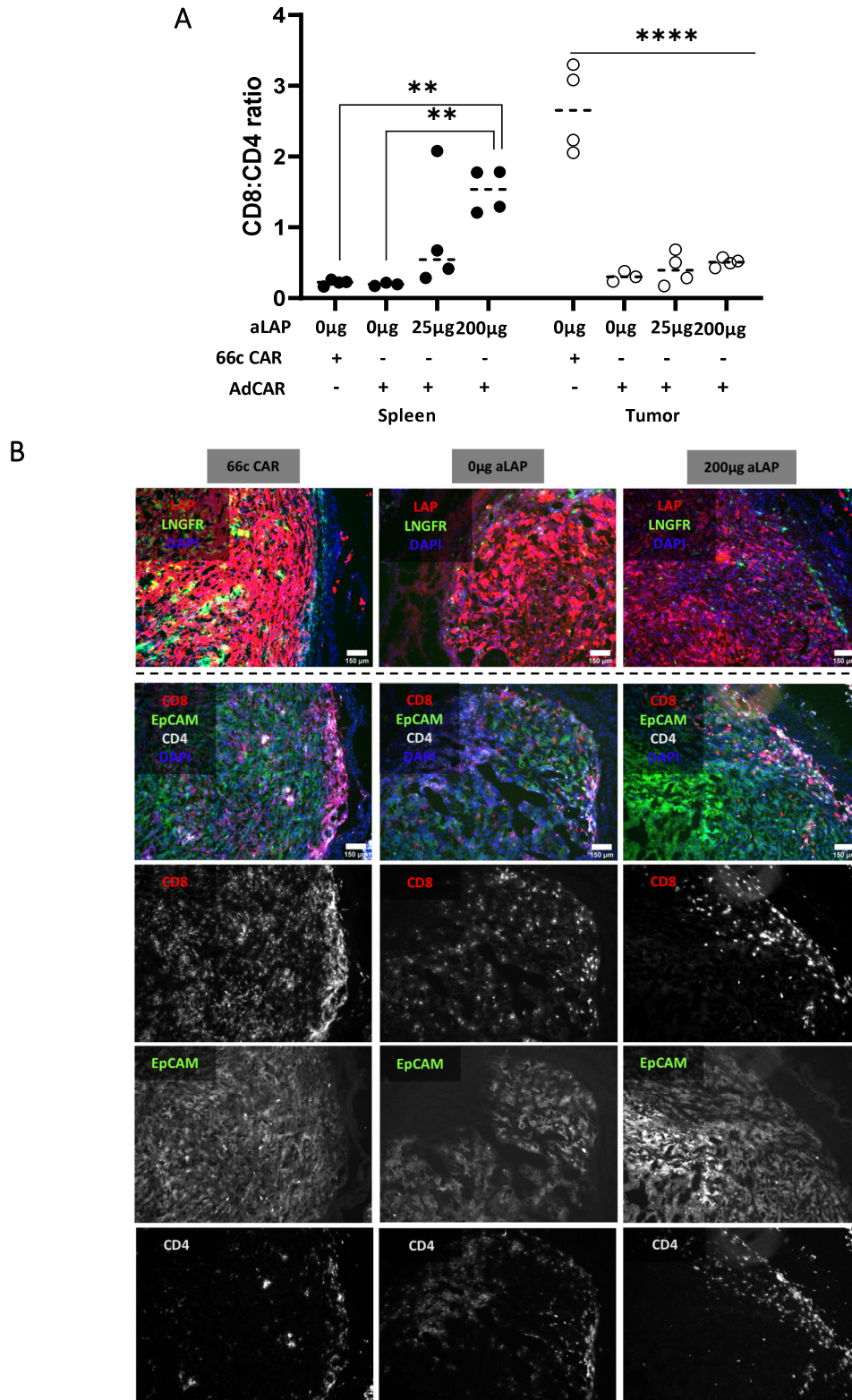


Figure 27: CD8 frequency and tumor infiltration of CAR T cells in AsPC-1-TGF tumor-bearing mice treated with AdCAR1 T cells plus aLAP or CD66c S CAR T cells.

(A) *Ex vivo* analysis of the expansion of CD8⁺ CAR T cells in AsPC-1-TGF tumor-bearing NSG mice. (B) T cell infiltration and CD4:CD8 ratio was analyzed by immunofluorescence of AsPC-1-TGF tumor sections. Consecutive tissue slices from the same animal are depicted for each treatment cohort. Images were taken with 10x magnification. Scale bars indicate 150 µm. Each dot presents one animal. Median values are plotted as solid lines. Statistical analysis was performed by Two-way ANOVA. Correction for multiple comparisons done with Holm-Sidak. Significance defined as: * $p \leq 0.05$; ** $p \leq 0.01$; *** $p \leq 0.001$; **** $p \leq 0.0001$.

5.3.5 Combined sensing of latent TGF- β with AdCAR T cells and targeting a TAA with CAR T cells *in trans* does not interfere with anti-tumor efficacy

To assess if the anti-tumor efficacy of a CD66c-directed CAR can be improved in the AsPC-1-TGF tumor model, and to examine a potential beneficial effect of soluble antigen targeting by AdCAR T cells, CD66c XS CAR T cells were co-infused with AdCAR1 T cells. In this way, the early induction of pro-inflammatory cytokine secretion induced by targeting a soluble antigen was aimed to be verified in presence of the XS CAR specific for CD66c. In contrast to the previously tested CD66c S CAR, the XS CAR contained a shorter hinge domain (XS). It was shown previously by Schaefer *et al.* that the CD66c XS CAR was outperforming the CD66c S CAR in a pancreatic tumor model²¹⁵. The incorporation of the XS CAR into the experimental set-up also allowed to investigate whether the comparably high level of TGF- β in the AsPC-1-TGF model is suppressing the cytotoxicity of CAR T cells. Therefore, combined TAA targeting and soluble antigen sensing was tested in AsPC-1-TGF tumor-bearing mice (**Figure 28 A**) and AsPC-1 WT tumor-bearing mice supplemented with human soluble latent TGF- β -containing IVIG (**Figure 28 D**). In the latter model, mice were i.p. injected with 10 mg of human IVIG one day before CAR T cell injection. To control for potential AdCAR1 T cell activation induced only by aLAP, all control groups received a control adapter conjugated to multiple LLE moieties comparable to aLAP. The CAR expression and CD4:CD8 ratio were analyzed prior to injection by flow cytometry. AdCAR1 was expressed in 52.81 % of the cells and CD66c XS CAR was expressed in 58.94 % of the cells. The CD4:CD8 ratio was comparable between both cellular products (AdCAR1: 45.38 % CD4⁺, 50.62 % CD8⁺; CD66c XS CAR: 45.79 % CD4⁺, 49.66 % CD8⁺)

In the AsPC-1-TGF tumor-bearing mice, the combination of CD66c XS CAR T cells with AdCAR1 T cells did not induce tumor eradication neither in presence or absence of aLAP (**Figure 28 B**). Nevertheless, animals that have been treated with aLAP clearly showed higher levels of IFN- γ in sera on day four compared to controls (**Figure 28 C**). These results supported the previous finding that AdCAR1 T cells convert the soluble latent TGF- β into a pro-inflammatory stimulus in presence of a specific adapter molecule.

In comparison, in the AsPC-1 WT tumor-bearing mice supplemented with human latent TGF- β , the combination of CD66c XS CAR T cells with the AdCAR1 T cells induced tumor clearance both in absence and presence of aLAP (**Figure 28 E**). Tumor eradication started on day seven independently of the presence of aLAP. The killing kinetics were comparable between both cohorts. It should be noted that one animal in the aLAP-treated cohort showed tumor outgrowth after initial tumor control, whereas in the cohort without aLAP the tumor was cleared in all animals. The IFN- γ levels on day four were significantly higher in presence of aLAP confirming activation of AdCAR T cells by exogenously added soluble latent TGF- β (**Figure 28 F**).

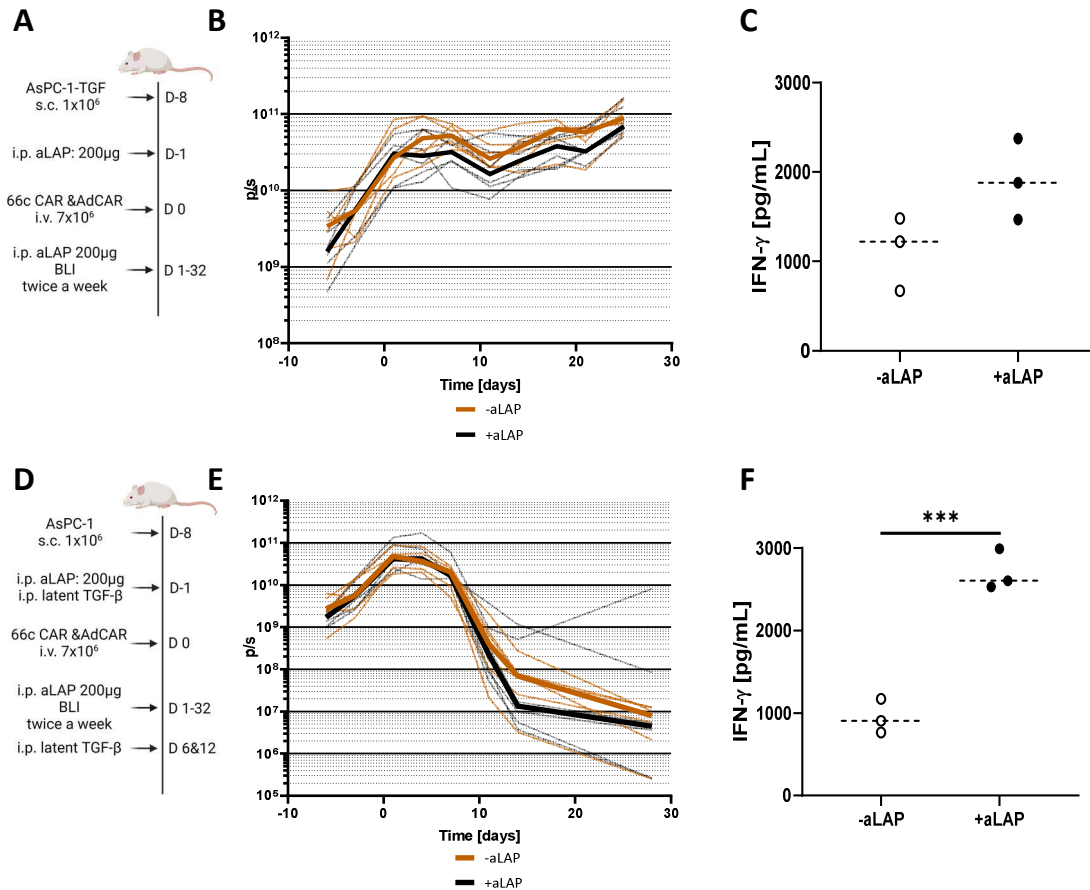


Figure 28: Treatment of AsPC-1-TGF- or AsPC-1 WT tumor-bearing mice with AdCAR1 T cells and CD66c xs CAR T cells in presence of aLAP.

Schematic representation of the study design to assess soluble antigen sensing and targeting a TAA in (A) AsPC-1-TGF tumor-bearing mice or (D) AsPC-1 WT tumor-bearing mice. Tumor growth of (B) AsPC-1-TGF and (E) AsPC-1 WT was analyzed by BLI imaging. Photon flux per second in presence of aLAP (black line: median; grey line: individual animals) or absence of aLAP (orange line: median; light orange line: individual animals) is plotted. Cytokine levels were determined of (C) AsPC-1-TGF tumor-bearing mice or (F) AsPC-1 WT tumor-bearing mice at day four after T cell infusion. Each dot represents one animal. Dashed lines represent median values. Statistical analysis was performed with unpaired two tailed t-test. Significance defined as: * $p \leq 0.05$; ** $p \leq 0.01$; *** $p \leq 0.001$; **** $p \leq 0.0001$. Illustrations were created with BioRender.com.

A comparison of the IFN- γ concentration between the AsPC-1-TGF and the AsPC-1 WT model supplemented with the soluble ligand showed higher cytokine secretion in the AsPC-1 WT model. This finding as well as the lack of anti-tumor efficacy observed in the AsPC-1-TGF model suggests that TGF- β was acting as a strong immunosuppressor in the AsPC-1-TGF tumor bearing mice. Surprisingly, the AdCAR1 T cells were still able to convert a soluble ligand into a pro-inflammatory stimulus. To get a better understanding of soluble target concentrations in both animal models, the levels of latent TGF- β in sera were analyzed by ELISA. Serum samples were collected five days after i.p. injection of IVIG-containing latent TGF- β . In sera of animals inoculated with AsPC-1 WT supplemented with latent TGF- β , no latent TGF- β was detected five days after first IVIG injection. In contrast, sera of animals bearing AsPC-1-TGF tumors contained approx. 200 ng/mL to 700 ng/mL of endogenously, tumor-secreted soluble latent TGF- β (Figure 29). This difference in systemic latent TGF- β concentrations may explain the difference in anti-tumor efficacy in both models.

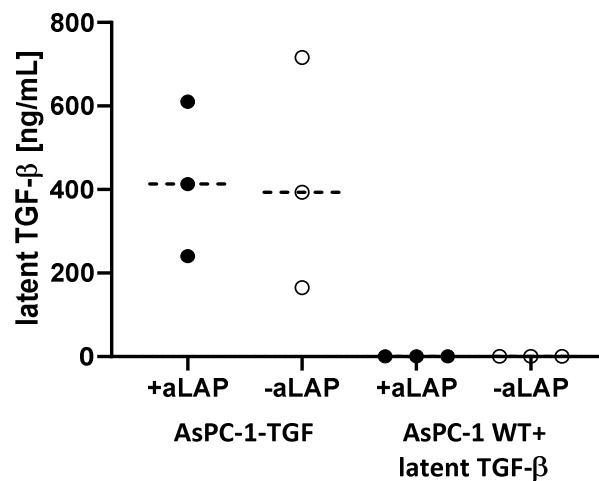


Figure 29: Concentration of soluble latent TGF- β in sera of AsPC-1-TGF or AsPC-1 WT-bearing mice.

Latent TGF- β quantified in sera of mice was sampled four days after T cell injection. Each dot represents one animal. Dashed lines represent median values.

Overall these data indicated no reduction in anti-tumor efficacy when AdCAR1 T cells and CAR T cells were combined to target different antigens. Based on the BLI measurement, the systemic activation of AdCAR1 T cells did not counteract local activation of CAR T cells *in trans*. The soluble antigen-mediated systemic activation and subsequent release of IFN- γ was confirmed. Although the CD66c XS CAR induced tumor reduction, a faster induction of IFN- γ release in dependency of aLAP indicated AdCAR stimulation by the soluble ligand. This showed that the previously observed differences in activation between CAR T cells and AdCAR T cells were not due to a nonfunctional CD66c CAR construct.

5.3.6 Endogenous immune cells enhance sensing of latent TGF- β and anti-tumor efficacy of AdCAR T cells in an immunosuppressive tumor model

One objective of this work was to demonstrate the feasibility of simultaneous targeting of a soluble ligand and a TAA with the same AdCAR. Within the TME of AsPC-1-TGF tumors, the presence of latent TGF- β has been shown previously (5.3.1). In principle, AdCAR T cells can bind both latent TGF- β and CD66c within the TME, when adapters for these targets are infused. This might result in synergies in controlling tumor growth. Local latent TGF- β might serve as an antigen for AdCAR T cells to destruct the TME in addition to tumor eradication via the TAA CD66c. However, the AsPC-1-TGF tumor model is challenging for CAR T cells as in all previous *in vivo* experiments the AsPC-1-TGF tumor model was shown to be very resistant to CAR T cell-induced killing. CD66c specific CAR T cells did only induce a transient control of AsPC-1-TGF tumors. Therefore, further improvement was needed to enhance therapeutic outcome in this highly immunosuppressive model.

To investigate whether a potential engagement of immune cells in addition to AdCAR T cells could lead to an improved anti-tumor response in such an immunosuppressive environment, AdCAR T cells were co-infused with autologous PBMCs. The importance of endogenous immune cells has been studied previously for targeting the TME of solid cancer with CAR T cells^{65,217}. In contrast, the treatment strategy presented in this work allowed to combine two different AdCAR-related modes of action. First, the targeting of a TAA and second, the novel sensing of a soluble ligand. Thus, mice were i.p. injected with either aCD66c or with a combination of aCD66c plus aLAP (**Figure 30 A**). Deviating from previous *in vivo* studies, T cells were transduced to express AdCAR2. Based on the previous observation that AdCAR2 showed higher tumor cell lysis at lower concentrations of aCD66c and simultaneously higher aLAP concentrations *in vitro*, this construct was used for *in vivo* testing here. The CAR expression and CD4:CD8 ratio were analyzed prior to injection by flow cytometry. AdCAR2 was expressed in 84.71 % of the cells. The cellular product was composed of 67.11 % CD4⁺ cells and 24.31 % CD8⁺ cells.

When AdCAR2 T cells were given in combination with autologous PBMCs reduction of tumors was observed in presence of aCD66c or aCD66c plus aLAP on day 18, whereas all other cohorts showed a progression of tumor growth (**Figure 30 B**). After day 18, in all cohorts, progression of tumor growth was observed. Nevertheless, AsPC-1-TGF tumor burden was significantly reduced in reconstituted mice treated with AdCAR2 T cells in combination with aCD66c or aCD66c plus aLAP at the endpoint on day 25. Interestingly, the anti-tumor effect was lost in absence of autologous PBMCs. In absence of PBMCs, the combinatorial targeting of soluble latent TGF- β and CD66c resulted in a higher tumor burden compared to animals treated with aCD66c alone. As in previous experiments, the release of IFN- γ on day four was used as a readout for soluble antigen-induced AdCAR T cell activation (**Figure 30 C**). The combination of aCD66c and aLAP led

to higher IFN- γ secretion compared to mice treated with aCD66c alone. Furthermore, the presence of autologous PBMCs enhanced IFN- γ production. Co-injection of AdCAR2 T cells and PBMCs induced significantly higher IFN- γ levels in cohorts treated with both adapter molecules. Surprisingly, this effect was observed in absence of adapter molecules as well, but was not seen in mice injected only with aCD66c. The unexpected high levels of IFN- γ in absence of adapter may indicated tonic signaling of the AdCAR2 construct as the cytokine secretion was suppressed in presence of aCD66c. In addition, it was observed that PBMC injection alone did not result in elevated IFN- γ production highlighting the importance of the mutual dependency between AdCAR2 T cells and PBMCs to boost pro-inflammatory cytokine secretion. Conclusively, AdCAR2 T cells were able to sense a soluble ligand and induced tumor cell killing simultaneously. For the first time AdCAR2 T cells controlled the tumor growth partially in the immunosuppressive AsPC-1-TGF model. In the same experimental setting, AdCAR2 T cells also responded to a soluble ligand. Most importantly, the sensing of a soluble ligand did not counteract the cytolytic potential of AdCAR2 T cells targeting a TAA. Overall, the enhanced anti-tumor effect can be attributed to the co-administration of PBMCs. Both the tumor control and the cytokine secretion were strengthened in this reconstituted model.

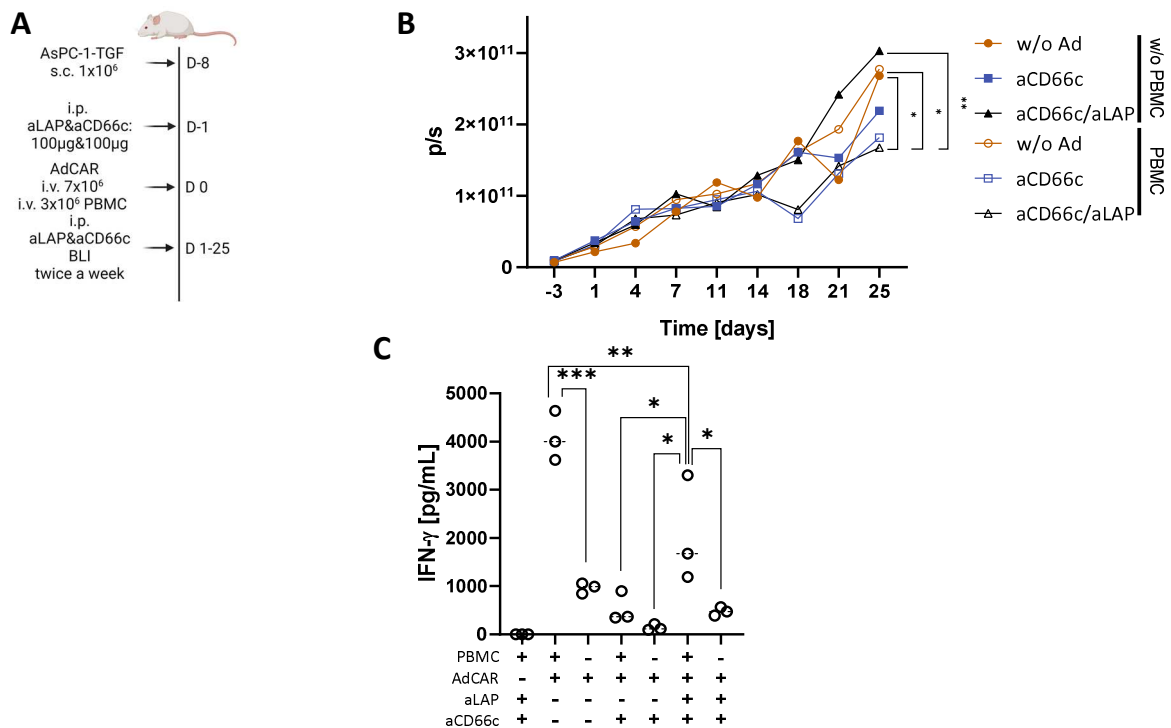


Figure 30: Treatment of AsPC-1-TGF tumor-bearing mice with autologous PBMCs and AdCAR2 T cells in presence of aLAP plus aCD66c.

(A) Schematic representation of the study design to investigate AdCAR2 T cell treatment combined with co-administration of autologous PBMCs in AsPC-1 TGF- β tumor bearing NSG mice. (B) Tumor growth of AsPC-1-TGF was analyzed by BLI imaging. At least five mice were analyzed per cohort and median values of photon flux are plotted. (C) Quantifications of IFN- γ levels in sera are shown. Blood was drawn at day four. Each dot represents one animal. dashed lines represent median values. Statistical analysis was performed with (B) Two-way ANOVA or (C) ordinary one-way ANOVA. Correction for multiple comparisons was done by Holm-Sidak correction. Significance defined as: * $p \leq 0.05$; ** $p \leq 0.01$; *** $p \leq 0.001$; **** $p \leq 0.0001$. Illustrations were created with BioRender.com.

5.3.7 Endogenous immune cells enhance proliferation and tumor infiltration of AdCAR2 T cells in an immunosuppressive tumor model

In addition to impacts on tumor growth and cytokine production as effector mechanisms of AdCAR2 T cells (5.3.6), the proportion of human cells infiltrating the spleen and the tumor tissue was assessed *ex vivo* at day 25 (**Figure 31 A-B**). In spleens and tumors, the co-administration of PBMCs together with AdCAR2 T cells led to higher frequencies of human immune cells compared to mice which did not receive autologous PBMCs. However, the increase of CD45⁺ cells was not adapter-dependent and the highest levels of CD45⁺ cells were found in spleens in absence of adapter. In contrast, mice treated with a combination of aLAP and aCD66c showed lowest frequencies of CD45⁺ cells in the spleens amongst PBMC reconstituted cohorts. Almost no CD45⁺ cells were detected in cohorts treated with PBMCs in absence of AdCAR2 T cells. In tumor tissue, the overall levels of CD45⁺ cells showed no significant differences between all reconstituted cohorts, irrespective of the adapter molecule administered. As observed in the spleens, the frequency of CD45⁺ cells was higher in tumor tissue when AdCAR2 T cells and PBMCs were combined independent of the adapter administration. In comparison to spleens, the frequency of immune cells was approx. two to three times lower in the tumors indicating good engraftment of cells but low tumor infiltration.

To further characterize the effects of autologous PBMCs on AdCAR2 T cells in the immunosuppressive environment of AsPC-1-TGF tumors, the detailed immune cell composition was analyzed in spleens and tumor tissues of cohorts co-injected with PBMCs (**Figure 31 C**). The immune cell composition was analyzed by flow cytometry (Table 10). Both in spleens and tumor tissues, T cells represented the majority of immune cells followed by NKT cells. In spleens, the proportion of T cells was increased when mice received both adapter molecules. In contrast to tumor tissues, B cells were found in spleens. Interestingly, the highest frequency of B cells was present in absence of any adapter and the lowest frequency was found in presence of aCD66c and aLAP. This shift in immune cell composition towards T cells may indicate antigen-induced T cell activation.

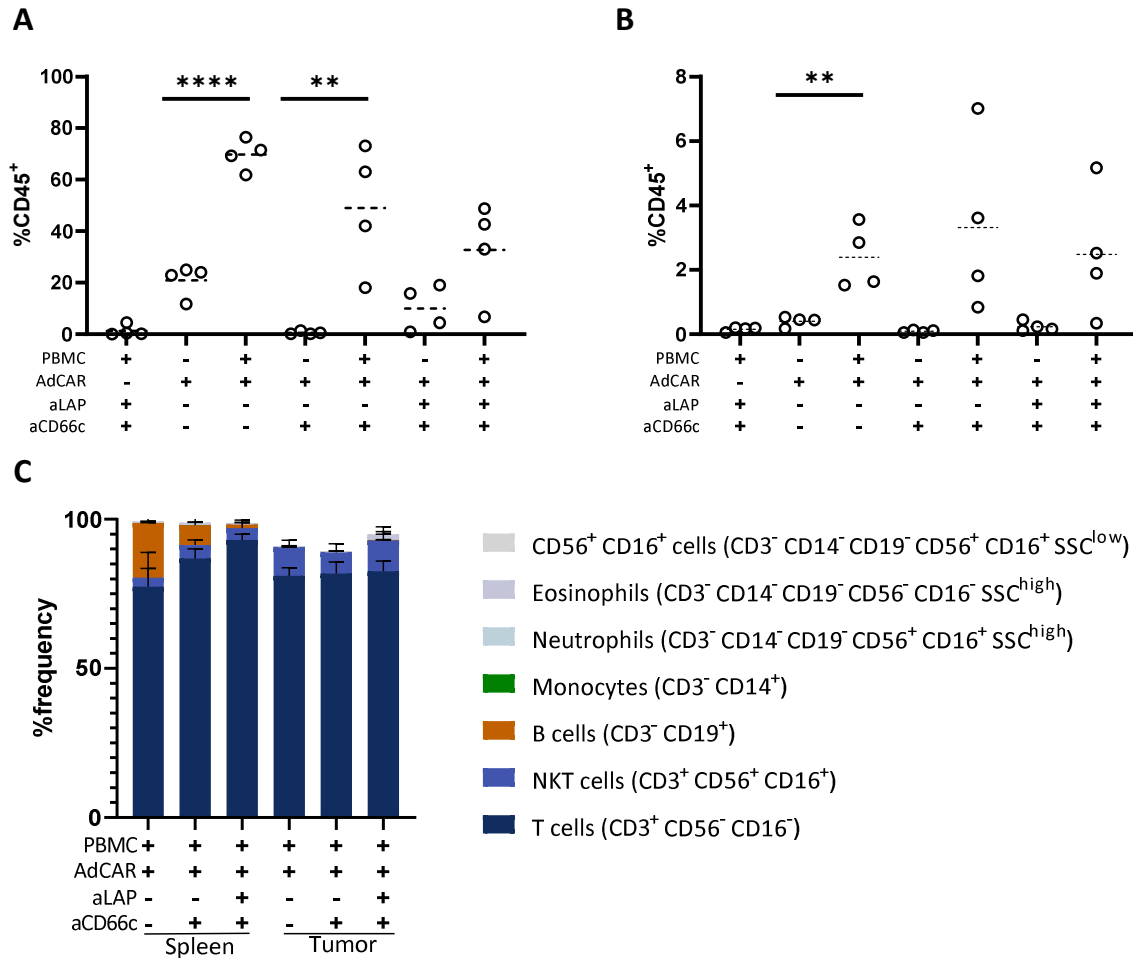


Figure 31: Immune cell engraftment and immune cell composition in AsPC-1-TGF tumor-bearing mice treated with AdCAR2 T cells and autologous PBMCs in presence of aLAP plus aCD66c.

Ex vivo analysis of viable CD45⁺ cells in (A) spleens and in (B) tumor tissues at day 25. Each dot represents one animal. Dashed lines represent median values. (C) *Ex vivo* analysis of immune cell compositions in spleens and tumor tissues. Statistical analysis was performed with unpaired t-test, correction for multiple comparisons was done by Holm-Sidak correction. Significance defined as: * $p \leq 0.05$; ** $p \leq 0.01$; *** $p \leq 0.001$; **** $p \leq 0.0001$.

To support this assumption, the CD8 frequency of T cells in spleens and tumors was analyzed as an indicator for adapter-mediated AdCAR2 activation (**Figure 32 A**). In spleens, a significantly higher frequency of CD8⁺ T cells was found in animals treated with aLAP and aCD66c compared to aCD66c treatment or in absence of adapter molecules. This finding might have been caused by the systemically present soluble latent TGF- β . In the tumor tissue the, frequency of CD8⁺ T cells was comparable between cohorts injected with aCD66c or a combination of both adapters. Both cohorts showed significantly more cytotoxic T cells compared to absence of adapter. Although T cells were stimulated in an adapter- and antigen-dependent manner no complete tumor control was observed. One explanation for this could be the exhaustion of T cells due to chronic antigen stimulation. To further analyze exhaustion, CD279 (PD-1), CD366 (TIM3) and CD223 (LAG3) expression on T cells isolated from spleens or tumor tissues were analyzed by flow cytometry (**Figure 32 B**). The tumor-infiltrating lymphocytes showed high levels of T cells

expressing PD-1, TIM3 and LAG3. Only a small fraction of T cells located in spleens showed this phenotype. The administration of adapters did not induce differences in the expression patterns of analyzed exhaustion markers. This finding may explain the tumor outgrowth after the initial tumor reduction as T cells expressed markers indicative for dysfunctionality within the TME of AsPC-1-TGF tumors.

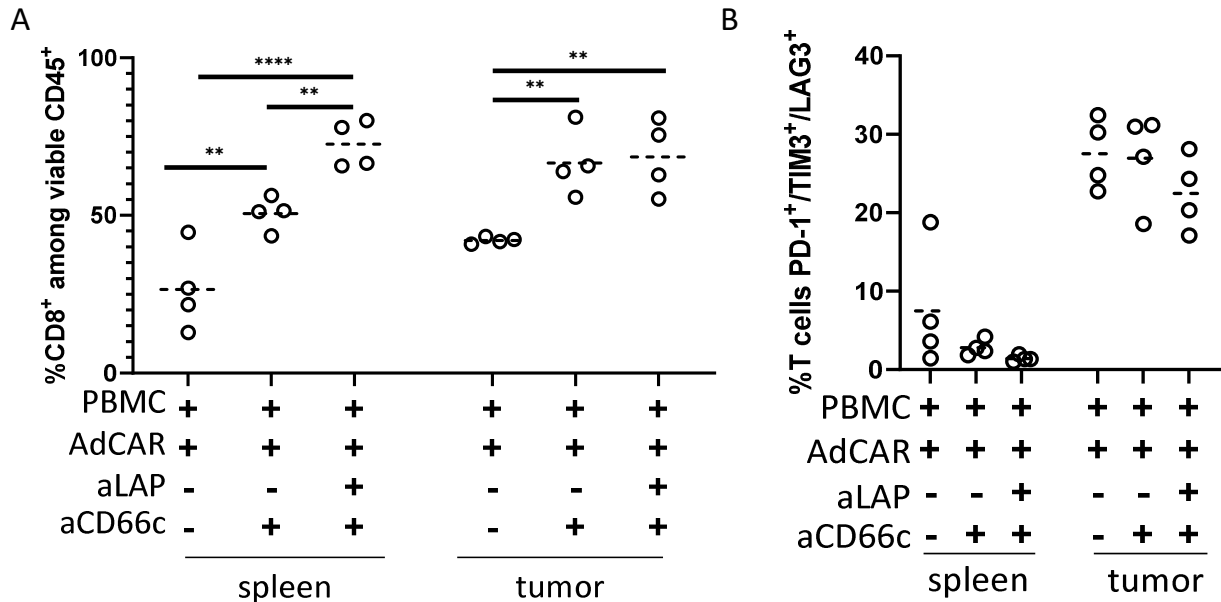


Figure 32: CD8 frequency and exhaustion marker expression on T cells isolated from AsPC-1-TGF tumor-bearing mice treated with AdCAR2 T cells in presence of aLAP plus aCD66c.

(A) *Ex vivo* analysis of viable CD8⁺ T cells was done by flow cytometry after immune cell isolation from spleens and tumor tissues, respectively. (B) In addition, T cells were used for *ex vivo* analysis of exhaustion marker expression on T cells isolated from spleens as well as tumor tissues. Each dot represents one animal. Dashed lines represent median values. Statistical analysis was performed with Two-way ANOVA. Correction for multiple comparisons was done with Holm-Sidak correction. Significance defined as: * $p < 0.05$; ** $p < 0.01$; *** $p < 0.001$; **** $p < 0.0001$.

These results showed that autologous PBMCs improve AdCAR2 T cell functionality by enhancing the engraftment of immune cells in an immunosuppressive TME that is rich in TGF- β . The survival of autologous PBMCs was dependent on the presence of AdCAR2 T cells as there was almost no engraftment seen in mice which only received PBMCs. In accordance with the cytokine data presented previously (5.3.6) AdCAR2 T cells demonstrated activation in absence of adapter indicated by elevated levels of CD45⁺ cells both in spleens and in tumor tissues. Nevertheless, the signature of CD8 expression revealed antigen-induced AdCAR2 T cell activation in presence of either the soluble antigen or the TAA. The monitored aLAP-dependent increase of CD8⁺ T cells in spleens confirmed that a soluble ligand was able to trigger cytotoxic T cell activation.

5.3.8 Cytotoxic T cells show adapter-dependent accumulation in the peritumor

In addition to the previously described flow cytometric analysis (5.3.7) the infiltration of T cells into the tumor was investigated by immunofluorescent imaging (**Figure 33**). In contrast to the *ex vivo* analysis of digested tumor material used for flow cytometry, this method adds spatial information on T cell penetration of the tumors. In this way, microscopy may provide a better understanding of possible limitations and hurdles with regard to incomplete tumor eradication. In absence of adapters, mostly CD4⁺ cells were found in the surroundings of the tumors. Only a minor fraction of cells was invading the tumor. In presence of either aCD66c or aCD66c plus aLAP mainly CD8⁺ T cells were detected prominently in the peritumor. Importantly, in these cohorts, the T cells showed invasion into the solid tumor mass as well, which was not seen in absence of adapter. Neither in the peritumor nor in the center of the tumor, aLAP altered the infiltration of T cells compared to treatment with aCD66c alone. The structure of the tumor tissue was comparable between cohorts treated with either aCD66c alone or both adapters. Based on this observation no structural changes in the stroma were observed.

In summary, this analysis of tumor tissue by immunofluorescent imaging validated the results obtained by flow cytometry. Only in presence of adapter molecules an increase in CD8⁺ T cells was observed indicating an antigen-dependent activation. Based on the immunohistochemistry data it can be concluded that T cells attach to the tumor edge but the ability to invade the tumor mass appears to be limited. The limited amount of cells penetrating the tumor may explain incomplete tumor eradication.

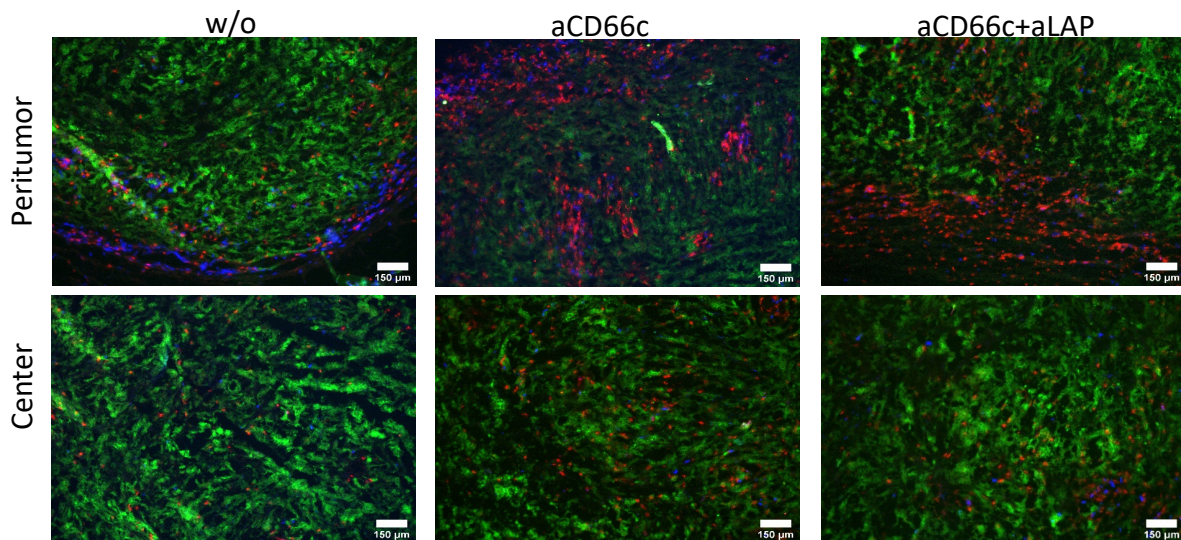


Figure 33: T cell infiltration in tumors of AsPC1-TGF tumor-bearing mice treated with AdCAR2 T cells and autologous PBMCs in presence of aLAP plus aCD66c.

The spatial distribution of T cells in AsPC1-TGF tumors and surrounding tissue was analyzed by immunofluorescence imaging (CD8: red, CD4: blue, EpCAM: green). Tumor slices (8 μm) of cohorts injected with AdCAR T cells and autologous PBMCs were analyzed at the endpoint of the *in vivo* study. Images from the peritumors and the center of tumors are shown. Images were taken with 10x magnification. Scale bar represents 150 μm.

Data shown in figures 8-13, 15-18, 20 and 30-32 are part of a published manuscript²¹⁸.

6. Discussion

Soluble molecules, e.g. cytokines or chemokines play a central role in cancer progression by orchestrating the interplay of malignant and non-malignant cells within the TME. Despite of their importance, soluble molecules have been omitted as antigens for CAR T cells to elicit or support anti-tumor response. The feasibility to target soluble TGF- β directly by CAR T cells was demonstrated recently²¹⁶. Nevertheless, targeting a soluble antigen alone will most probably not be sufficient to elicit complete tumor eradication. An additional limitation of directly targeting soluble antigens with CAR T cells is on-target off-tumor toxicity as soluble CAR ligands are not tumor confined. Therefore, a tight control is required when using soluble ligands as CAR antigens. In principle, the recently developed AdCAR technology would allow a controllable multiplexed targeting of different antigens, as shown for membrane bound antigens but not for soluble ligands⁸⁷. The response of AdCAR T cells towards soluble ligands has not been described so far.

The data obtained within the presented study demonstrated that AdCAR T cells are sensitive for sensing soluble antigens *in vitro* and *in vivo* upon complexing the soluble ligand by an adapter molecule. The activation was dependent on the adapter and the antigen concentration and thus controllable. The concept of converting latent TGF- β , an immune-suppressive cytokine involved in a variety of solid cancers, into a pro-inflammatory trigger for AdCAR T cell activation was functional *in vivo* as well. Importantly, it could be combined with targeting a TAA employing the very same AdCAR T cell product.

6.1 Latent TGF- β is localized in the TME of ovarian tumors

The TME of solid tumors is a complex structure composed of malignant and non-malignant cells. In addition to cellular components, soluble factors play a major role in shaping the immune responses to cancer. TGF- β is known as a potent inhibitor of T cell-mediated anti-tumor immune response²¹⁹. Interestingly, TGF- β is secreted and can be anchored to the ECM within the tumor stroma in its latent form²²⁰. Therefore, latent TGF- β represents a potential target for CAR T cell therapy targeting the TME rather than the tumor itself. To decipher the spatial distribution of latent TGF- β in human tumors and its co-localization with other cellular- or ECM-components within the TME, human ovarian cancer tissue was analyzed with cyclic fluorescent imaging. This technique allowed to visualize the localization of latent TGF- β within the TME and to quantify the co-expression of latent TGF- β in relation to other surface markers on tumor and non-tumor tissue. Latent TGF- β was found to be expressed in desmoplastic areas of human ovarian cancer. Within these areas it was co-localized with CD90 and CD49a. CD49a showed the highest correlation with LAP in the analyzed human ovarian cancer tissue. This integrin is binding to collagen in the ECM of malignant tissue. In ovarian cancer, CD49a expression was

reported and low CD49a expression was linked to drug resistance in ovarian cancer²²¹. CD49a was also linked to other solid cancers, e.g. PDAC in which CD49a was necessary for chemotherapy resistance of PDAC cells, cell attachment and spreading²²². CD90, which showed the second highest correlation, is a fibroblast marker that can be found on CAFs²²³. The existence of CAFs in the stroma of ovarian cancer has been described previously^{112,224,225}. CAFs are reported to enhance tumor invasiveness through direct cell-cell interactions or by secreting chemokines. For instance, CAF-derived CCL5 was reported to be a regulator of metastasis in ovarian cancer^{112,226}. Overall, these reports highlight the relevance of CD90 and CD49a within the TME and support the cyclic fluorescent imaging data obtained in this work.

The co-expression of LAP, as a surrogate for TGF- β , with CD90 and CD49a can be linked to biological processes that are mediated by TGF- β in the TME. Ovarian cancer cells were reported to secrete TGF- β for active recruitment of CAFs. TGF- β is reported to promote the conversion of mesothelial cells to myofibroblasts. After transitioning to this mesenchymal phenotype, CAFs contribute to ECM remodeling and cancer invasiveness by secreting, e.g. fibronectin^{227,228}. In addition, CAFs themselves were reported to secrete TGF- β . CAF-derived TGF- β was shown to be a potent mediator of ECM remodeling in ovarian cancer by inducing signaling cascades leading to MMP secretion²²⁹. Furthermore, an interplay of CD49a and TGF- β was demonstrated as well. CD49a and TGF- β response genes were found to be co-expressed in samples of pancreatic cancer patients, indicating functional relations of both proteins²²². In TMEs rich of collagen, CD49a and TGF- β were found to synergistically drive cancer progression and therapy resistance²²².

In summary, these studies support the observed co-expression of LAP with CD90 and CD49a found in this work. Therefore, latent TGF- β appears to be a potential target for directing AdCAR T cells to the TME and tumor stroma regions.

Similar approaches were already tested successfully for CAR T cells by targeting a splice variant of fibronectin or the fibroblast activation protein (FAP) expressed by fibroblasts^{65,217}. For further validation of LAP expression and spatial distribution in human cancer tissue, the correlation of known LAP binding partners e.g. LTPB, integrins or GARP should be included into, e.g. cyclic fluorescent imaging analysis²³⁰⁻²³².

For the clinical translation of a therapeutic concept targeting the stroma rather than the tumor, one paradigm is to minimize on-target off-tumor toxicity. One way to achieve this is to target molecules which are predominately present in malignant stroma. However, based on the cyclic fluorescent imaging data shown here, LAP was also expressed in absence of tumor cells. For a comprehensive conclusion whether LAP is suitable to distinguish between tumor and non-tumor tissue quantitative data rather than qualitative expression data would be required. In a study by Cao *et al.*, clinical samples of gastric cancer patients showed high LAP expression in

the tumor, whereas less LAP expression was found in the peritumor. This study described LAP expression in gastric cancer as a suitable prognostic factor for patient survival and found evidence for a correlation of high LAP expression and dysfunctional T cells²³³. The differential expression intensity further highlights the possibility to use LAP for discrimination between healthy and malignant tissue. Although LAP was found to be expressed in less desmoplastic regions of tumors as well, different expressions levels across a patient's tissue may nonetheless be suitable to direct the cytotoxic activity of AdCAR T cells to the tumor area.

In addition to its localization in the ECM, LAP was also found as a soluble protein circulating in the plasma of healthy subjects, demonstrating that latent TGF- β can occur either ECM bound or as soluble protein circulating in the blood²³⁴. This is in accordance with observations within this work, since latent TGF- β was detected in the supernatant of the glioblastoma cell line H4, the pancreatic tumor cell line AsPC-1-TGF and in the serum of mice inoculated with AsPC-1-TGF.

Besides its localization and prognostic relevance in the TME, the LAP TGF- β complex is a relevant target because it is involved in the regulation of the immune response. A central role of LAP is to control TGF- β activity upon secretion since membrane tethering by LAP allows TGF- β to signal either in an autocrine or paracrine manner²³¹. In addition, TGF- β independent functionality was described. LAP acts as a chemoattractant for monocytes and showed anti-inflammatory response in a mouse model independently of TGF- β ²³⁵. Furthermore, LAP was described as a chemoattractant for squamous carcinoma cells promoting cancer cell invasion²³⁶. The role of LAP as a chemoattractant is of particular interest as this implies that LAP can build a gradient which could be exploited for CAR T cell therapies to guide CAR T cells towards the tumor. Interestingly, the process of squamous carcinoma cell invasion was inhibited by the soluble form of LAP, indicating differential modes of action depending on LAP being present in its ECM anchored or soluble form²³⁶.

The significance of LAP as a suitable target moiety for CAR T cells is further supported by a study conducted by Gabriely *et al.* using an anti-LAP antibody to improve anti-tumor response in mouse tumor models²³⁷. The application of anti-LAP antibodies led to a reduction of tumor growth in different immunocompetent mouse tumor models, e.g. melanoma, orthotopic glioblastoma and orthotopic colorectal cancer²³⁷. Mechanistically, the authors found a reduction of CD103⁺ tolerogenic T cells, T_{regs} and immature immunosuppressive LAP⁺ DCs^{237,238}. This study highlights that LAP is suitable to target a diverse set of immunosuppressive cell types commonly found in the TME of various cancers.

The conclusive assessment of latent TGF- β as a CAR target is complex and involves numerous aspects. Latent TGF- β is either contributing or actively promoting a variety of processes involved in immune evasion of tumor cells, which argues for latent TGF- β being a relevant target to treat cancer. This is further supported by first promising results obtained in mouse models

targeting LAP by mAb therapy. The most critical point to keep in mind when latent TGF- β is considered as a CAR target is its localization. Although LAP can be found in the TME of solid cancers and shows a prognostic relevance, it is not exclusively tumor confined, especially as it is present as a soluble molecule. Therefore, potential on-target off-tumor toxicities need to be evaluated in future studies. However, the presence of latent TGF- β , as both membrane-bound and soluble molecule distinguishes this cytokine complex from other antigens to target the TME by CAR T cells. Utilizing this soluble antigen thus may improve CAR T cell therapy for solid tumors²¹⁶.

6.2 AdCAR T cells are activated by soluble antigens and effector responses are tunable by both adapter and antigen dose

CAR T cells were initially designed to directly recognize antigens expressed on the surface of cells for targeted killing of malignant cells, independent of HLA presented antigens. Typically, the specificity of a CAR is mediated by an extracellular scFv coupled to intracellular signaling molecules which are derived from the endogenous T cell activation cascade⁵⁹. In the study presented here, T cells were engineered to express an AdCAR specific for LC-LC biotin. In contrast to a conventional CAR, the AdCAR does not directly bind to its targeted molecule but to the tag of an adapter, e.g. antibodies or fragments thereof. Hence, only in combination with an adapter molecule the CAR will be able to bind to its target and induce T cell effector function. Indeed, the data obtained within the presented study demonstrated that soluble hLAP and soluble latent TGF- β in presence of a tagged IgG₁ adapter molecule do trigger AdCAR T cell phenotypic activation and cytokine secretion. Importantly, this response was dependent on the adapter as well as on the soluble ligand concentration.

In the past, the effect of soluble ligands on engineered T cells was mainly investigated with a focus on potential inhibitory effects on T cells. For instance, it was reported that soluble CD30, CEA, Lewis-Y or CEA do not inhibit the anti-tumor effect of T cells specific for the respective membrane bound antigen^{239–241}. Soluble BCMA was described not to limit expansion or anti-tumor effect *in vivo*. However, Pont *et al.* described reduced cytokine secretion of CAR T cells in presence of soluble BCMA^{242,243}. In addition, anti-Glypican-3 CAR T cells showed reduced anti-tumor response in a hepatocellular carcinoma secreting the soluble target antigen²⁴⁴. In this light, the seminal work of Chang *et al.* opened up an entirely new perspective for soluble CAR targets. The authors demonstrated that CAR T cells can be engineered to respond to soluble ligands and convert *per se* inhibitory signals, e.g. TGF- β , into stimulatory cues of T cell effector functions^{216,245}. As a pre-requisite, the soluble antigen needed to complex at least two CAR molecules, subsequently leading to intracellular activation of the CAR downstream signaling cascade²¹⁶.

To meet the criteria of CAR complexation upon soluble antigen sensing with AdCAR T cells, a homodimeric soluble antigen and an adapter with multiple tags were used in this study. Both LAP and latent TGF- β are homodimers. Therefore, one antigen molecule can form a complex with two adapter molecules and subsequently crosslink at least two CAR molecules to induce downstream signaling. However, not all antigens that might appear attractive in the future to target within the TME do form homodimers. In this case, AdCARs would be advantageous compared to a conventional CAR approach because crosslinking of CARs with proteins not forming homodimers would require the expression of two CARs with different specificities. This would mean a more labor intensive CAR T cell transduction and higher production costs, whereas AdCAR T cells can target multiple antigens by applying different imparting adapters⁸⁷. In addition, the mode of operation of an AdCAR does further support multimerization of CAR molecules on T cells surface through multivalency of the adapter and multiple tags conjugated to one adapter. Due to the multivalency of the IgG₁-derived adapter molecule, one CAR engages two antigens. In combination with a homodimeric target, this enables a concatenation of CARs on the T cell surface. As the adapter molecules used in the presented study contained multiple binding sites, it can be assumed that this contributes to CAR multimerization as well. In sum, AdCARs have advantages in terms of dimerization by soluble antigens compared to a CAR approach.

One important characteristic to consider is the sensitivity at which the soluble antigen-CAR-complex induces intracellular signaling. Although AdCAR T cells tested in this work sensed antigens in a dose dependent manner, the sensitivity towards latent TGF- β was clearly lower than the sensitivity of the conventional CAR to TGF- β . The AdCAR was activated from 2 $\mu\text{g}/\text{mL}$ to 193 $\mu\text{g}/\text{mL}$ latent TGF- β , whereas the CAR detected TGF- β at concentration approx. one log scale lower²¹⁶. Due to the low concentrations of latent TGF- β secreted by various tumor cell lines *in vitro*, the AdCAR system would not be sensitive enough to get activated by the supernatants of these cell lines. Of the tested cell lines, H4 a neuroglioma cell line, was found to secrete the highest amount of latent TGF- β at approx. 200 ng/mL. That concentration would still be below the detection limit of AdCAR T cells. To ensure stable and reasonable secretion of latent TGF- β by tumor cells to characterize the system for soluble antigen sensing *in vitro* and *in vivo*, the AsPC-1 WT tumor cell line was modified to constitutively express latent TGF- β . It should be noted that the concentration of latent TGF- β measured *in vitro* cannot be predictive for the concentrations later found *in vivo*, as latent TGF- β can either accumulate or diffuse within the TME. Furthermore, the amount of soluble antigen depends on the amount of tumor cells inoculated *in vivo* and subsequent tumor growth kinetics.

To improve the sensitivity of the system several modifications of the CAR architecture can be made. Chang *et al.* proposed a mechanotransduction model that requires a reasonable stiffness of the CAR construct²¹⁶. Based on this model it can be deduced that the AdCAR design is crucial

for sensing soluble antigens. In this context, it was essential to prove in AdCAR T cells that coupling of the CAR to its soluble antigen via an antibody indeed resulted in T cell activation, since this coupling is expected to be less rigid compared to a conventional CAR. Hence, it can be assumed that an increased affinity between AdCAR and adapter, as well as between adapter and antigen, would lower the detection limit of soluble antigen sensing. As already mentioned the CAR design, e.g. the length of the spacer domain, can influence the performance of the CAR. Reducing the length of the extracellular spacer domain resulted in higher sensitivity of the CAR towards TGF- β in the proof of concept study done by Chang *et al.*²¹⁶. Since the AdCAR tested in the study presented here already contained the short IgG₄ hinge domain this structural element is most probably not the main cause for the lower sensitivity of AdCAR T cells. One major difference between the two CAR architectures, besides the adapter molecule, is the TM domain. The AdCAR has a CD8 TM domain in comparison to the anti TGF- β CAR which contained a CD28 TM. In previous studies it was shown that the TM can have a significant impact on CAR performance. In a comparative study of CD28 TM and CD8 TM only the CD28 TM was able to activate endogenous CD28⁷⁰. Therefore, the TM can change the composition of the immunological synapse formed by the CAR by engaging with endogenous T cell signaling molecules and lower the activation threshold²⁴⁶.

Another critical component influencing the sensitivity of a CAR is the configuration of co-stimulatory endodomains for efficient intracellular signaling. In this study, a third generation CAR containing CD28 and 4-1BB co-stimulatory domains was used. This signaling complex may need further optimization to increase the sensitivity of the AdCAR T cells. Previously, improved antigen sensitivity of CARs was achieved by adding two CD3 ζ elements to a 4-1BB co-stimulation domain²⁴⁶. In addition, besides the commonly used co-stimulatory domains CD28 and 4-1BB, other intracellular signaling moieties need to be considered. Breuning *et al.* incorporated signaling motifs of CD6 which is a co-receptor of T cells involved in synapse formation and demonstrated improved CAR T cell effector function when compared to 4-1BB mediated signaling^{247,248}. These results highlight that the identification of the best CAR design is still an empirical process. To this end, an empirical evaluation of the best CAR design for AdCARs which are re-directed to sense soluble antigens is just at the beginning.

6.3 AdCAR T cells can target a soluble antigen and a TAA simultaneously

In principle, AdCARs allow to target multiple target antigens by sequential or even simultaneous administration of adapter molecules which differ in specificity. Indeed, using three different adapter molecules specific for CD19, CD20 and ROR1, Seitz *et al.* demonstrated the combination of different adapters. The adapters functioned as an “OR” gate and led to differential killing

of target cells in dependency of TAAs expressed on the target cell⁸⁷. The transferability of simultaneous TAA targeting to the simultaneous targeting of a soluble ligand and a TAA was investigated within the study presented here. To this end, AdCAR T cells were co-cultured with AsPC-1 WT and AsPC-1-TGF in presence of different mixtures of aLAP and aCD66c. It could be shown that both killing of CD66c⁺ tumor cells and sensing of latent TGF- β was mediated simultaneously by AdCAR T cells. In accordance with previous results obtained with hLAP, AdCAR T cells were activated in dependency of aLAP concentration when cultured with supernatant of AsPC-1-TGF. Surprisingly, an activation of AdCAR T cells was also observed in an aCD66c-dependent manner when supernatant of AsPC-1 WT was provided. In theory, the activation of AdCAR T cells might have been induced by crosslinking of CAR molecules by the multiple-biotinylated aCD66c. However, this activation was not observed with multiple-biotinylated aLAP in absence of aCD66c. Thus, an adapter-induced activation can be excluded as trigger for AdCAR T cell activation. In fact, this unexpected finding indicates that the supernatant of AsPC-1 WT contains soluble CD66c. Grunert *et al.* found concentrations of approx. 40 ng/mL to 100 ng/mL CD66c in sera of patients diagnosed with uterus carcinoma²⁴⁹. As described earlier, AdCAR T cells got stimulated by soluble hLAP provided in comparable concentrations. Therefore, soluble CD66c secreted by AsPC-1 WT is likely to have induced the stimulation of AdCAR T cells. It should be noted that the activation strength induced by potential soluble CD66c was lower compared to the activation observed in presence of soluble latent TGF- β . Different concentrations of the soluble target antigens may explain this observation. To validate this hypothesis, and to definitely confirm the presence of soluble CD66c, the CD66c concentration in supernatant of AsPC-1 WT needs to be determined in future studies as it cannot be excluded that residual cells or debris might have triggered AdCAR T cell activation.

Furthermore, two different CAR constructs were tested and compared for simultaneous sensing of TAAs and soluble antigens in this study. The main difference between these constructs were the LLE specific scFv fragments. Based on data generated by our group, it is inferred that scFv hBio2 4G10 used in AdCAR2 has a higher affinity towards LC-LC-biotin. Interestingly, AdCAR2 T cells outperformed AdCAR1 T cells *in vitro* as the AdCAR2 T cells showed superior effector function at lower aCD66c concentrations with concomitant higher concentrations of aLAP. These data indicate that the AdCAR2 construct is more suitable for the simultaneous targeting of two antigens. Apart from a different promotor sequence, the affinity is the main difference between the two constructs. The affinity of the scFv appeared to be crucial for the performance of AdCAR2 in comparison to AdCAR1. It is not clear yet which affinity is needed to have optimal CAR activation. Previous research described that low affinity scFvs outperform binders of higher affinity, however, also the opposite finding was made^{63,250}. For the AdCAR concept, the role of affinity is even more complex, as the affinity of the CAR to its tagged adapter and the affinity of the adapter towards the antigen impacts the efficacy of the AdCAR T cells. For a leucine

zipper based AdCAR T cell approach, Cho *et al.* reported a positive correlation of effector functions and affinity of the CAR to the adapter molecule indicating the need for strong binding between an AdCAR and the corresponding adapter⁹⁰. Although this result is in line with the findings reported here, it needs to be clarified if this principle is universal and thus translatable to LLE-specific AdCARs as well.

In previous reports, conventional CARs were used to target multiple antigens. Different approaches, e.g. double transduction of T cells or mixing of different CAR T cell products have been described²⁵¹. A double transduction will lead to an undefined CAR T cell product consisting of single and double transduced T cells, which is not favorable for clinical translation. In addition, and as an alternative to double transductions, two CARs were encoded on a bicistronic vector to circumvent double transduction, as shown for BCMA-SLAMF7 CAR T cells²⁵². One drawback of this approach is the size of the transgene that needs to be packed into the LVV. The larger size of the bicistronic transgene will lead to lower LVV titers and reduced transduction efficacy compared to a monocistronic construct due to limited packaging capacity of LVVs²⁵³. In principle, one solution could be to equip a CAR with two scFv fragments with different specificities to create tandem CARs. Indeed, a CD19/20 tandem CAR developed by Schneider *et al.* is currently tested in a clinical trial (NCT03870945) to treat patients suffering from diffuse large B cell lymphoma²⁵⁴. In theory, a tandem CAR targeting CD66c and latent TGF- β could be used to induce tumor cell killing with combined soluble antigen sensing as well. However, the safety profile of such a cellular immunotherapy approach needs to be considered. Especially when targeting soluble antigens that are potentially more abundant in tumor tissue but also systemically available to infused CAR T cells. On-target off-tumor toxicity is a major risk for CAR T cell applications in the clinics, as severe side effects were observed in patients treated with Her2 and GD2 specific CAR T cells^{255,256}. To this end, especially latent TGF- β targeted by CAR T cells are anticipated to require a safety strategy since latent TGF- β can be found systemically in healthy individuals as well²³⁴. In this regard, AdCARs offer the advantage that T cell activity can be controlled by adapter removal or withdrawal of adapter injections. Thus, the AdCAR T cell concept enables simple CAR T cell generation for targeting multiple antigens and appears ideal for combined sensing of soluble antigen.

6.4 In the subcutaneous AsPC-1-TGF mouse model latent TGF- β is present both in serum and the TME

To investigate the sensing of soluble antigens *in vivo*, NSG mice were s.c. inoculated with AsPC-1-TGF. Analysis by immunofluorescence imaging of the solid tumor mass identified latent TGF- β within the TME of AsPC-1-TGF tumors. Latent TGF- β was found to be co-localized with tumor cells and fibronectin. In accordance with previous reports, which described latent TGF- β as not only being anchored to the ECM but also as a soluble molecule, latent TGF- β was detectable in the sera of AsPC-1-TGF tumor bearing mice as well. The concentration of the soluble ligand ranged from approx. 400 ng/mL to 10 μ g/mL depending on tumor size and time point of blood sampling.

The clinical relevance of this model is critical for evaluation of the potential clinical applicability of soluble latent TGF- β sensing with AdCAR T cells. However, knowledge about the local concentrations of latent TGF- β within the TME of human tumors is limited. For example, Hawinkels *et al.* analyzed the spatial distribution of total TGF- β and quantified total TGF- β in tissue homogenates of gastric tumors. Significantly higher levels of total TGF- β were found in tumor tissue homogenates (21.1 to 620.1 pg/mg) compared to adjacent control mucosa²⁵⁷. In addition, the spatial distribution of total TGF- β was compared between gastric tumor tissue and adjacent control tissue by immunohistochemistry. Total TGF- β was preferentially associated with epithelial and stromal staining²⁵⁷. The AsPC-1-TGF mouse model established in the presented study recapitulated this TGF- β distribution pattern, as latent TGF- β was found to be co-localized with tumor cells and fibronectin. In sum, and in line with the immunostaining of human ovarian cancer tissue presented in this study, these data indicate the presence of TGF- β in the TME at concentrations higher compared to non-malignant tissue.

Besides attached to the ECM, soluble latent TGF- β concentrations, ranging from 400 ng/mL to 10 μ g/mL, were also found in sera of mice inoculated with AsPC-1-TGF. In humans, elevated levels of TGF- β in sera of cancer patients suffering from, e.g. hepatocellular carcinoma or pancreatic ductal adenocarcinoma have been reported as well. Absolute values ranged from 1.69 \pm 1.46 ng/mL in hepatocellular carcinoma to 237.6 \pm 45.3 ng/mL in PDAC^{258,259}. These data indicate that clinical levels of TGF- β are depending on the particular disease and prone to inter-individual variation. For any comparison of latent TGF- β levels between the AsPC-1-TGF mouse model and clinical data, it is essential to stress that the cited clinical data refer to concentrations of TGF- β . Unfortunately, it is not clearly indicated whether the investigators of these studies quantified total or active TGF- β . If these studies were only referring to active TGF- β the levels of latent TGF- β in serum could change up to 65-fold²⁶⁰. In addition, a positive correlation of the TGF- β level with the tumor size was found, further showing the dynamic of the TGF- β concentration in tumor patients²⁶¹. This correlation was observed in the AsPC-1-TGF mouse model as well. Serum samples collected at day four contained approx. 400 ng/mL latent TGF- β , whereas

at day 30, latent TGF- β went up to approx. 10 $\mu\text{g}/\text{mL}$. Thus, at day four, latent TGF- β serum levels of AsPC-1-TGF-bearing mice were comparable to levels reported for PDAC. However, as tumor growth continued over time, the latent TGF- β levels in the AsPC-1-TGF mouse model exceeded clinically relevant levels.

For a more comprehensive understanding whether AdCAR T cells sense clinically relevant levels of latent TGF- β co-culture assays with patient-derived serum samples are advisable. Potentially, also the eligibility of a patient to such a soluble antigen targeting approach could be evaluated in this way.

Sensing of soluble latent TGF- β was also assessed in the AsPC-1 WT model in which exogenous latent TGF- β was supplemented by i.p. injection of IVIG. IVIG, which was injected to block Fc-receptor binding of adapter molecules, was found to also contain human latent TGF- β as shown by own ELISA data and confirming reports by Rißmann *et al.*²⁶². Mice received approx. 20 ng latent TGF- β i.p. which was sufficient to induce activation of AdCAR T cells. Interestingly, no latent TGF- β was detected by ELISA five days after the last i.p. injection. It could be assumed that due to renal clearance the concentration was below the detection limit of the ELISA²⁶³. This result indicates that AdCAR T cells do not require the high latent TGF- β concentrations observed in the AsPC-1-TGF mouse model to become activated. However, the AsPC-1 WT model was suitable to validate the stimulation of AdCAR T cells in presence of soluble latent TGF- β in absence of the ECM attached form. It further demonstrates that AdCAR T cells can sense latent TGF- β in a broad concentration range *in vivo*. Nevertheless, it does most likely not recapitulate the immunosuppressive TME due to the absence of latent TGF- β anchored to the stroma as it is found in primary cancer tissue.

However, to allow a more comprehensive evaluation of the clinical relevance of soluble antigen sensing by AdCARs, a mouse model with TGF- β concentrations equivalent to cancer patients is required for future studies. One option to investigate the impact of latent TGF- β and its gradients even better in pre-clinical models could be the use of mouse models in which the tumor arises spontaneously, rather than being transplanted. In previous reports it was demonstrated that the same tumor type can secrete different levels of TGF- β depending on whether it was transplanted or developed spontaneously²⁶⁴. In more detail, Guerin *et al.* found a seven-fold higher mRNA expression of TGF- β in the spontaneous MMTV-PyMT tumor model compared to the transplanted model²⁶⁴. Furthermore, the improved anti-tumor effect of TGF- β blocking antibodies combined with DMXAA was only observed in the spontaneous tumor model, whereas in a transplanted PyMT tumor additional blocking of TGF- β was not improving tumor regression²⁶⁴. This indicates that the level of TGF- β as well as the therapeutic translation of therapies targeting TGF- β are indeed a function of the tumor origin which needs to be considered to

improve the significance of pre-clinical results. Therefore, such a tumor model would be favorable as well to decipher the effect of sensing soluble latent TGF- β by AdCAR T cells on tumor rejection.

The TME is a major limitation of this study. In this study, an immune compromised subcutaneous xenograft tumor model was applied by inoculating NSG mice with AsPC-1-TGF. For this reason, central components of the TME, e.g. stroma organization, vascularization or immune infiltration, are not comparable to primary tumors. The stroma of primary tumors is typically organized by stromal cells like fibroblasts²⁶⁵. Xenografts, even when patient-derived, lose stromal cells during *in vitro* cell cultivation. Therefore, tumor matched fibroblasts can no longer contribute to build up stromal structures in mouse models as found in primary human tumors. Consequently, the stroma of the implanted tumor is either reconstituted by mouse stroma and/or tumor cells²⁶⁶. Extensively cultured tumor cells can undergo EMT switch *in vitro* and therefore segregate fibronectin on their own differently than fibroblasts would do. The stroma organized by tumor cells does not show the characteristic islet like organization of malignant cells surrounded by stroma tissue as seen e.g. for carcinoma cells. In contrast, the connective tissue is distributed more uniform within the tumor mass²⁶⁵. This tumor cell-mediated uniform distribution of fibronectin was also observed in the AsPC-1-TGF model used in the presented study. This indicates an artificial stroma architecture that is lacking a well-organized stroma and fibroblasts. However, the development of a tumor stroma resembling human malignant tissue as much as possible is of particular interest for targeting latent TGF- β with AdCAR T cells. Since latent TGF- β can be anchored to the ECM, the stroma organization impacts the spatial distribution as well as the local concentration of the target antigen. In addition, the stromal architecture organized by fibronectin was shown to influence the spatial distribution of infiltrating immune cells²⁶⁷. As shown by Salmon *et al.*, both the alignment and the density of the fibers are decisive for the migratory trajectory of T cells. Immune cells fail to migrate properly through dense matrix structures and in addition the orientation of stromal fibers specifies the direction of T cell migration¹²⁶. Therefore, the stroma does significantly influence the migration of T cells within the tumor as well as the anti-tumor efficacy of AdCAR T cells. This further highlights the need for a clinically relevant stroma of tumor models to predict the therapeutic outcome of new immunotherapies more precisely.

CAFs are potential targets for AdCAR T cells targeting latent TGF- β . Thus, it can be assumed that the eradication of those CAFs could lead to different therapeutic outcome in a tumor model that depends on stromal cells to organize the ECM around the tumor. For better prediction of clinical efficacy, the use of freshly patient-derived xenografts or autochthonous models is recommended²⁶⁸. However, it is important to stress that spontaneous tumor models are usually more difficult to establish and take longer to engraft compared to transplanted tumors which make them not suitable for initial functional assessment of AdCAR T cells²⁶⁵.

As an alternative, orthotopic models need to be considered in future. Substantial differences in vascularization as well as a more immunosuppressive TME in orthotopic tumors compared to s.c. tumors were described²⁶⁹. Therefore, orthotopic models might overcome limitations of subcutaneous models as they are described to recapitulate the features of spontaneous tumors better than a subcutaneous tumor^{265,270}. In sum, future studies of AdCAR T cells targeting the TME of cancer should include mouse models which recapitulate many more facets that shape solid tumors and determine treatment efficacy.

6.5 Sensing of soluble latent TGF- β *in vivo* induces systemic AdCAR T cell activation characterized by an early induction of pro-inflammatory cytokine secretion

In this work the sensing of soluble antigens was investigated in three different s.c. xenograft mouse models. NSG mice received either (1) AsPC-1 WT and were in addition supplemented with soluble latent TGF- β , (2) AsPC-1-TGF which directly secrete latent TGF- β or (3) AsPC-1-TGF plus autologous PBMCs to investigate synergistic effects of AdCAR T cells with endogenous immune cells.

Independent of the model used, soluble latent TGF- β was found to trigger IFN- γ release by AdCAR T cells in presence of an anti-LAP specific adapter. Furthermore, the induction of cytokine release *in vivo* was compared between targeting a TAA or a soluble antigen. The differential induction of cytokine secretion was analyzed in the AsPC-1 WT model and in the AsPC-1-TGF model. Using these two models, the cytokine secretion of two different anti-CD66c CAR T cells was compared to AdCAR T cells targeting soluble latent TGF- β . The cytokine secretion was induced remarkably earlier by soluble ligands targeted by the AdCAR compared to a CAR targeting a TAA.

One major advantage of the AdCAR concept is its flexibility to redirect the AdCAR to multiple target molecules by applying different adapters. Therefore, simultaneous targeting of a TAA and a soluble antigen with one AdCAR T cell was evaluated in the AsPC-1-TGF model as well. In animals that were treated with aLAP plus aCD66c elevated levels of systemic IFN- γ were found at day four compared to animals treated with aCD66c only. Importantly, when targeting a TAA alone or simultaneously with a soluble antigen using the same AdCAR, the anti-tumor efficacy was similar in both settings. This demonstrated no interference of soluble antigen sensing and tumor killing. In addition, the activation of AdCARs by soluble antigens did not impair tumor trafficking and TAA induced activation of AdCAR T cells, as frequencies of infiltrating lymphocytes and the proportion of CD8⁺ T cells in the tumors were comparable between the cohorts that received either aCD66c plus aLAP or only aCD66c. However, a remarkable shift towards

CD8⁺ AdCAR T cells was observed in spleens in presence of latent TGF- β and aLAP. This indicates latent TGF- β induced AdCAR T cell activation independent of AdCAR T cells engaging a TAA.

To better understand the elevated IFN- γ concentrations four days after AdCAR T injection, the availability of latent TGF- β and the route of AdCAR T cell administration in these mouse models needs to be considered. Upon i.v. administration most transplanted cells are trapped in the lung for the first 24 h and persist for up to three days followed by homing to the tumor site²⁷¹. Within this time frame, truly TAA specific T cells lack antigen-dependent stimulation. This is supported by the observation that the efficacy of PSCA-mCAR T cells was improved in a lung metastatic model compared to the corresponding prostate tumor model. The authors assumed that the initial trapping of i.v. injected CAR T cells in the lung is limiting the survival in the periphery due to missing antigen stimulation in the non-metastatic model. In a metastatic model, CAR T cells engage their antigen rapidly after infusion and thus get stimulated already in the lung²⁷². Furthermore, T cells were described to not only lack sufficient antigen stimulus but also to receive inhibitory signals in the periphery before reaching the tumor tissue. For instance, MDSCs were found to circulate in the periphery of melanoma and lung cancer patients after chemotherapy²⁷³. As already discussed, soluble latent TGF- β is circulating in the serum, therefore AdCAR T cells receive antigen stimulation already in the periphery distant from the tumor. Thus, the early induction of IFN- γ secretion by AdCAR T cells targeting a soluble antigen in presence of aLAP and soluble latent TGF- β clearly identifies a peripheral stimulation of AdCAR T cells by soluble latent TGF- β distant from the tumor site. In sum, the mechanistic feature may circumvent the lack of initial antigen encounter of CAR T cells targeting TAAs.

One mechanistic feature of sensing soluble antigens with AdCAR T cells *in vivo* was the production of IFN- γ . The systemic administration of IFN- γ was reported to elicit remodeling of the TME. For example, systemic exogenous administration of IFN- γ was already evaluated in a phase 0 clinical trial²⁷⁴. In detail, patients suffering from synovial sarcoma and myxoid/round cell liposarcoma were injected with IFN- γ to induce inflammation of the TME. Mechanistically, Zhang *et al.* found an upregulation of MHC-I expression on tumor cells and less exhausted T cells within the tumor in this phase 0 study²⁷⁴. It needs to be clarified by future work whether the systemic stimulation of AdCAR T cells by soluble antigens and the secretion of pro-inflammatory cytokines is beneficial to also activate bystander immune cells systemically or if activation is limited to AdCAR T cells. To comprehensively answer this question, a fully immune competent mouse model is required. This would allow to also study the involvement of, e.g. B cells, NK cells or DCs in systemic activation and tumor infiltration²⁷⁵.

In the mouse studies presented here, secretion of cytokines in absence of adapter was noticed. Interestingly, this background cytokine secretion was diminished in presence of adapter when the target was absent. This data indicates an adapter-independent stimulation of the AdCAR early after injection. One phenomenon that is described to cause such antigen-independent

stimulation of CAR T cells is tonic signaling. Tonic signaling was reported to be dependent on various factors such as intracellular signaling, the scFv or CAR expression level. Frigault *et al.* could show a link of tonic signaling between the CD28 intracellular signaling domain and a high expression level of the CAR²⁷⁶. As both, the AdCAR1 and AdCAR2 contain a CD28 signaling domain, a possible correlation of the expression level and tonic signaling needs to be investigated. Furthermore, it cannot be excluded that the scFv binds a second target in addition to the LLE. A potential off-target binding may explain why CAR activation is blocked in presence of adapter molecules. In sum, more data are needed to identify the cause of the antigen-independent signaling in absence of adapter. It is likely that this phenomenon is caused by a combination of multiple factors, e.g. CAR architecture, expression level and choice of CAR binding moiety.

6.6 The anti-tumor effect of AdCAR T cells is enhanced in NSG mice reconstituted with autologous PBMCs

Within this study, the NSG mouse strain was used for all three tumor models, and for all of them the principle of sensing soluble antigens with AdCAR T cells was confirmed. However, complete tumor eradication, even for functional CD66c CAR T cells, was only observed in NSG mice bearing the AsPC-1 WT tumor, whereas in NSG mice bearing the AsPC-1-TGF tumor no anti-tumor effect was found. A similar trend was observed with AdCAR T cells simultaneously targeting soluble latent TGF- β and CD66c. No anti-tumor response was elicited in the NSG AsPC-1-TGF model. Surprisingly, AdCAR T cells were able to induce growth control of highly immunosuppressive AsPC-1-TGF tumors in PBMC reconstituted NSG mice. Tumor burden in mice treated with AdCAR T cells and aLAP plus aCD66c was significantly lower in presence of autologous PBMCs compared to non-reconstituted mice. Moreover, in reconstituted mice, the frequency of human cells was significantly higher indicating improved engraftment and expansion of immune cells in secondary lymphoid organs, e.g. spleens. Additionally, elevated frequencies of CD45⁺ cells were found in dissociated AsPC-1-TGF tumors of reconstituted NSG mice compared to non-reconstituted mice, which might explain the superior anti-tumor response.

Pyo *et al.* engrafted NSG mice with human PBMCs of healthy donors. By comparing the cytokine secretion pattern of human cytokines before and after engraftment, the authors found a significantly higher secretion of, e.g. IFN- γ and GM-CSF²⁷⁷. Furthermore, Onoe *et al.* adoptively transferred CD34⁺ cells into lymphopenic NOD/SCID mice and reported a rapid proliferation and conversion of naïve CD8 and CD4 T cells into memory like T cells with the capability to secrete IFN- γ upon stimulation²⁷⁸. The pronounced secretion of IFN- γ reported by Pyo *et al.* and Onoe *et al.* is in line with the increased IFN- γ levels found in PBMC reconstituted mice bearing AsPC-1-TGF tumors after treatment with AdCAR T cells. It is likely that the cytokine milieu established by the engraftment of human PBMCs and AdCAR T cells into lymphopenic mice explains the

improved anti-tumor response of AdCAR T cells in the otherwise immunosuppressive AsPC-1-TGF model. There is evidence that IFN- γ , besides its pro-apoptotic role, can enhance the proliferation and cytolytic potential of T cells, therefore a positive effect on AdCAR T cells is assumed^{279–282}. IFN- γ can improve survival of CD4⁺ T cells in absence of antigen stimulation. CD4⁺ T cells pre-treated with IFN- γ *in vitro* demonstrated improved expansion upon antigen stimulation, since the fraction of cells entering replicating cell cycle was increased by IFN- γ ²⁸³. Thus, IFN- γ could prepare AdCAR T cells to elicit an anti-tumor response as soon as reaching the tumor and contribute to the survival of T cells during circulation in the periphery.

In the presented study, the reconstitution of immunodeficient mice was required but not sufficient for anti-tumor response in the AsPC-1-TGF model. It is hypothesized that the pool of AdCAR T cells was systemically increased in AsPC-1-TGF bearing mice reconstituted with autologous PBMCs, whereas the AdCAR T cell proliferation was suppressed by active TGF- β in absence of autologous PBMCs. Additionally, no engraftment of immune cells was observed in AsPC-1-TGF-bearing mice treated with PBMCs only, indicating a suppression of the previously observed rapid proliferation in absence of AdCAR T cells. Zhang *et al.* identified TGF- β as a suppressor of T cells proliferation in a lymphopenic environment. After transferring mouse T cells, harboring a knockout of the TGF- β RII or WT T cells into RAG1^{-/-} mice, only the knockout T cells showed proliferation under lymphopenic conditions²⁸⁴. This indicates that TGF- β is a mediator of T cell proliferation under lymphopenic conditions. Consequently, the TGF- β present in the AsPC-1-TGF model most likely suppressed the lymphopenia-induced proliferation of immune cells. However, when AdCAR T cells and autologous PBMCs were co-injected to mice bearing AsPC-1-TGF tumors a proliferation of human immune cells was observed. Cytokine driven stimulation of T cells, e.g. by IL-12, TNF- α and to some extent IFN- γ is known to overcome the suppressive effect TGF- β is exerting on T cells²⁸⁴. Therefore, the level of those cytokines should be monitored in future experiments when treating AsPC-1-TGF-bearing mice with autologous immune cells and/or AdCAR T cells to decipher their contribution to overcome the suppressive effect of TGF- β .

However, this highlights the potential of a combined application of AdCAR T cells and autologous PBMCs to overcome a suppressive TME marked by TGF- β . Although the simultaneous targeting of CD66c and latent TGF- β enhanced IFN- γ secretion in humanized mice no improved tumor clearance was found compared to targeting CD66c alone. Nevertheless, Boulch *et al.* described a beneficial effect of IFN- γ and IL-12 in orchestrating the crosstalk of CD19-CAR T cells with host immune cells in an immune competent mouse model²⁸⁵. IFN- γ was shown to recruit a wide range of immune cells to the TME, e.g. DCs, monocytes, NK- and NKT cells. In addition, DC-derived IL-12 was needed to elicit full CAR T cell functionality²⁸⁵. This feedback loop might be relevant for AdCAR T cells sensing soluble latent TGF- β as well but could not be investigated in the NSG model.

It should be noted that the induction of rapid proliferation of immune cells observed in this study was adapter-independent, whereas the anti-tumor response was strictly dependent on aCD66c. The previously discussed tonic signaling of AdCAR T cells is assumed to support the reconstitution of NSG mice also in absence of an adapter, since IFN- γ secretion was observed. Therefore, a system without background activation of AdCAR T cells is needed to clarify whether the improved expansion of AdCAR T cells in presence of PBMCs can be triggered in a soluble antigen and/or a TAA-dependent manner.

Furthermore, B cells acting as APCs were identified to be essential for the rapid proliferation of CD8⁺ cytotoxic T cells under lymphopenic conditions²⁷⁸. In the study presented here, B cells were found to be persistent in spleens after injection of human PBMCs into NSG mice. Thus, B cells potentially served as APCs for adoptively transferred T cells and/or AdCAR T cells to induce rapid proliferation in the AsPC-1 TGF model. This may further contributed to the elevated frequencies of T cells found in spleens and tumors. Although the injection of human PBMCs into NSG mice is a straight-forward approach for in-depth investigations of CAR T cell therapy, the used model harbors some disadvantages. In this study mainly T cells, B cells and NKT cells were found in the spleens or the tumors after 25 days of engraftment. However, the myeloid compartment and NK cells were mostly missing, due to a lack of human cytokine support in NSG mice. An improved engraftment of neutrophils and monocytes was reported for NSG-SGM3 mice, expressing human GM-CSF, IL-3 and stem cell factor²⁸⁶. Thus, the investigation of anti-tumor efficacy of AdCAR T cells in such a humanized mouse model is required in the future, as they much more mimic the setting in a patient. The rationale to target the TME with AdCAR T cells in immunocompetent models is further supported by results obtained with anti-EIIIB⁺ CAR T cells and anti-FAP CAR T cells. Both CAR T cells demonstrated anti-tumor responses *in vivo* in immunocompetent mouse models but were not functional in immunodeficient hosts^{65,217}.

In sum, it appears reasonable to speculate that the effects of targeting the TME via soluble latent TGF- β would be much more pronounced in a tumor mouse model with a fully reconstituted human immune system and a more physiological tumor stroma.

6.7 AdCAR T cells show deficits to infiltrate solid tumor tissue

AdCAR T cells either targeting CD66c or CD66c and latent TGF- β showed a transient control of AsPC-1-TGF tumors in reconstituted NSG mice. However, AdCAR T cells failed to achieve complete tumor eradication. To get a more comprehensive understanding what caused the tumor outgrowth of AsPC-1-TGF tumors, the frequency of T cells infiltrating spleens and tumors as well as their exhaustion marker expression was analyzed *ex vivo*.

T cells were mainly found in spleens, whereas the frequency of T cells in the tumors was markedly reduced. Interestingly, these lymphocyte accumulations were accompanied by phenotypic differences. T cells in the tumor showed higher frequencies of PD-1, TIM3 and LAG3 expression compared to T cells isolated from spleens. This phenotype is considered as an indication of exhaustion and low cellular fitness²⁸⁷. Despite the immunosuppressive conditions present in the AsPC-1-TGF model, T cells showed persistence in the spleens more than three weeks after transfer. Thus, T cells located in the spleens seem to be an untapped reservoir of functional cells for tumor treatment which have not been recruited to the tumor site. Interestingly, similar observations were made in an autochthonous prostate cancer model. Tumor specific T cells harboring a knockout of the TGF- β RII receptor showed persistence in the spleen but not in the tumor²⁸⁸. Here, the authors found LAG3 to be expressed preferentially in T cells isolated from the tumor but not on cells from the periphery²⁸⁸. These observations are supported by gene expression data obtained from melanoma patients showing an exhaustion related gene profile and reduced IFN- γ production only in the tumor or draining lymph nodes but not in circulating cells²⁸⁹.

Lesch *et al.* reported that engineering CAR T cells to co-express CXCR6 improved tumor infiltration and enhanced anti-tumor response in an orthotopic pancreas tumor model²⁹⁰. This approach seems to be an elegant way to induce migration of less exhausted AdCAR T cells from secondary lymphoid organs to the tumor site. By combining chemokine-induced tumor infiltration and sensing of soluble antigens with AdCAR T cells, systemically activated CAR T cells could potentially be recruited to the tumor site. The analysis of the spatial distribution of AdCAR T cells further validates the need to improve the penetration of AdCAR T cell into the tumor. Whereas anti-CD66c CAR T cells showed accumulation in tumor layers more distant from the periphery, AdCAR T cells preferential accumulated in the peritumor as observed in the AsPC-1-TGF model. This migration behavior of AdCAR T cells may counteract anti-tumor efficacy. In general, two requirements for effective anti-tumor response of AdCAR T cells must be met, e.g. (1) sufficient infiltration of the tumor tissue by AdCAR T cells and in contrast to CAR T cells, (2) tumor penetration of the adapter molecules at therapeutic relevant concentration. As an adapter IgG₁ molecules tagged with the LLE epitope were used in this study. It can be assumed that these molecules distribute similar in tumor tissue compared to antibody drug conjugates (ADCs) as both molecules share most biochemical properties. In regions of high antigen density,

ADC penetration is less homogenous and declines rapidly the more the antibody diffuses into the tumor^{291,292}. Furthermore, it was shown for human head and neck cancer tumors that the size of the tumors is negatively correlated with antibody accumulation²⁹³. One caveat for bivalent adapter formats in penetrating solid tumor tissues is their relatively high affinity. Highly affine binding molecules showed limited diffusion due to the low level of unbound antibodies which can diffuse further into the tumor tissue^{294,295}. This is further supported by clinical data of patients suffering from head and neck squamous cell carcinomas. Here, anti-EGFR antibodies showed declining tumor penetration with increased distance from tumor edges leading to heterogeneously labeled tumors, thus potentially limiting the efficacy of the ADC²⁹⁶. Antibody fragments of smaller size, e.g. Fab-fragments or scFvs, demonstrated improved intratumoral distribution and thus have the potential to overcome the shortcoming of full length IgGs²⁹⁷. However, limitations of antigen binding moieties with lower molecular weight, are a faster renal clearance and a lower plasma concentration. Nessler *et al.* fused nanobodies to an albumin binding domain to elongate serum half-life. This increased tissue penetration and efficacy of an ADC in a mouse xenograft prostate cancer model compared to a full length IgG²⁹⁸. It can be assumed that both the aLAP and the aCD66c adapter also penetrated only outer layers of the tumors resulting in the accumulation of AdCAR T cells in this region.

In summary, both the accumulation of adapter molecules and the migration pattern need to be quantified within the tumor mass in future studies, either by *ex vivo* immunofluorescent analysis of sequential tumor slices or imaging of the whole tumor by ultramicroscopy²⁹⁹. In addition, adapter formats of low molecular weight, e.g. Fabs, scFvs or nanobodies, should be considered for AdCAR T cells in solid tumor treatment, instead of full length IgG molecules.

6.8 Outlook

The introduction of CAR T cells has offered new therapeutic options for patients suffering from hematological malignancies. However, CAR T cell therapies targeting solid cancers have not yet been approved. A major difference between liquid and solid tumors is the TME, and its complex and immunosuppressive composition that currently renders CAR T cell therapy inefficient.

Most of the current CAR T cell approaches focus on membrane bound molecules expressed by the tumor with only a few examples targeting the stroma of solid tumors^{65,217}. To allow communication of the tumor with surrounding stroma, and in order to orchestrate immune evasion, soluble molecules like chemokines or cytokines are indispensable. However, chemokines, cytokines or shed tumor antigens have only poorly been considered as CAR targets so far due to the dogma of antigens requiring cell surface expression.

In the study presented here it was shown that AdCAR T cells in combination with an adapter molecule get stimulated by soluble antigens both *in vitro* and *in vivo*. The AdCAR technology

allowed to combine soluble antigen sensing with direct tumor targeting without any further genetic modification of the T cell except of the AdCAR expression. Therefore, the therapeutic spectrum of future AdCAR approaches can be expanded simply by adding new adapter specificities to the treatment protocol. The omission of additional genetic modifications facilitates clinical translation since the already existing AdCAR architecture is used for sensing soluble antigens as well as TAAs. This allows to target antigens present in the TME, which can be both ECM-bound or secreted. This concept was inspected in this work using the immunosuppressive latent TGF- β . However, in addition to TGF- β , other chemokines are described to contribute to the immune evasion of tumors as well, for instance by attracting immunosuppressive cells like T_{regs}, MDSCs or neutrophils into the TME. Therefore, CCL22, CCL2 or CXCL5 appear attractive to be targeted by AdCAR T cells for conversion into pro-inflammatory stimuli in future work³⁰⁰⁻³⁰². In addition, tumors do escape the CAR T cell anti-tumor effector function by shedding TAAs, as described for Glypican-3²⁴⁴. These antigens are usually not considered as CAR targets. However, with the technique presented here the higher serum concentrations of shed antigens can be used as a specific trigger of AdCAR T cells in the periphery before reaching the tumor lesion. By sensing shed tumor antigens and subsequent secretion of pro-inflammatory cytokines, AdCAR T cells have the potential to compensate the lack of antigen stimuli in the periphery.

Another class of new potential CAR targets are soluble checkpoint molecules which suppress the immune response. For instance, soluble PD-L1 or soluble CTLA-4 have been identified in sera of cancer patients^{303,304}. A complexation of soluble checkpoint molecules with AdCAR T cells could counteract their inhibitory effect in two ways. First, the AdCAR T cells would be triggered by those molecules instead of being inhibited. Second, the adapter could be engineered to neutralize those molecules and thereby reduce the inhibitory effect otherwise exerted on non-AdCAR T cells as well. This strategy has the potential to promote an enhanced and systemic immunity.

It was demonstrated within this study that soluble antigens trigger the secretion of endogenous IFN- γ but can induce transgene expression as well. It is conceivable that this system can be used to induce expression of therapeutically relevant transgenes within a specific environment, e.g. at high concentrations of TGF- β at the tumor site. In this way, AdCAR T cells can be used for instance to sense latent TGF- β and induce the expression of a dominant negative T β RII. Thereby, AdCAR T cells could help to overcome TGF- β -mediated inhibition of cytotoxicity as AdCAR T cells would act as a sink for TGF- β ²¹³. Overall, the concept of soluble antigen sensing with AdCAR T cells may provide a new therapeutic option to patients suffering from solid cancer.

7. References

1. Hansemann D. Ueber asymmetrische Zelltheilung in Epithelkrebsen und deren biologische Bedeutung. *Arch. für Pathol. Anat. und Physiol. und für Klin. Med.* 1890;119(2):299–326. doi:10.1007/BF01882039
2. Boveri T. *Zur Frage der Entstehung maligner Tumoren.* Fischer; 1914.
3. Danaei G, Vander Hoorn S, Lopez AD, Murray CJ, Ezzati M. Causes of cancer in the world: comparative risk assessment of nine behavioural and environmental risk factors. *Lancet.* 2005;366(9499):1784–1793. doi:10.1016/S0140-6736(05)67725-2
4. Henle G, Henle W, Clifford P, Diehl V, Kafuko GW, Kirya BG, Klein G, Morrow RH, Munube GM, Pike P, et al. Antibodies to Epstein-Barr virus in Burkitt's lymphoma and control groups. *J. Natl. Cancer Inst.* 1969;43(5):1147–1157.
5. Walboomers JMM, Jacobs M V, Manos MM, Bosch FX, Kummer JA, Shah K V, Snijders PJF, Peto J, Meijer CJLM, Muñoz N. Human papillomavirus is a necessary cause of invasive cervical cancer worldwide. *J. Pathol.* 1999;189(1):12–19. doi:10.1002/(SICI)1096-9896(199909)189:1<12::AID-PATH431>3.0.CO;2-F
6. Moan J, Grigalavicius M, Baturaite Z, Dahlback A, Juzeniene A. The relationship between UV exposure and incidence of skin cancer. *Photodermatol. Photoimmunol. Photomed.* 2015;31(1):26–35. doi:10.1111/phpp.12139
7. Lindahl T, Barnes DE. Repair of endogenous DNA damage. *Cold Spring Harb. Symp. Quant. Biol.* 2000;65:127–133. doi:10.1101/sqb.2000.65.127
8. Lindahl T. Instability and decay of the primary structure of DNA. *Nature.* 1993;362(6422):709–715. doi:10.1038/362709a0
9. Modrich P. Mechanisms and biological effects of mismatch repair. *Annu. Rev. Genet.* 1991;25(1):229–53. doi:10.1146/annurev.ge.25.120191.001305
10. Petit C, Sancar A. Nucleotide excision repair: From E. coli to man. *Biochimie.* 1999;81(1–2):15–25. doi:10.1016/S0300-9084(99)80034-0
11. Tubbs A, Nussenzweig A. Endogenous DNA Damage as a Source of Genomic Instability in Cancer. *Cell.* 2017;168(4):644–656. doi:10.1016/J.CELL.2017.01.002
12. Stratton MR, Campbell PJ, Futreal PA. The cancer genome. *Nature.* 2009;458(7239):719–724. doi:10.1038/nature07943
13. Goh HS, Elnatan J, Low CH, Smith DR. p53 point mutation and survival in colorectal cancer patients: effect of disease dissemination and tumour location. *Int. J. Oncol.* 1999;15(3):491–498. doi:10.3892/ijo.15.3.491
14. Daley GQ, Van Etten RA, Baltimore D. Induction of Chronic Myelogenous Leukemia in Mice by the P210 bcr/abl Gene of the Philadelphia Chromosome. *Science (80-).* 1990;247(4944):824–830. doi:10.1126/science.2406902
15. Thomas L. On immunosurveillance in human cancer. *Yale J. Biol. Med.* 1982;55(3–4):329.
16. Burnet FM. Immunological Surveillance in Neoplasia. *Immunol. Rev.* 1971;7(1):3–25. doi:10.1111/j.1600-065X.1971.tb00461.x
17. Burnet FM. Immunological aspects of malignant disease. *Lancet (London, England).* 1967;1(7501):1171–4. doi:10.1016/s0140-6736(67)92837-1

18. Birkeland SA, Storm HH, Lamm LU, Barlow L, Blohmé I, Forsberg B, Eklund B, Fjeldborg O, Friedberg M, Frödin L, et al. Cancer risk after renal transplantation in the nordic countries, 1964-1986. *Int. J. Cancer*. 1995;60(2):183–189. doi:10.1002/ijc.2910600209
19. Gutierrez-Dalmau A, Campistol JM. Immunosuppressive Therapy and Malignancy in Organ Transplant Recipients. *Drugs*. 2007;67(8):1167–1198. doi:10.2165/00003495-200767080-00006
20. Challenor S, Tucker D. SARS-CoV-2-induced remission of Hodgkin lymphoma. *Br. J. Haematol*. 2021;192(3):415–415. doi:10.1111/bjh.17116
21. Buckner TW, Dunphy C, Fedoriw YD, van Deventer HW, Foster MC, Richards KL, Park SI. Complete Spontaneous Remission of Diffuse Large B-Cell Lymphoma of the Maxillary Sinus After Concurrent Infections. *Clin. Lymphoma Myeloma Leuk*. 2012;12(6):455–458. doi:10.1016/j.clml.2012.06.007
22. Sung H, Ferlay J, Siegel RL, Laversanne M, Soerjomataram I, Jemal A, Bray F. Global Cancer Statistics 2020: GLOBOCAN Estimates of Incidence and Mortality Worldwide for 36 Cancers in 185 Countries. *CA. Cancer J. Clin*. 2021;71(3):209–249. doi:10.3322/caac.21660
23. Dunn GP, Old LJ, Schreiber RD. The three Es of cancer immunoediting. *Annu. Rev. Immunol*. 2004;22(4):329–360. doi:10.1146/annurev.immunol.22.012703.104803
24. Bauer S, Groh V, Wu J, Steinle A, Phillips JH, Lanier LL, Spies T. Activation of NK Cells and T Cells by NKG2D, a Receptor for Stress-Inducible MICA. *Science (80-)*. 1999;285(5428):727–729. doi:10.1126/science.285.5428.727
25. Diefenbach A, Jensen ER, Jamieson AM, Raulet DH. Rae1 and H60 ligands of the NKG2D receptor stimulate tumour immunity. *Nature*. 2001;413(6852):165–171. doi:10.1038/35093109
26. Vicari AP, Caux C. Chemokines in cancer. *Cytokine Growth Factor Rev*. 2002;13(2):143–154. doi:10.1016/S1359-6101(01)00033-8
27. Schmiegel WH, Caesar J, Kalthoff H, Greten H, Schreiber HW, Thiele H-G. Antiproliferative Effects Exerted by Recombinant Human Tumor Necrosis Factor- α (TNF- α) and Interferon- γ (IFN- γ) on Human Pancreatic Tumor Cell Lines. *Pancreas*. 1988;3(2):180–188. doi:10.1097/00006676-198804000-00012
28. Detjen KM, Farwig K, Welzel M, Wiedenmann B, Rosewicz S. Interferon γ inhibits growth of human pancreatic carcinoma cells via caspase-1 dependent induction of apoptosis. *Gut*. 2001;49(2):251–262. doi:10.1136/gut.49.2.251
29. Boost KA, Sadik CD, Bachmann M, Zwissler B, Pfeilschifter J, Mühl H. IFN- γ Impairs Release of IL-8 by IL-1 β -stimulated A549 Lung Carcinoma Cells. *BMC Cancer*. 2008;8(1):265. doi:10.1186/1471-2407-8-265
30. Lacina L, Čoma M, Dvořánková B, Kodet O, Melegová N, Gál P, Smetana K. Evolution of Cancer Progression in the Context of Darwinism. *Anticancer Res*. 2019;39(1):1–16. doi:10.21873/anticancer.13074
31. Pelosi E, Castelli G, Testa U. Pancreatic Cancer: Molecular Characterization, Clonal Evolution and Cancer Stem Cells. *Biomedicines*. 2017;5(4):65. doi:10.3390/biomedicines5040065
32. Fortunato A, Boddy A, Mallo D, Aktipis A, Maley CC, Pepper JW. Natural Selection in Cancer Biology: From Molecular Snowflakes to Trait Hallmarks. *Cold Spring Harb. Perspect. Med*. 2017;7(2):1–14. doi:10.1101/cshperspect.a029652

33. Dhatchinamoorthy K, Colbert JD, Rock KL. Cancer Immune Evasion Through Loss of MHC Class I Antigen Presentation. *Front. Immunol.* 2021;12(636568). doi:10.3389/fimmu.2021.636568
34. Liu S, Ren J, ten Dijke P. Targeting TGF β signal transduction for cancer therapy. *Signal Transduct. Target. Ther.* 2021;6(1):8. doi:10.1038/s41392-020-00436-9
35. Han Y, Liu D, Li L. PD-1/PD-L1 pathway: current researches in cancer. *Am. J. Cancer Res.* 2020;10(3):727–742.
36. GILMAN A. Therapeutic applications of chemical warfare agents. *Fed. Proc.* 1946;5:285–292.
37. Kuai R, Ochyl LJ, Bahjat KS, Schwendeman A, Moon JJ. Designer vaccine nanodiscs for personalized cancer immunotherapy. *Nat. Mater.* 2017;16(4):489–496. doi:10.1038/nmat4822
38. Henley SJ, Ward EM, Scott S, Ma J, Anderson RN, Firth AU, Thomas CC, Islami F, Weir HK, Lewis DR, et al. Annual report to the nation on the status of cancer, part I: National cancer statistics. *Cancer.* 2020;126(10):2225–2249. doi:10.1002/cncr.32802
39. COLEY WB. CONTRIBUTION TO THE KNOWLEDGE OF SARCOMA. *Ann. Surg.* 1891;14(3):199–220. doi:10.1097/00000658-189112000-00015
40. Thomas L, Lawrence H. Cellular and humoral aspects of the hypersensitive states. New York Hoeber-Harper. 1959:529–532.
41. Burnet FM. The concept of immunological surveillance. *Prog. Exp. Tumor Res.* 1970;13:1–27. doi:10.1159/000386035
42. Rituximab - Product Approval Information - Licensing Action. [accessed January 27, 2022]. https://www.accessdata.fda.gov/drugsatfda_docs/applletter/1997/ritugen112697L.htm
43. Biologics License Application approval letter YERVOY. [accessed January 27, 2022]. https://www.accessdata.fda.gov/drugsatfda_docs/applletter/2011/125377s000ltr.pdf
44. Schadendorf D, Hodi FS, Robert C, Weber JS, Margolin K, Hamid O, Patt D, Chen T-T, Berman DM, Wolchok JD. Pooled Analysis of Long-Term Survival Data From Phase II and Phase III Trials of Ipilimumab in Unresectable or Metastatic Melanoma. *J. Clin. Oncol.* 2015;33(17):1889–1894. doi:10.1200/JCO.2014.56.2736
45. U.S. Food and Drug Administration. Biologics License Application approval letter Keytruda. [accessed January 27, 2022]. https://www.accessdata.fda.gov/drugsatfda_docs/applletter/2014/125514Orig1s000ltr.pdf
46. U.S. Food and Drug Administration. Biologics License Application approval letter OPDIVO. [accessed January 27, 2022]. https://www.accessdata.fda.gov/drugsatfda_docs/applletter/2015/125527Orig1s000ltr.pdf
47. Herbst RS, Baas P, Kim D-W, Felip E, Pérez-Gracia JL, Han J-Y, Molina J, Kim J-H, Arvis CD, Ahn M-J, et al. Pembrolizumab versus docetaxel for previously treated, PD-L1-positive, advanced non-small-cell lung cancer (KEYNOTE-010): a randomised controlled trial. *Lancet.* 2016;387(10027):1540–1550. doi:10.1016/S0140-6736(15)01281-7
48. Ferris RL, Blumenschein G, Fayette J, Guigay J, Colevas AD, Licitra L, Harrington K, Kasper S, Vokes EE, Even C, et al. Nivolumab for Recurrent Squamous-Cell Carcinoma of the Head and Neck. *N. Engl. J. Med.* 2016;375(19):1856–1867. doi:10.1056/NEJMoa1602252
49. Baas P, Scherpereel A, Nowak AK, Fujimoto N, Peters S, Tsao AS, Mansfield AS, Popat S,

- Jahan T, Antonia S, et al. First-line nivolumab plus ipilimumab in unresectable malignant pleural mesothelioma (CheckMate 743): a multicentre, randomised, open-label, phase 3 trial. *Lancet*. 2021;397(10272):375–386. doi:10.1016/S0140-6736(20)32714-8
50. Hellmann MD, Paz-Ares L, Bernabe Caro R, Zurawski B, Kim S-W, Carcereny Costa E, Park K, Alexandru A, Lupinacci L, de la Mora Jimenez E, et al. Nivolumab plus Ipilimumab in Advanced Non–Small-Cell Lung Cancer. *N. Engl. J. Med.* 2019;381(21):2020–2031. doi:10.1056/NEJMoa1910231
51. Motzer RJ, Tannir NM, McDermott DF, Arén Frontera O, Melichar B, Choueiri TK, Plimack ER, Barthélémy P, Porta C, George S, et al. Nivolumab plus Ipilimumab versus Sunitinib in Advanced Renal-Cell Carcinoma. *N. Engl. J. Med.* 2018;378(14):1277–1290. doi:10.1056/NEJMoa1712126
52. Southam CM, Brunschwig A, Levin AG, Dizon QS. Effect of leukocytes on transplantability of human cancer. *Cancer*. 1966;19.
53. Rosenberg SA, Yang JC, Sherry RM, Kammula US, Hughes MS, Phan GQ, Citrin DE, Restifo NP, Robbins PF, Wunderlich JR, et al. Durable Complete Responses in Heavily Pretreated Patients with Metastatic Melanoma Using T-Cell Transfer Immunotherapy. *Clin. Cancer Res.* 2011;17(13):4550–4557. doi:10.1158/1078-0432.CCR-11-0116
54. Dudley ME, Yang JC, Sherry R, Hughes MS, Royal R, Kammula U, Robbins PF, Huang J, Citrin DE, Leitman SF, et al. Adoptive Cell Therapy for Patients With Metastatic Melanoma: Evaluation of Intensive Myeloablative Chemoradiation Preparative Regimens. *J. Clin. Oncol.* 2008;26(32):5233–5239. doi:10.1200/JCO.2008.16.5449
55. Robbins PF, Morgan RA, Feldman SA, Yang JC, Sherry RM, Dudley ME, Wunderlich JR, Nahvi A V., Helman LJ, Mackall CL, et al. Tumor Regression in Patients With Metastatic Synovial Cell Sarcoma and Melanoma Using Genetically Engineered Lymphocytes Reactive With NY-ESO-1. *J. Clin. Oncol.* 2011;29(7):917–924. doi:10.1200/JCO.2010.32.2537
56. Merchant AM, Zhu Z, Yuan JQ, Goddard A, Adams CW, Presta LG, Carter P. An efficient route to human bispecific IgG. *Nat. Biotechnol.* 1998;16(7):677–81. doi:10.1038/nbt0798-677
57. Przepiorka D, Ko CW, Deisseroth A, Yancey CL, Candau-Chacon R, Chiu HJ, Gehrke BJ, Gomez-Broughton C, Kane RC, Kirshner S, et al. FDA Approval: Blinatumomab. *Clin. Cancer Res.* 2015;21(18):4035–4039. doi:10.1158/1078-0432.CCR-15-0612
58. Slaney CY, Wang P, Darcy PK, Kershaw MH. CARs versus BiTEs: A Comparison between T Cell–Redirection Strategies for Cancer Treatment. *Cancer Discov.* 2018;8(8):924–934. doi:10.1158/2159-8290.CD-18-0297
59. Eshhar Z, Waks T, Gross G, Schindler DG. Specific activation and targeting of cytotoxic lymphocytes through chimeric single chains consisting of antibody-binding domains and the gamma or zeta subunits of the immunoglobulin and T-cell receptors. *Proc. Natl. Acad. Sci.* 1993;90(2):720–724. doi:10.1073/pnas.90.2.720
60. U.S. Food and Drug Administration. Approved Cellular and Gene Therapy Products | FDA. [accessed March 14, 2022]. <https://www.fda.gov/vaccines-blood-biologics/cellular-gene-therapy-products/approved-cellular-and-gene-therapy-products>
61. Munshi NC, Anderson LD, Shah N, Madduri D, Berdeja J, Lonial S, Raje N, Lin Y, Siegel D, Oriol A, et al. Idecabtagene Vicleucel in Relapsed and Refractory Multiple Myeloma. *N. Engl. J. Med.* 2021;384(8):705–716. doi:10.1056/NEJMoa2024850

62. Zhang Z, Jiang D, Yang H, He Z, Liu X, Qin W, Li L, Wang C, Li Y, Li H, et al. Modified CAR T cells targeting membrane-proximal epitope of mesothelin enhances the antitumor function against large solid tumor. *Cell Death Dis.* 2019;10(7):476. doi:10.1038/s41419-019-1711-1
63. Ghorashian S, Kramer AM, Onuoha S, Wright G, Bartram J, Richardson R, Albon SJ, Casanovas-Company J, Castro F, Popova B, et al. Enhanced CAR T cell expansion and prolonged persistence in pediatric patients with ALL treated with a low-affinity CD19 CAR. *Nat. Med.* 2019;25(9):1408–1414. doi:10.1038/s41591-019-0549-5
64. Caruso HG, Hurton L V., Najjar A, Rushworth D, Ang S, Olivares S, Mi T, Switzer K, Singh H, Huls H, et al. Tuning Sensitivity of CAR to EGFR Density Limits Recognition of Normal Tissue While Maintaining Potent Antitumor Activity. *Cancer Res.* 2015;75(17):3505–3518. doi:10.1158/0008-5472.CAN-15-0139
65. Xie YJ, Dougan M, Jaikhan N, Ingram J, Fang T, Kummer L, Momin N, Pishesha N, Rickelt S, Hynes RO, et al. Nanobody-based CAR T cells that target the tumor microenvironment inhibit the growth of solid tumors in immunocompetent mice. *Proc. Natl. Acad. Sci. U. S. A.* 2019;116(33):16656. doi:10.1073/pnas.1912487116
66. Kahlon KS, Brown C, Cooper L J N, Raubitschek A, Forman SJ, Jensen MC. Specific Recognition and Killing of Glioblastoma Multiforme by Interleukin 13-Zetakine Redirected Cytolytic T Cells. *Cancer Res.* 2004;64(24):9160–9166. doi:10.1158/0008-5472.CAN-04-0454
67. Patasic L, Seifried J, Bezler V, Kaljanac M, Schneider IC, Schmitz H, Tondera C, Hartmann J, Hombach A, Buchholz CJ, et al. Designed Ankyrin Repeat Protein (DARPin) to target chimeric antigen receptor (CAR)-redirected T cells towards CD4+ T cells to reduce the latent HIV+ cell reservoir. *Med. Microbiol. Immunol.* 2020;209(6):681–691. doi:10.1007/s00430-020-00692-0
68. Zhang A, Sun Y, Du J, Dong Y, Pang H, Ma L, Si S, Zhang Z, He M, Yue Y, et al. Reducing Hinge Flexibility of CAR-T Cells Prolongs Survival In Vivo With Low Cytokines Release. *Front. Immunol.* 2021;12(724211). doi:10.3389/fimmu.2021.724211
69. Hudecek M, Sommermeyer D, Kosasih PL, Silva-Benedict A, Liu L, Rader C, Jensen MC, Riddell SR. The Nonsignaling Extracellular Spacer Domain of Chimeric Antigen Receptors Is Decisive for In Vivo Antitumor Activity. *Cancer Immunol. Res.* 2015;3(2):125–135. doi:10.1158/2326-6066.CIR-14-0127
70. Muller YD, Nguyen DP, Ferreira LMR, Ho P, Raffin C, Valencia RVB, Congrave-Wilson Z, Roth TL, Eyquem J, Van Gool F, et al. The CD28-Transmembrane Domain Mediates Chimeric Antigen Receptor Heterodimerization With CD28. *Front. Immunol.* 2021;12(639818):1–13. doi:10.3389/fimmu.2021.639818
71. Bridgeman JS, Hawkins RE, Bagley S, Blaylock M, Holland M, Gilham DE. The Optimal Antigen Response of Chimeric Antigen Receptors Harboring the CD3 ζ Transmembrane Domain Is Dependent upon Incorporation of the Receptor into the Endogenous TCR/CD3 Complex. *J. Immunol.* 2010;184(12):6938–6949. doi:10.4049/jimmunol.0901766
72. Wan Z, Shao X, Ji X, Dong L, Wei J, Xiong Z, Liu W, Qi H. Transmembrane domain-mediated Lck association underlies bystander and costimulatory ICOS signaling. *Cell. Mol. Immunol.* 2020;17(2):143–152. doi:10.1038/s41423-018-0183-z
73. Brocker T, Karjalainen K. Signals through T cell receptor-zeta chain alone are insufficient to prime resting T lymphocytes. *J. Exp. Med.* 1995;181(5):1653–1659. doi:10.1084/jem.181.5.1653

74. Till BG, Jensen MC, Wang J, Chen EY, Wood BL, Greisman HA, Qian X, James SE, Raubitschek A, Forman SJ, et al. Adoptive immunotherapy for indolent non-Hodgkin lymphoma and mantle cell lymphoma using genetically modified autologous CD20-specific T cells. *Blood*. 2008;112(6):2261–2271. doi:10.1182/blood-2007-12-128843
75. Maher J, Brentjens RJ, Gunset G, Rivière I, Sadelain M. Human T-lymphocyte cytotoxicity and proliferation directed by a single chimeric TCR ζ /CD28 receptor. *Nat. Biotechnol.* 2002;20(1):70–75. doi:10.1038/nbt0102-70
76. Schubert M-L, Schmitt A, Neuber B, Hückelhoven-Krauss A, Kunz A, Wang L, Gern U, Michels B, Sellner L, Hofmann S, et al. Third-Generation CAR T Cells Targeting CD19 Are Associated with an Excellent Safety Profile and Might Improve Persistence of CAR T Cells in Treated Patients. *Blood*. 2019;134(Supplement_1):51–51. doi:10.1182/blood-2019-125423
77. Hombach AA, Heiders J, Foppe M, Chmielewski M, Abken H. OX40 costimulation by a chimeric antigen receptor abrogates CD28 and IL-2 induced IL-10 secretion by redirected CD4 + T cells. *Oncoimmunology*. 2012;1(4). doi:10.4161/onci.19855
78. Guedan S, Posey AD, Shaw C, Wing A, Da T, Patel PR, McGettigan SE, Casado-Medrano V, Kawalekar OU, Uribe-Herranz M, et al. Enhancing CAR T cell persistence through ICOS and 4-1BB costimulation. *JCI Insight*. 2018;3(1). doi:10.1172/jci.insight.96976
79. Hombach A, Barden M, Hannappel L, Chmielewski M, Rappl G, Sachinidis A, Abken H. IL12 integrated into the CAR exodomain converts CD8+ T cells to poly-functional NK-like cells with superior killing of antigen-loss tumors. *Mol. Ther.* 2022;30(2):593–605. doi:10.1016/j.ymthe.2021.10.011
80. Kueberuwa G, Kalaitidou M, Cheadle E, Hawkins RE, Gilham DE. CD19 CAR T Cells Expressing IL-12 Eradicate Lymphoma in Fully Lymphoreplete Mice through Induction of Host Immunity. *Mol. Ther. - Oncolytics*. 2018;8:41–51. doi:10.1016/j.omto.2017.12.003
81. Kunert A, Chmielewski M, Wijers R, Berrevoets C, Abken H, Debets R. Intra-tumoral production of IL18, but not IL12, by TCR-engineered T cells is non-toxic and counteracts immune evasion of solid tumors. *Oncoimmunology*. 2018;7(1). doi:10.1080/2162402X.2017.1378842
82. Wang Y, Jiang H, Luo H, Sun Y, Shi B, Sun R, Li Z. An IL-4/21 Inverted Cytokine Receptor Improving CAR-T Cell Potency in Immunosuppressive Solid-Tumor Microenvironment. *Front. Immunol.* 2019;10(1691). doi:10.3389/fimmu.2019.01691
83. Kagoya Y, Tanaka S, Guo T, Anczurowski M, Wang CH, Saso K, Butler MO, Minden MD, Hirano N. A novel chimeric antigen receptor containing a JAK-STAT signaling domain mediates superior antitumor effects. *Nat. Med.* 2018;24(3):352–359. doi:10.1038/nm.4478
84. Golay J, Manganini M, Facchinetti V, Gramigna R, Broady R, Borleri G, Rambaldi A, Introna M. Rituximab-mediated antibody-dependent cellular cytotoxicity against neoplastic B cells is stimulated strongly by interleukin-2. *Haematologica*. 2003;88(9):1002–1012.
85. Gennari R, Menard S, Fagnoni F, Ponchio L, Scelsi M, Tagliabue E, Castiglioni F, Villani L, Magalotti C, Gibelli N, et al. Pilot Study of the Mechanism of Action of Preoperative Trastuzumab in Patients with Primary Operable Breast Tumors Overexpressing HER2. *Clin. Cancer Res.* 2004;10(17):5650–5655. doi:10.1158/1078-0432.CCR-04-0225
86. Ochi F, Fujiwara H, Tanimoto K, Asai H, Miyazaki Y, Okamoto S, Mineno J, Kuzushima K, Shiku H, Barrett J, et al. Gene-Modified Human α/β -T Cells Expressing a Chimeric CD16-CD3 ζ Receptor

- as Adoptively Transferable Effector Cells for Anticancer Monoclonal Antibody Therapy. *Cancer Immunol. Res.* 2014;2(3):249–262. doi:10.1158/2326-6066.CIR-13-0099-T
87. Seitz CM, Mittelstaet J, Atar D, Hau J, Reiter S, Illi C, Kieble V, Engert F, Drees B, Bender G, et al. Novel adapter CAR-T cell technology for precisely controllable multiplex cancer targeting. *Oncoimmunology.* 2021;10(1). doi:10.1080/2162402X.2021.2003532
88. Tamada K, Geng D, Sakoda Y, Bansal N, Srivastava R, Li Z, Davila E. Redirecting gene-modified T cells toward various cancer types using tagged antibodies. *Clin. Cancer Res.* 2012;18(23):6436–6445. doi:10.1158/1078-0432.CCR-12-1449
89. Cartellieri M, Loff S, von Bonin M, Bejestani EP, Ehninger A, Feldmann A, Koristka S, Arndt C, Ehninger G, Bachmann MP. Unicar: A Novel Modular Retargeting Platform Technology for CAR T Cells. *Blood.* 2015;126(23):5549–5549. doi:10.1182/blood.V126.23.5549.5549
90. Cho JH, Collins JJ, Wong WW. Universal Chimeric Antigen Receptors for Multiplexed and Logical Control of T Cell Responses. *Cell.* 2018;173(6):1426–1438. doi:10.1016/J.CELL.2018.03.038
91. Minutolo NG, Sharma P, Poussin M, Shaw LC, Brown DP, Hollander EE, Smole A, Rodriguez-Garcia A, Hui JZ, Zappala F, et al. Quantitative Control of Gene-Engineered T-Cell Activity through the Covalent Attachment of Targeting Ligands to a Universal Immune Receptor. *J. Am. Chem. Soc.* 2020;142(14):6554–6568. doi:10.1021/jacs.9b11622
92. Rodgers DT, Mazagova M, Hampton EN, Cao Y, Ramadoss NS, Hardy IR, Schulman A, Du J, Wang F, Singer O, et al. Switch-mediated activation and retargeting of CAR-T cells for B-cell malignancies. *Proc. Natl. Acad. Sci.* 2016;113(4):459–468. doi:10.1073/pnas.1524155113
93. Lee YG, Chu H, Lu Y, Leamon CP, Srinivasarao M, Putt KS, Low PS. Regulation of CAR T cell-mediated cytokine release syndrome-like toxicity using low molecular weight adapters. *Nat. Commun.* 2019;10(1). doi:10.1038/S41467-019-10565-7
94. Albert S, Arndt C, Feldmann A, Bergmann R, Bachmann D, Koristka S, Ludwig F, Ziller-Walter P, Kegler A, Gärtner S, et al. A novel nanobody-based target module for retargeting of T lymphocytes to EGFR-expressing cancer cells via the modular UniCAR platform. *Oncoimmunology.* 2017;6(4). doi:10.1080/2162402X.2017.1287246
95. Mitwasi N, Feldmann A, Bergmann R, Berndt N, Arndt C, Koristka S, Kegler A, Jureczek J, Hoffmann A, Ehninger A, et al. Development of novel target modules for retargeting of UniCAR T cells to GD2 positive tumor cells. *Oncotarget.* 2017;8(65):108584–108603. doi:10.18632/oncotarget.21017
96. Mankarious S, Lee M, Fischer S, Pyun KH, Ochs HD, Oxelius VA, Wedgwood RJ. The half-lives of IgG subclasses and specific antibodies in patients with primary immunodeficiency who are receiving intravenously administered immunoglobulin. *J. Lab. Clin. Med.* 1988;112(5):634–640.
97. Flinn IW, Westin JR, Cohen JB, Akard LP, Jaglowski S, Sachs J, Ranger A, Harris P, Payumo F, Bachanova V. Preliminary Clinical Results from a Phase 1 Study of ACTR707 in Combination with Rituximab in Subjects with Relapsed or Refractory CD20+ non-Hodgkin Lymphoma. *Blood.* 2019;134(Supplement_1):1587–1587. doi:10.1182/blood-2019-125995
98. UNITED STATES, SECURITIES AND EXCHANGE COMMISSION. Form 8-K. Unum Therapeutics, Inc. 2020 Mar 4. [accessed March 8, 2022]. <http://content-archive.fast-edgar.com/20200309/AL22322CZZ2R52ZZ27TH2MYLBTRSE22Z222/>
99. ClinicalTrials.gov. Dose-escalating Trial With UniCAR02-T Cells and CD123 Target Module

- (TM123) in Patients With Hematologic and Lymphatic Malignancies. [accessed January 31, 2022]. <https://clinicaltrials.gov/ct2/show/NCT04230265>
100. ClinicalTrials.gov. CLBR001 and SWI019 in Patients With Relapsed / Refractory B-cell Malignancies. [accessed January 31, 2022]. <https://clinicaltrials.gov/ct2/show/NCT04450069>
101. Wermke M, Kraus S, Ehninger A, Bargou RC, Goebeler M-E, Middeke JM, Kreissig C, von Bonin M, Koedam J, Pehl M, et al. Proof of concept for a rapidly switchable universal CAR-T platform with UniCAR-T-CD123 in relapsed/refractory AML. *Blood*. 2021;137(22):3145–3148. doi:10.1182/blood.2020009759
102. Hou B, Tang Y, Li W, Zeng Q, Chang D. Efficiency of CAR-T Therapy for Treatment of Solid Tumor in Clinical Trials: A Meta-Analysis. *Dis. Markers*. 2019;2019:1–11. doi:10.1155/2019/3425291
103. Baghban R, Roshangar L, Jahanban-Esfahlan R, Seidi K, Ebrahimi-Kalan A, Jaymand M, Kolahian S, Javaheri T, Zare P. Tumor microenvironment complexity and therapeutic implications at a glance. *Cell Commun. Signal*. 2020;18(1):59. doi:10.1186/s12964-020-0530-4
104. Henke E, Nandigama R, Ergün S. Extracellular Matrix in the Tumor Microenvironment and Its Impact on Cancer Therapy. *Front. Mol. Biosci*. 2020;6:160. doi:10.3389/fmolb.2019.00160
105. Giraldo NA, Becht E, Remark R, Damotte D, Sautès-Fridman C, Fridman WH. The immune contexture of primary and metastatic human tumours. *Curr. Opin. Immunol*. 2014;27(1):8–15. doi:10.1016/j.coi.2014.01.001
106. Giraldo NA, Sanchez-Salas R, Peske JD, Vano Y, Becht E, Petitprez F, Validire P, Ingels A, Cathelineau X, Fridman WH, et al. The clinical role of the TME in solid cancer. *Br. J. Cancer*. 2019;120(1):45–53. doi:10.1038/s41416-018-0327-z
107. Yamakoshi Y, Tanaka H, Sakimura C, Deguchi S, Mori T, Tamura T, Toyokawa T, Muguruma K, Hirakawa K, Ohira M. Immunological potential of tertiary lymphoid structures surrounding the primary tumor in gastric cancer. *Int. J. Oncol*. 2020;57(1):171–182. doi:10.3892/ijo.2020.5042
108. Munoz-Eraza L, Rhodes JL, Marion VC, Kemp RA. Tertiary lymphoid structures in cancer – considerations for patient prognosis. *Cell. Mol. Immunol*. 2020;17(6):570–575. doi:10.1038/s41423-020-0457-0
109. J. Gunderson A, Rajamanickam V, Bui C, Bernard B, Pucilowska J, Ballesteros-Merino C, Schmidt M, McCarty K, Philips M, Piening B, et al. Germinal center reactions in tertiary lymphoid structures associate with neoantigen burden, humoral immunity and long-term survivorship in pancreatic cancer. *Oncoimmunology*. 2021;10(1). doi:10.1080/2162402X.2021.1900635
110. Duan Q, Zhang H, Zheng J, Zhang L. Turning Cold into Hot: Firing up the Tumor Microenvironment. *Trends in Cancer*. 2020;6(7):605–618. doi:10.1016/j.trecan.2020.02.022
111. Henze J, Tacke F, Hardt O, Alves F, Al Rawashdeh W. Enhancing the Efficacy of CAR T Cells in the Tumor Microenvironment of Pancreatic Cancer. *Cancers (Basel)*. 2020;12(6):1389. doi:10.3390/cancers12061389
112. Mitra AK, Zillhardt M, Hua Y, Tiwari P, Murmann AE, Peter ME, Lengyel E. MicroRNAs Reprogram Normal Fibroblasts into Cancer-Associated Fibroblasts in Ovarian Cancer. *Cancer Discov*. 2012;2(12):1100–1108. doi:10.1158/2159-8290.CD-12-0206
113. Raz Y, Cohen N, Shani O, Bell RE, Novitskiy S V., Abramovitz L, Levy C, Milyavsky M, Leider-Trejo L, Moses HL, et al. Bone marrow-derived fibroblasts are a functionally distinct stromal

- cell population in breast cancer. *J. Exp. Med.* 2018;215(12):3075–3093. doi:10.1084/jem.20180818
114. Kidd S, Spaeth E, Watson K, Burks J, Lu H, Klopp A, Andreeff M, Marini FC. Origins of the Tumor Microenvironment: Quantitative Assessment of Adipose-Derived and Bone Marrow-Derived Stroma Rameshwar P, editor. *PLoS One.* 2012;7(2):e30563. doi:10.1371/journal.pone.0030563
115. San Francisco IF, DeWolf WC, Peehl DM, Olumi AF. Expression of transforming growth factor-beta 1 and growth in soft agar differentiate prostate carcinoma-associated fibroblasts from normal prostate fibroblasts. *Int. J. Cancer.* 2004;112(2):213–218. doi:10.1002/ijc.20388
116. Cheng J, Deng Y, Yi H, Wang G, Fu B, Chen W, Liu W, Tai Y, Peng Y, Zhang Q. Hepatic carcinoma-associated fibroblasts induceIDO-producing regulatory dendritic cells through IL-6-mediated STAT3 activation. *Oncogenesis.* 2016;5(2):e198–e198. doi:10.1038/oncsis.2016.7
117. Zhang A, Qian Y, Ye Z, Chen H, Xie H, Zhou L, Shen Y, Zheng S. Cancer-associated fibroblasts promote M2 polarization of macrophages in pancreatic ductal adenocarcinoma. *Cancer Med.* 2017;6(2):463–470. doi:10.1002/cam4.993
118. Ahmadzadeh M, Rosenberg SA. TGF- β 1 Attenuates the Acquisition and Expression of Effector Function by Tumor Antigen-Specific Human Memory CD8 T Cells. *J. Immunol.* 2005;174(9):5215–5223. doi:10.4049/jimmunol.174.9.5215
119. Dumont N, Liu B, DeFilippis RA, Chang H, Rabban JT, Karnezis AN, Tjoe JA, Marx J, Parvin B, Tlsty TD. Breast Fibroblasts Modulate Early Dissemination, Tumorigenesis, and Metastasis through Alteration of Extracellular Matrix Characteristics. *Neoplasia.* 2013;15(3):249–262. doi:10.1593/neo.121950
120. Johansson A-C, Ansell A, Jerhammar F, Lindh MB, Grénman R, Munck-Wikland E, Östman A, Roberg K. Cancer-Associated Fibroblasts Induce Matrix Metalloproteinase-Mediated Cetuximab Resistance in Head and Neck Squamous Cell Carcinoma Cells. *Mol. Cancer Res.* 2012;10(9):1158–1168. doi:10.1158/1541-7786.MCR-12-0030
121. Mahadevan D, Von Hoff DD. Tumor-stroma interactions in pancreatic ductal adenocarcinoma. *Mol. Cancer Ther.* 2007;6(4):1186–1197. doi:10.1158/1535-7163.MCT-06-0686
122. Bergamaschi A, Tagliabue E, Sørli T, Naume B, Triulzi T, Orlandi R, Russnes H, Nesland J, Tammi R, Auvinen P, et al. Extracellular matrix signature identifies breast cancer subgroups with different clinical outcome. *J. Pathol.* 2008;214(3):357–367. doi:10.1002/path.2278
123. Hanahan D, Weinberg RA. The hallmarks of cancer. *Cell.* 2000;100(1):57–70. doi:10.1016/s0092-8674(00)81683-9
124. Hanahan D, Weinberg RA. Hallmarks of Cancer: The Next Generation. *Cell.* 2011;144(5):646–674. doi:10.1016/j.cell.2011.02.013
125. Hanahan D. Hallmarks of Cancer: New Dimensions. *Cancer Discov.* 2022;12(1):31–46. doi:10.1158/2159-8290.CD-21-1059
126. Salmon H, Franciszkiewicz K, Damotte D, Dieu-Nosjean M-C, Validire P, Trautmann A, Mami-Chouaib F, Donnadieu E. Matrix architecture defines the preferential localization and migration of T cells into the stroma of human lung tumors. *J. Clin. Invest.* 2012;122(3):899–910. doi:10.1172/JCI45817
127. Kobayashi N, Miyoshi S, Mikami T, Koyama H, Kitazawa M, Takeoka M, Sano K, Amano J,

- Isogai Z, Niida S, et al. Hyaluronan Deficiency in Tumor Stroma Impairs Macrophage Trafficking and Tumor Neovascularization. *Cancer Res.* 2010;70(18):7073–7083. doi:10.1158/0008-5472.CAN-09-4687
128. Torre C, Wang SJ, Xia W, Bourguignon LYW. Reduction of Hyaluronan-CD44-Mediated Growth, Migration, and Cisplatin Resistance in Head and Neck Cancer Due to Inhibition of Rho Kinase and PI-3 Kinase Signaling. *Arch. Otolaryngol. Neck Surg.* 2010;136(5):493. doi:10.1001/archoto.2010.25
129. Bourguignon LW, Zhu H, Shao L, Chen Y-W. CD44 Interaction with c-Src Kinase Promotes Cortactin-mediated Cytoskeleton Function and Hyaluronic Acid-dependent Ovarian Tumor Cell Migration. *J. Biol. Chem.* 2001;276(10):7327–7336. doi:10.1074/jbc.M006498200
130. Hamidi H, Ivaska J. Every step of the way: integrins in cancer progression and metastasis. *Nat. Rev. Cancer.* 2018;18(9):533–548. doi:10.1038/s41568-018-0038-z
131. Lorusso G, Rüegg C, Kuonen F. Targeting the Extra-Cellular Matrix—Tumor Cell Crosstalk for Anti-Cancer Therapy: Emerging Alternatives to Integrin Inhibitors. *Front. Oncol.* 2020;10(1231). doi:10.3389/fonc.2020.01231
132. Sethi T, Rintoul RC, Moore SM, MacKinnon AC, Salter D, Choo C, Chilvers ER, Dransfield I, Donnelly SC, Strieter R, et al. Extracellular matrix proteins protect small cell lung cancer cells against apoptosis: A mechanism for small cell lung cancer growth and drug resistance in vivo. *Nat. Med.* 1999;5(6):662–668. doi:10.1038/9511
133. Yang D, Tang Y, Fu H, Xu J, Hu Z, Zhang Y, Cai Q. Integrin $\beta 1$ promotes gemcitabine resistance in pancreatic cancer through Cdc42 activation of PI3K p110 β signaling. *Biochem. Biophys. Res. Commun.* 2018;505(1):215–221. doi:10.1016/j.bbrc.2018.09.061
134. Lesniak D, Xu Y, Deschenes J, Lai R, Thoms J, Murray D, Gosh S, Mackey JR, Sabri S, Abdulkarim B. $\beta 1$ -integrin circumvents the antiproliferative effects of trastuzumab in human epidermal growth factor receptor-2-positive breast cancer. *Cancer Res.* 2009;69(22):8620–8628. doi:10.1158/0008-5472.CAN-09-1591
135. Munger JS, Huang X, Kawakatsu H, Griffiths MJD, Dalton SL, Wu J, Pittet JF, Kaminski N, Garat C, Matthay MA, et al. The integrin alpha v beta 6 binds and activates latent TGF beta 1: a mechanism for regulating pulmonary inflammation and fibrosis. *Cell.* 1999;96(3):319–28. doi:10.1016/s0092-8674(00)80545-0
136. Cambier S, Gline S, Mu D, Collins R, Araya J, Dolganov G, Einheber S, Boudreau N, Nishimura SL. Integrin alpha(v)beta8-mediated activation of transforming growth factor-beta by perivascular astrocytes: an angiogenic control switch. *Am. J. Pathol.* 2005;166(6):1883–94. doi:10.1016/s0002-9440(10)62497-2
137. Roberts AB, Sporn MB, Assoian RK, Smith JM, Roche NS, Wakefield LM, Heine UI, Liotta LA, Falanga V, Kehrl JH. Transforming growth factor type beta: rapid induction of fibrosis and angiogenesis in vivo and stimulation of collagen formation in vitro. *Proc. Natl. Acad. Sci.* 1986;83(12):4167–4171. doi:10.1073/pnas.83.12.4167
138. Roberts AB, Anzano MA, Wakefield LM, Roche NS, Stern DF, Sporn MB. Type beta transforming growth factor: a bifunctional regulator of cellular growth. *Proc. Natl. Acad. Sci.* 1985;82(1):119–123. doi:10.1073/pnas.82.1.119
139. Miyazono K, Hellman U, Wernstedt C, Heldin CH. Latent high molecular weight complex of transforming growth factor $\beta 1$. Purification from human platelets and structural

- characterization. *J. Biol. Chem.* 1988;263(13):6407–6415. doi:10.1016/s0021-9258(18)68800-3
140. Gray AM, Mason AJ. Requirement for activin A and transforming growth factor--beta 1 pro-regions in homodimer assembly. *Science* (80-.). 1990;247(4948):1328–30. doi:10.1126/science.2315700
141. Dubois CM, Laprise M-H, Blanchette F, Gentry LE, Leduc R. Processing of Transforming Growth Factor β 1 Precursor by Human Furin Convertase. *J. Biol. Chem.* 1995;270(18):10618–10624. doi:10.1074/jbc.270.18.10618
142. Shi M, Zhu J, Wang R, Chen X, Mi L, Walz T, Springer TA. Latent TGF- β structure and activation. *Nature.* 2011;474(7351):343–349. doi:10.1038/nature10152
143. Todorovic V, Rifkin DB. LTBPs, more than just an escort service. *J. Cell. Biochem.* 2012;113(2):410–418. doi:10.1002/jcb.23385
144. Taipale J, Miyazono K, Heldin C, Keski-Oja J. Latent transforming growth factor-beta 1 associates to fibroblast extracellular matrix via latent TGF-beta binding protein. *J. Cell Biol.* 1994;124(1):171–181. doi:10.1083/jcb.124.1.171
145. Taylor AW. Review of the activation of TGF-beta in immunity. *J. Leukoc. Biol.* 2009;85(1):29–33. doi:10.1189/jlb.0708415
146. Wang R, Kozhaya L, Mercer F, Khaitan A, Fujii H, Unutmaz D. Expression of GARP selectively identifies activated human FOXP3+ regulatory T cells. *Proc. Natl. Acad. Sci.* 2009;106(32):13439–13444. doi:10.1073/pnas.0901965106
147. Tran DQ, Andersson J, Wang R, Ramsey H, Unutmaz D, Shevach EM. GARP (LRRC32) is essential for the surface expression of latent TGF- β on platelets and activated FOXP3 + regulatory T cells. *Proc. Natl. Acad. Sci.* 2009;106(32):13445–13450. doi:10.1073/pnas.0901944106
148. Qin Y, Garrison BS, Ma W, Wang R, Jiang A, Li J, Mistry M, Bronson RT, Santoro D, Franco C, et al. A Milieu Molecule for TGF- β Required for Microglia Function in the Nervous System. *Cell.* 2018;174(1):156–171. doi:10.1016/j.cell.2018.05.027
149. Batlle E, Massagué J. Transforming Growth Factor- β Signaling in Immunity and Cancer. *Immunity.* 2019;50(4):924–940. doi:10.1016/j.immuni.2019.03.024
150. Travis MA, Sheppard D. TGF- β Activation and Function in Immunity. *Annu. Rev. Immunol.* 2014;32(1):51–82. doi:10.1146/annurev-immunol-032713-120257
151. Annes JP, Munger JS, Rifkin DB. Making sense of latent TGF β activation. *J. Cell Sci.* 2003;116(2):217–224. doi:10.1242/jcs.00229
152. Cho H-R, Hong S-B, Kim Y II, Lee J-W, Kim N-I. Differential expression of TGF-beta isoforms during differentiation of HaCaT human keratinocyte cells: implication for the separate role in epidermal differentiation. *J. Korean Med. Sci.* 2004;19(6):853–858. doi:10.3346/jkms.2004.19.6.853
153. Ferguson MWJ, O’Kane S. Scar-free healing: from embryonic mechanisms to adult therapeutic intervention. *Philos. Trans. R. Soc. London. Ser. B, Biol. Sci.* 2004;359(1445):839–850. doi:10.1098/rstb.2004.1475
154. Gupta A, Budhu S, Fitzgerald K, Giese R, Michel AO, Holland A, Campesato LF, van Snick J, Uyttenhove C, Ritter G, et al. Isoform specific anti-TGF β therapy enhances antitumor efficacy

- in mouse models of cancer. *Commun. Biol.* 2021;4(1):1296. doi:10.1038/s42003-021-02773-z
155. Danielpour D, Dart LL, Flanders KC, Roberts AB, Sporn MB. Immunodetection and quantitation of the two forms of transforming growth factor-beta (TGF- β 1 and TGF- β 2) secreted by cells in culture. *J. Cell. Physiol.* 1989;138(1):79–86. doi:10.1002/jcp.1041380112
156. de Saint-Vis B, Fugier-Vivier I, Massacrier C, Gaillard C, Vanbervliet B, Ait-Yahia S, Banchereau J, Liu Y-J, Lebecque S, Caux C. The Cytokine Profile Expressed by Human Dendritic Cells Is Dependent on Cell Subtype and Mode of Activation. *J. Immunol.* 1998;160(4):1666 LP – 1676.
157. Kehrl JH, Wakefield LM, Roberts AB, Jakowlew S, Alvarez-Mon M, Derynck R, Sporn MB, Fauci AS. Production of transforming growth factor beta by human T lymphocytes and its potential role in the regulation of T cell growth. *J. Exp. Med.* 1986;163(5):1037–1050. doi:10.1084/jem.163.5.1037
158. Kehrl JH, Roberts AB, Wakefield LM, Jakowlew S, Sporn MB, Fauci AS. Transforming growth factor beta is an important immunomodulatory protein for human B lymphocytes. *J. Immunol.* 1986;137(12).
159. Zhang D, Qiu X, Li J, Zheng S, Li L, Zhao H. TGF- β secreted by tumor-associated macrophages promotes proliferation and invasion of colorectal cancer via miR-34a-VEGF axis. *Cell Cycle.* 2018;17(24):2766–2778. doi:10.1080/15384101.2018.1556064
160. Kobayashi T, Iijima K, Kita H. Marked Airway Eosinophilia Prevents Development of Airway Hyper-responsiveness During an Allergic Response in IL-5 Transgenic Mice. *J. Immunol.* 2003;170(11):5756–5763. doi:10.4049/jimmunol.170.11.5756
161. Yu Y, Xiao C-H, Tan L-D, Wang Q-S, Li X-Q, Feng Y-M. Cancer-associated fibroblasts induce epithelial–mesenchymal transition of breast cancer cells through paracrine TGF- β signalling. *Br. J. Cancer.* 2014;110(3):724–732. doi:10.1038/bjc.2013.768
162. Guo Y, Cui W, Pei Y, Xu D. Platelets promote invasion and induce epithelial to mesenchymal transition in ovarian cancer cells by TGF- β signaling pathway. *Gynecol. Oncol.* 2019;153(3):639–650. doi:10.1016/j.ygyno.2019.02.026
163. Lyons RM, Keski-Oja J, Moses HL. Proteolytic activation of latent transforming growth factor-beta from fibroblast-conditioned medium. *J. Cell Biol.* 1988;106(5):1659–1665. doi:10.1083/jcb.106.5.1659
164. Tatti O, Vehviläinen P, Lehti K, Keski-Oja J. MT1-MMP releases latent TGF-beta1 from endothelial cell extracellular matrix via proteolytic processing of LTBP-1. *Exp. Cell Res.* 2008;314(13):2501–14. doi:10.1016/j.yexcr.2008.05.018
165. Annes JP, Chen Y, Munger JS, Rifkin DB. Integrin α V β 6-mediated activation of latent TGF- β requires the latent TGF- β binding protein-1. *J. Cell Biol.* 2004;165(5):723–734. doi:10.1083/jcb.200312172
166. Unsold C, Hyytiäinen M, Bruckner-Tuderman L, Keski-Oja J. Latent TGF-beta binding protein LTBP-1 contains three potential extracellular matrix interacting domains. *J. Cell Sci.* 2001;114(1):187–197. doi:10.1242/jcs.114.1.187
167. Mu D, Cambier S, Fjellbirkeland L, Baron JL, Munger JS, Kawakatsu H, Sheppard D, Broaddus VC, Nishimura SL. The integrin α V β 8 mediates epithelial homeostasis through MT1-MMP-dependent activation of TGF- β 1. *J. Cell Biol.* 2002;157(3):493–507. doi:10.1083/jcb.200109100

168. Heldin C-H, Moustakas A. Signaling Receptors for TGF- β Family Members. *Cold Spring Harb. Perspect. Biol.* 2016;8(8). doi:10.1101/cshperspect.a022053
169. Busch S, Acar A, Magnusson Y, Gregersson P, Rydén L, Landberg G. TGF-beta receptor type-2 expression in cancer-associated fibroblasts regulates breast cancer cell growth and survival and is a prognostic marker in pre-menopausal breast cancer. *Oncogene.* 2015;34(1):27–38. doi:10.1038/onc.2013.527
170. Hempel N, How T, Cooper SJ, Green TR, Dong M, Copland JA, Wood CG, Blobe GC. Expression of the type III TGF- β receptor is negatively regulated by TGF- β . *Carcinogenesis.* 2008;29(5):905–912. doi:10.1093/carcin/bgn049
171. Panchenko MP, Williams MC, Brody JS, Yu Q. Type I receptor serine-threonine kinase preferentially expressed in pulmonary blood vessels. *Am. J. Physiol. Cell. Mol. Physiol.* 1996;270(4):547–558. doi:10.1152/ajplung.1996.270.4.L547
172. Beger B, Robertson K, Evans A, Grant A, Berg J. Expression of endoglin and the activin receptor-like kinase 1 in skin suggests a role for these receptors in normal skin function and skin tumorigenesis. *Br. J. Dermatol.* 2006;154(2):379–382. doi:10.1111/j.1365-2133.2005.07043.x
173. König H-G, Kögel D, Rami A, Prehn JHM. TGF- β 1 activates two distinct type I receptors in neurons. *J. Cell Biol.* 2005;168(7):1077–1086. doi:10.1083/jcb.200407027
174. Cheifetz S, Like B, Massague J. Cellular distribution of type I and type II receptors for transforming growth factor-beta. *J. Biol. Chem.* 1986;261(21):9972–9978. doi:10.1016/S0021-9258(18)67611-2
175. Shi Y, Massagué J. Mechanisms of TGF- β Signaling from Cell Membrane to the Nucleus. *Cell.* 2003;113(6):685–700. doi:10.1016/S0092-8674(03)00432-X
176. Esparza-López J, Montiel JL, Vilchis-Landeros MM, Okadome T, Miyazono K, López-Casillas F. Ligand Binding and Functional Properties of Betaglycan, a Co-receptor of the Transforming Growth Factor- β Superfamily. *J. Biol. Chem.* 2001;276(18):14588–14596. doi:10.1074/jbc.M008866200
177. Tazat K, Hector-Greene M, Blobe GC, Henis YI. T β RIII independently binds type I and type II TGF- β receptors to inhibit TGF- β signaling Luo K, editor. *Mol. Biol. Cell.* 2015;26(19):3535–3545. doi:10.1091/mbc.E15-04-0203
178. Luo K. Positive and negative regulation of type II TGF-beta receptor signal transduction by autophosphorylation on multiple serine residues. *EMBO J.* 1997;16(8):1970–1981. doi:10.1093/emboj/16.8.1970
179. Nakao A. TGF-beta receptor-mediated signalling through Smad2, Smad3 and Smad4. *EMBO J.* 1997;16(17):5353–5362. doi:10.1093/emboj/16.17.5353
180. Gingery A, Bradley EW, Pederson L, Ruan M, Horwood NJ, Oursler MJ. TGF- β coordinately activates TAK1/MEK/AKT/NF κ B and SMAD pathways to promote osteoclast survival. *Exp. Cell Res.* 2008;314(15):2725–2738. doi:10.1016/j.yexcr.2008.06.006
181. Remy I, Montmarquette A, Michnick SW. PKB/Akt modulates TGF- β signalling through a direct interaction with Smad3. *Nat. Cell Biol.* 2004;6(4):358–365. doi:10.1038/ncb1113
182. Hannon GJ, Beach D. p15^{INK4B} is a potential effector of TGF- β -induced cell cycle arrest. *Nature.* 1994;371(6494):257–261. doi:10.1038/371257a0

183. Datto MB, Li Y, Panus JF, Howe DJ, Xiong Y, Wang XF. Transforming growth factor beta induces the cyclin-dependent kinase inhibitor p21 through a p53-independent mechanism. *Proc. Natl. Acad. Sci.* 1995;92(12):5545–5549. doi:10.1073/pnas.92.12.5545
184. Dardare J, Witz A, Merlin J-L, Gilson P, Harlé A. SMAD4 and the TGF β Pathway in Patients with Pancreatic Ductal Adenocarcinoma. *Int. J. Mol. Sci.* 2020;21(10):3534. doi:10.3390/ijms21103534
185. Goggins M, Shekher M, Turnacioglu K, Yeo CJ, Hruban RH, Kern SE. Genetic alterations of the transforming growth factor beta receptor genes in pancreatic and biliary adenocarcinomas. *Cancer Res.* 1998;58(23):5329–32.
186. Miettinen PJ, Ebner R, Lopez AR, Derynck R. TGF-beta induced transdifferentiation of mammary epithelial cells to mesenchymal cells: involvement of type I receptors. *J. Cell Biol.* 1994;127(6):2021–2036. doi:10.1083/jcb.127.6.2021
187. Nieto MA, Huang RY-J, Jackson RA, Thiery JP. EMT: 2016. *Cell.* 2016;166(1):21–45. doi:10.1016/j.cell.2016.06.028
188. Zheng X, Carstens JL, Kim J, Scheible M, Kaye J, Sugimoto H, Wu C-C, LeBleu VS, Kalluri R. Epithelial-to-mesenchymal transition is dispensable for metastasis but induces chemoresistance in pancreatic cancer. *Nature.* 2015;527(7579):525–530. doi:10.1038/nature16064
189. Tsukamoto H, Shibata K, Kajiyama H, Terauchi M, Nawa A, Kikkawa F. Irradiation-induced epithelial–mesenchymal transition (EMT) related to invasive potential in endometrial carcinoma cells. *Gynecol. Oncol.* 2007;107(3):500–504. doi:10.1016/j.ygyno.2007.08.058
190. Laouar Y, Sutterwala FS, Gorelik L, Flavell RA. Transforming growth factor- β controls T helper type 1 cell development through regulation of natural killer cell interferon- γ . *Nat. Immunol.* 2005;6(6):600–607. doi:10.1038/ni1197
191. Castriconi R, Cantoni C, Della Chiesa M, Vitale M, Marcenaro E, Conte R, Biassoni R, Bottino C, Moretta L, Moretta A. Transforming growth factor β 1 inhibits expression of NKp30 and NKG2D receptors: Consequences for the NK-mediated killing of dendritic cells. *Proc. Natl. Acad. Sci.* 2003;100(7):4120–4125. doi:10.1073/pnas.0730640100
192. Viel S, Marçais A, Guimaraes FS-F, Loftus R, Rabilloud J, Grau M, Degouve S, Djebali S, Sanlaville A, Charrier E, et al. TGF- β inhibits the activation and functions of NK cells by repressing the mTOR pathway. *Sci. Signal.* 2016;9(415). doi:10.1126/scisignal.aad1884
193. Fainaru O, Shay T, Hantisteanu S, Goldenberg D, Domany E, Groner Y. TGF β -dependent gene expression profile during maturation of dendritic cells. *Genes Immun.* 2007;8(3):239–244. doi:10.1038/sj.gene.6364380
194. Papaspyridonos M, Matei I, Huang Y, do Rosario Andre M, Brazier-Mitouart H, Waite JC, Chan AS, Kalter J, Ramos I, Wu Q, et al. Id1 suppresses anti-tumour immune responses and promotes tumour progression by impairing myeloid cell maturation. *Nat. Commun.* 2015;6(1):6840. doi:10.1038/ncomms7840
195. Chen C-H, Seguin-Devaux C, Burke NA, Oriss TB, Watkins SC, Clipstone N, Ray A. Transforming Growth Factor β Blocks Tec Kinase Phosphorylation, Ca²⁺ Influx, and NFATc Translocation Causing Inhibition of T Cell Differentiation. *J. Exp. Med.* 2003;197(12):1689–1699. doi:10.1084/jem.20021170
196. Lin JT, Martin SL, Xia L, Gorham JD. TGF-beta 1 uses distinct mechanisms to inhibit IFN-

- gamma expression in CD4+ T cells at priming and at recall: differential involvement of Stat4 and T-bet. *J. Immunol.* 2005;174(10):5950–5958. doi:10.4049/jimmunol.174.10.5950
197. Brabletz T, Pfeuffer I, Schorr E, Siebelt F, Wirth T, Serfling E. Transforming growth factor beta and cyclosporin A inhibit the inducible activity of the interleukin-2 gene in T cells through a noncanonical octamer-binding site. *Mol. Cell. Biol.* 1993;13(2):1155–1162. doi:10.1128/mcb.13.2.1155-1162.1993
198. Chen W, Jin W, Hardegen N, Lei K, Li L, Marinos N, McGrady G, Wahl SM. Conversion of Peripheral CD4+CD25– Naive T Cells to CD4+CD25+ Regulatory T Cells by TGF- β Induction of Transcription Factor Foxp3. *J. Exp. Med.* 2003;198(12):1875–1886. doi:10.1084/jem.20030152
199. Zhou L, Lopes JE, Chong MMW, Ivanov II, Min R, Victora GD, Shen Y, Du J, Rubtsov YP, Rudensky AY, et al. TGF- β -induced Foxp3 inhibits TH17 cell differentiation by antagonizing ROR γ t function. *Nature.* 2008;453(7192):236–240. doi:10.1038/nature06878
200. Liu C, Cheng H, Luo G, Lu Y, Jin K, Guo M, Ni Q, Yu X. Circulating regulatory T cell subsets predict overall survival of patients with unresectable pancreatic cancer. *Int. J. Oncol.* 2017;51(2):686–694. doi:10.3892/ijo.2017.4032
201. Stevenson JP, Kindler HL, Papasavvas E, Sun J, Jacobs-Small M, Hull J, Schwed D, Ranganathan A, Newick K, Heitjan DF, et al. Immunological effects of the TGF β -blocking antibody GC1008 in malignant pleural mesothelioma patients. *Oncoimmunology.* 2013;2(8). doi:10.4161/onci.26218
202. Santiago B, Gutierrez-Cañas I, Dotor J, Palao G, Lasarte JJ, Ruiz J, Prieto J, Borrás-Cuesta F, Pablos JL. Topical Application of a Peptide Inhibitor of Transforming Growth Factor- β 1 Ameliorates Bleomycin-Induced Skin Fibrosis. *J. Invest. Dermatol.* 2005;125(3):450–455. doi:10.1111/j.0022-202X.2005.23859.x
203. Bogdahn U, Hau P, Stockhammer G, Venkataramana NK, Mahapatra AK, Suri A, Balasubramaniam A, Nair S, Oliushine V, Parfenov V, et al. Targeted therapy for high-grade glioma with the TGF- 2 inhibitor trabedersen: results of a randomized and controlled phase IIb study. *Neuro. Oncol.* 2011;13(1):132–142. doi:10.1093/neuonc/noq142
204. Yap TA, Vieito M, Baldini C, Sepúlveda-Sánchez JM, Kondo S, Simonelli M, Cosman R, van der Westhuizen A, Atkinson V, Carpentier AF, et al. First-In-Human Phase I Study of a Next-Generation, Oral, TGF β Receptor 1 Inhibitor, LY3200882, in Patients with Advanced Cancer. *Clin. Cancer Res.* 2021;27(24):6666–6676. doi:10.1158/1078-0432.CCR-21-1504
205. Nemunaitis J, Dillman RO, Schwarzenberger PO, Senzer N, Cunningham C, Cutler J, Tong A, Kumar P, Pappen B, Hamilton C, et al. Phase II Study of Belagenpumatucel-L, a Transforming Growth Factor Beta-2 Antisense Gene-Modified Allogeneic Tumor Cell Vaccine in Non–Small-Cell Lung Cancer. *J. Clin. Oncol.* 2006;24(29):4721–4730. doi:10.1200/JCO.2005.05.5335
206. Knudson KM, Hicks KC, Luo X, Chen J-Q, Schlom J, Gameiro SR. M7824, a novel bifunctional anti-PD-L1/TGF β Trap fusion protein, promotes anti-tumor efficacy as monotherapy and in combination with vaccine. *Oncoimmunology.* 2018;7(5). doi:10.1080/2162402X.2018.1426519
207. Merck KGaA. Bintrafusp Alfa Update - News | Merck. [accessed February 2, 2022]. <https://www.merckgroup.com/en/news/bintrafusp-alfa-update-23-08-2021.html>
208. Rolfo C, Sortino G, Smits E, Passiglia F, Bronte G, Castiglia M, Russo A, Santos ES, Janssens A, Pauwels P, et al. Immunotherapy: is a minor god yet in the pantheon of treatments for lung cancer? *Expert Rev. Anticancer Ther.* 2014;14(10):1173–1187.

doi:10.1586/14737140.2014.952287

209. Giaccone G, Bazhenova LA, Nemunaitis J, Tan M, Juhász E, Ramlau R, van den Heuvel MM, Lal R, Kloecker G., Eaton KD, et al. A phase III study of belagenpumatucel-L, an allogeneic tumour cell vaccine, as maintenance therapy for non-small cell lung cancer. *Eur. J. Cancer.* 2015;51(16):2321–2329. doi:10.1016/j.ejca.2015.07.035

210. Novartis AG. Novartis receives FDA Orphan Drug Designation for NIS793 in pancreatic cancer | Novartis. [accessed February 2, 2022]. <https://www.novartis.com/news/novartis-receives-fda-orphan-drug-designation-nis793-pancreatic-cancer>

211. ClinicalTrials.gov. Study of Efficacy and Safety of NIS793 in Combination With Standard of Care (SOC) Chemotherapy in First-line Metastatic Pancreatic Ductal Adenocarcinoma (mPDAC). [accessed February 2, 2022]. <https://clinicaltrials.gov/ct2/show/NCT04935359>

212. Alabanza LM, Xiong Y, Vu B, Webster B, Wu D, Hu P, Zhu Z, Dropulic B, Dash P, Schneider D. Armored BCMA CAR T Cells Eliminate Multiple Myeloma and Are Resistant to the Suppressive Effects of TGF- β . *Front. Immunol.* 2022;13(832645). doi:10.3389/fimmu.2022.832645

213. Webster B, Xiong Y, Hu P, Wu D, Alabanza L, Orentas RJ, Dropulic B, Schneider D. Self-driving armored CAR-T cells overcome a suppressive milieu and eradicate CD19+ Raji lymphoma in preclinical models. *Mol. Ther.* 2021;29(9):2691–2706. doi:10.1016/j.ymthe.2021.05.006

214. Bollard CM, Tripic T, Cruz CR, Dotti G, Gottschalk S, Torrano V, Dakhova O, Carrum G, Ramos CA, Liu H, et al. Tumor-Specific T-Cells Engineered to Overcome Tumor Immune Evasion Induce Clinical Responses in Patients With Relapsed Hodgkin Lymphoma. *J. Clin. Oncol.* 2018;36(11):1128–1139. doi:10.1200/JCO.2017.74.3179

215. Schäfer D, Tomiuk S, Küster LN, Rawashdeh W Al, Henze J, Tischler-Höhle G, Agorku DJ, Brauner J, Linnartz C, Lock D, et al. Identification of CD318, TSPAN8 and CD66c as target candidates for CAR T cell based immunotherapy of pancreatic adenocarcinoma. *Nat. Commun.* 2021;12(1):1453. doi:10.1038/s41467-021-21774-4

216. Chang ZL, Lorenzini MH, Chen X, Tran U, Nathanael J, Chen YY. Rewiring T-cell responses to soluble factors with chimeric antigen receptors. *Nat Chem Biol.* 2018;14(3):317–324. doi:10.1038/nchembio.2565.

217. Wang L-CS, Lo A, Scholler J, Sun J, Majumdar RS, Kapoor V, Antzis M, Cotner CE, Johnson LA, Durham AC, et al. Targeting Fibroblast Activation Protein in Tumor Stroma with Chimeric Antigen Receptor T Cells Can Inhibit Tumor Growth and Augment Host Immunity without Severe Toxicity. *Cancer Immunol. Res.* 2014;2(2):154–166. doi:10.1158/2326-6066.CIR-13-0027

218. Werchau N, Kotter B, Criado-Moronati E, Gosselink A, Cordes N, Lock D, Lennartz S, Kolbe C, Winter N, Teppert K, et al. Combined targeting of soluble latent TGF- β and a solid tumor-associated antigen with adapter CAR T cells. *Oncoimmunology.* 2022;11(1):2140534. doi:10.1080/2162402X.2022.2140534

219. Pickup M, Novitskiy S, Moses HL. The roles of TGF β in the tumour microenvironment. *Nat. Rev. Cancer.* 2013;13(11):788–799. doi:10.1038/nrc3603

220. Gleizes P, Munger JS, Nunes I, Harpel JG, Mazziari R, Noguera I, Rifkin DB. TGF- β Latency: Biological Significance and Mechanisms of Activation. *Stem Cells.* 1997;15(3):190–197. doi:10.1002/stem.150190

221. Wei L, Yin F, Zhang W, Li L. ITGA1 and cell adhesion-mediated drug resistance in ovarian

- cancer. *Int J Clin Exp Pathol.* 2017;10(5):5522–5529.
222. Gharibi A, La Kim S, Molnar J, Brambilla D, Adamian Y, Hoover M, Hong J, Lin J, Wolfenden L, Kelber JA. ITGA1 is a pre-malignant biomarker that promotes therapy resistance and metastatic potential in pancreatic cancer. *Sci. Rep.* 2017;7(1):1–14. doi:10.1038/s41598-017-09946-z
223. Sukowati CHC, Anfuso B, Crocé LS, Tiribelli C. The role of multipotent cancer associated fibroblasts in hepatocarcinogenesis. *BMC Cancer.* 2015;15(1):188. doi:10.1186/s12885-015-1196-y
224. Spaeth EL, Dembinski JL, Sasser AK, Watson K, Klopp A, Hall B, Andreeff M, Marini F. Mesenchymal Stem Cell Transition to Tumor-Associated Fibroblasts Contributes to Fibrovascular Network Expansion and Tumor Progression Blagosklonny M V., editor. *PLoS One.* 2009;4(4):e4992. doi:10.1371/journal.pone.0004992
225. Kerim AAA, Ellity MM, El-Shorbagy SH, El-Guindy DM. Cancer-associated fibroblasts in epithelial ovarian carcinoma: relation to clinicopathologic characteristics and microvessel density. *Egypt. J. Pathol.* 2019;39(1):89. doi:10.4103/EGJP.EGJP_12_19
226. Labernadie A, Kato T, Brugués A, Serra-Picamal X, Derzsi S, Arwert E, Weston A, González-Tarragó V, Elosegui-Artola A, Albertazzi L, et al. A mechanically active heterotypic E-cadherin/N-cadherin adhesion enables fibroblasts to drive cancer cell invasion. *Nat. Cell Biol.* 2017;19(3):224–237. doi:10.1038/ncb3478
227. Kenny HA, Chiang C-Y, White EA, Schryver EM, Habis M, Romero IL, Ladanyi A, Penicka C V., George J, Matlin K, et al. Mesothelial cells promote early ovarian cancer metastasis through fibronectin secretion. *J. Clin. Invest.* 2014;124(10):4614–4628. doi:10.1172/JCI74778
228. Sandoval P, Jiménez-Heffernan JA, Rynne-Vidal Á, Pérez-Lozano ML, Gilsanz Á, Ruiz-Carpio V, Reyes R, García-Bordas J, Stamatakis K, Dotor J, et al. Carcinoma-associated fibroblasts derive from mesothelial cells via mesothelial-to-mesenchymal transition in peritoneal metastasis. *J. Pathol.* 2013;231(4):517–531. doi:10.1002/path.4281
229. Yeung T-L, Leung CS, Wong K-K, Samimi G, Thompson MS, Liu J, Zaid TM, Ghosh S, Birrer MJ, Mok SC. TGF- β Modulates Ovarian Cancer Invasion by Upregulating CAF-Derived Versican in the Tumor Microenvironment. *Cancer Res.* 2013;73(16):5016–5028. doi:10.1158/0008-5472.CAN-13-0023
230. Robertson IB, Horiguchi M, Zilberberg L, Dabovic B, Hadjiolova K, Rifkin DB. Latent TGF- β -binding proteins. *Matrix Biol.* 2015;47:44–53. doi:10.1016/j.matbio.2015.05.005
231. Taylor AW. Review of the activation of TGF-beta in immunity. *J. Leukoc. Biol.* 2008;85(1):29–33. doi:10.1189/jlb.0708415
232. Stockis J, Colau D, Coulie PG, Lucas S. Membrane protein GARP is a receptor for latent TGF- β on the surface of activated human Treg. *Eur. J. Immunol.* 2009;39(12):3315–3322. doi:10.1002/eji.200939684
233. Cao Y, He H, Li R, Liu X, Chen Y, Qi Y, Yu K, Wang J, Lin C, Liu H, et al. Latency-associated Peptide Identifies Immuno-evasive Subtype Gastric Cancer With Poor Prognosis and Inferior Chemotherapeutic Responsiveness. *Ann. Surg.* 2022;275(1):e163–e173. doi:10.1097/sla.0000000000003833
234. Areström I, Zuber B, Bengtsson T, Ahlborg N. Measurement of human latent transforming growth factor- β 1 using a latency associated protein-reactive ELISA. *J. Immunol. Methods.*

2012;379(1–2):23–29. doi:10.1016/j.jim.2012.02.016

235. Ali NA, Gaughan AA, Orosz CG, Baran CP, McMaken S, Wang Y, Eubank TD, Hunter M, Lichtenberger FJ, Flavahan NA, et al. Latency Associated Peptide Has In Vitro and In Vivo Immune Effects Independent of TGF- β 1 Unutmaz D, editor. PLoS One. 2008;3(4):e1914. doi:10.1371/journal.pone.0001914

236. Thomas GJ, Hart IR, Speight PM, Marshall JF. Binding of TGF- β 1 latency-associated peptide (LAP) to α v β 6 integrin modulates behaviour of squamous carcinoma cells. Br. J. Cancer 2002 878. 2002;87(8):859–867. doi:10.1038/sj.bjc.6600545

237. Gabriely G, da Cunha AP, Rezende RM, Kenyon B, Madi A, Vandeventer T, Skillin N, Rubino S, Garo L, Mazzola MA, et al. Targeting latency-associated peptide promotes antitumor immunity. Sci. Immunol. 2017;2(11):1738. doi:10.1126/sciimmunol.aaj1738

238. Gandhi R, Anderson DE, Weiner HL. Cutting Edge: Immature Human Dendritic Cells Express Latency-Associated Peptide and Inhibit T Cell Activation in a TGF- β -Dependent Manner. J. Immunol. 2007;178(7):4017–4021. doi:10.4049/jimmunol.178.7.4017

239. Hombach A, Heuser C, Sircar R, Tillmann T, Diehl V, Pohl C, Abken H. An anti-CD30 chimeric receptor that mediates CD3-zeta-independent T-cell activation against Hodgkin's lymphoma cells in the presence of soluble CD30. Cancer Res. 1998;58(6):1116–9.

240. Nolan KF, Yun CO, Akamatsu Y, Murphy JC, Leung SO, Beecham EJ, Junghans RP. Bypassing immunization: Optimized design of “designer T cells” against carcinoembryonic antigen (CEA)-expressing tumors, and lack of suppression by soluble CEA. Clin. Cancer Res. 1999;5(12):3928–3941.

241. Westwood JA, Murray WK, Trivett M, Haynes NM, Solomon B, Mileshekin L, Ball D, Michael M, Burman A, Mayura-Guru P, et al. The lewis-Y carbohydrate antigen is expressed by many human tumors and can serve as a target for genetically redirected T cells despite the presence of soluble antigen in serum. J. Immunother. 2009;32(3):292–301. doi:10.1097/CJI.0b013e31819b7c8e

242. Friedman KM, Garrett TE, Evans JW, Horton HM, Latimer HJ, Seidel SL, Horvath CJ, Morgan RA. Effective Targeting of Multiple B-Cell Maturation Antigen-Expressing Hematological Malignancies by Anti-B-Cell Maturation Antigen Chimeric Antigen Receptor T Cells. Hum. Gene Ther. 2018;29(5):585–601. doi:10.1089/hum.2018.001

243. Pont MJ, Hill T, Cole GO, Abbott JJ, Kelliher J, Salter AI, Hudecek M, Comstock ML, Rajan A, Patel BKR, et al. γ -Secretase inhibition increases efficacy of BCMA-specific chimeric antigen receptor T cells in multiple myeloma. Blood. 2019;134(19):1585–1597. doi:10.1182/blood.2019000050

244. Sun L, Gao F, Gao Z, Ao L, Li N, Ma S, Jia M, Li N, Lu P, Sun B, et al. Shed antigen-induced blocking effect on CAR-T cells targeting Glypican-3 in Hepatocellular Carcinoma. J. Immunother. Cancer. 2021;9(4):1–14. doi:10.1136/jitc-2020-001875

245. Hou AJ, Chang ZL, Lorenzini MH, Zah E, Chen YY. TGF- β -responsive CAR-T cells promote anti-tumor immune function. Bioeng. Transl. Med. 2018;3(2):75–86. doi:10.1002/btm2.10097

246. Majzner RG, Rietberg SP, Sotillo E, Dong R, Vachharajani VT, Labanieh L, Myklebust JH, Kadapakkam M, Weber EW, Tousley AM, et al. Tuning the Antigen Density Requirement for CAR T-cell Activity. 2020;10(5):702–723. doi:10.1158/2159-8290.CD-19-0945

247. Breuning J, Philip B, Brown MH. Addition of the C-terminus of CD6 to a chimeric antigen

- receptor enhances cytotoxicity and does not compromise expression. *Immunology*. 2019;156(2):130–135. doi:10.1111/IMM.13009
248. Ampudia J, Young-Greenwald WW, Badrani J, Gatto S, Pavlicek A, Doherty T, Connelly S, Ng CT. CD6-ALCAM signaling regulates multiple effector/memory T cell functions. *J. Immunol*. 2020;204(1 Supplement):150.13 LP-150.13.
249. Grunert F, Daniel S, Nagel G, Kleist S Von, Jantscheff P. CD66b, CD66c and carcinoembryonic antigen (CEA) are independently regulated markers in sera of tumor patients. *Int. J. Cancer*. 1995;63(3):349–355. doi:10.1002/ijc.2910630308
250. Hudecek M, Lupo-Stanghellini MT, Kosasih PL, Sommermeyer D, Jensen MC, Rader C, Riddell SR. Receptor affinity and extracellular domain modifications affect tumor recognition by ROR1-specific chimeric antigen receptor T cells. *Clin. Cancer Res*. 2013. doi:10.1158/1078-0432.CCR-13-0330
251. Hegde M, Corder A, Chow KK, Mukherjee M, Ashoori A, Kew Y, Zhang YJ, Baskin DS, Merchant FA, Brawley VS, et al. Combinational Targeting Offsets Antigen Escape and Enhances Effector Functions of Adoptively Transferred T Cells in Glioblastoma. *Mol. Ther*. 2013;21(11):2087–2101. doi:10.1038/mt.2013.185
252. Chen KH, Wada M, Pinz KG, Liu H, Shuai X, Chen X, Yan LE, Petrov JC, Salman H, Senzel L, et al. A compound chimeric antigen receptor strategy for targeting multiple myeloma. *Leukemia*. 2018;32(2):402–412. doi:10.1038/leu.2017.302
253. Kumar M, Keller B, Makalou N, Sutton RE. Systematic Determination of the Packaging Limit of Lentiviral Vectors. *Hum. Gene Ther*. 2001;12(15):1893–1905. doi:10.1089/104303401753153947
254. Schneider D, Xiong Y, Wu D, Schmitz S, Haso W, Kaiser A, Dropulic B, Orentas RJ, Nölle V, Schmitz S, et al. A tandem CD19/CD20 CAR lentiviral vector drives on-target and off-target antigen modulation in leukemia cell lines. *J. Immunother. cancer*. 2017;5(1):42. doi:10.1186/s40425-017-0246-1
255. Morgan RA, Yang JC, Kitano M, Dudley ME, Laurencot CM, Rosenberg SA. Case report of a serious adverse event following the administration of T cells transduced with a chimeric antigen receptor recognizing ERBB2. *Mol. Ther*. 2010;18(4):843–851. doi:10.1038/MT.2010.24
256. Richman SA, Nunez-Cruz S, Moghimi B, Li LZ, Gershenson ZT, Mourelatos Z, Barrett DM, Grupp SA, Milone MC. High-Affinity GD2-Specific CAR T Cells Induce Fatal Encephalitis in a Preclinical Neuroblastoma Model. *Cancer Immunol. Res*. 2018;6(1):36–46. doi:10.1158/2326-6066.CIR-17-0211
257. Hawinkels LJAC, Verspaget HW, van Duijn W, van der Zon JM, Zuidwijk K, Kubben FJGM, Verheijen JH, Hommes DW, Lamers CBHW, Sier CFM. Tissue level, activation and cellular localisation of TGF- β 1 and association with survival in gastric cancer patients. *Br. J. Cancer*. 2007;97(3):398–404. doi:10.1038/sj.bjc.6603877
258. Kohla MAS, Attia A, Darwesh N, Obada M, Taha H, Youssef MF. Association of serum levels of transforming growth factor b1 with disease severity in patients with hepatocellular carcinoma. *Hepatoma Res*. 2017;3(12):294. doi:10.20517/2394-5079.2017.40
259. Zhao J, Liang Y, Yin Q, Liu S, Wang Q, Tang Y, Cao C. Clinical and prognostic significance of serum transforming growth factor-beta1 levels in patients with pancreatic ductal adenocarcinoma. *Brazilian J. Med. Biol. Res*. 2016;49(8). doi:10.1590/1414-431x20165485

260. Khan SA, Joyce J, Tsuda T. Quantification of active and total transforming growth factor- β levels in serum and solid organ tissues by bioassay. *BMC Res. Notes.* 2012;5:636. doi:10.1186/1756-0500-5-636
261. Lee D, Chung Y-H, Kim JA, Lee YS, Lee D, Jang MK, Kim KM, Lim Y-S, Lee HC, Lee YS. Transforming Growth Factor Beta 1 Overexpression Is Closely Related to Invasiveness of Hepatocellular Carcinoma. *Oncology.* 2012;82(1):11–18. doi:10.1159/000335605
262. Rißmann A, Pieper S, Adams I, Brune T, Wiemann D, Reinhold D. Increased blood plasma concentrations of TGF- β 1 and TGF- β 2 after treatment with intravenous immunoglobulins in childhood autoimmune diseases. *Pediatr. Allergy Immunol.* 2009;20(3):261–265. doi:10.1111/j.1399-3038.2008.00789.x
263. Li Z, Krippendorff B-F, Shah DK. Influence of Molecular size on the clearance of antibody fragments. *Pharm. Res.* 2017;34(10):2131–2141. doi:10.1007/s11095-017-2219-y
264. Guerin M V., Regnier F, Feuillet V, Vimeux L, Weiss JM, Bismuth G, Altan-Bonnet G, Guilbert T, Thoreau M, Finisguerra V, et al. TGF β blocks IFN α/β release and tumor rejection in spontaneous mammary tumors. *Nat. Commun.* 2019;10(1):4131. doi:10.1038/s41467-019-11998-w
265. Guerin M V., Finisguerra V, Van den Eynde BJ, Bercovici N, Trautmann A. Preclinical murine tumor models: a structural and functional perspective. *Elife.* 2020;9. doi:10.7554/eLife.50740
266. Day C-P, Merlino G, Van Dyke T. Preclinical Mouse Cancer Models: A Maze of Opportunities and Challenges. *Cell.* 2015;163(1):39–53. doi:10.1016/j.cell.2015.08.068
267. Weiss JM, Guérin M V., Regnier F, Renault G, Galy-Fauroux I, Vimeux L, Feuillet V, Peranzoni E, Thoreau M, Trautmann A, et al. The STING agonist DMXAA triggers a cooperation between T lymphocytes and myeloid cells that leads to tumor regression. *Oncoimmunology.* 2017;6(10). doi:10.1080/2162402X.2017.1346765
268. Talmadge JE, Singh RK, Fidler IJ, Raz A. Murine Models to Evaluate Novel and Conventional Therapeutic Strategies for Cancer. *Am. J. Pathol.* 2007;170(3):793–804. doi:10.2353/ajpath.2007.060929
269. Devaud C, Westwood JA, John LB, Flynn JK, Paquet-Fifield S, Duong CPM, Yong CSM, Pegram HJ, Stacker SA, Achen MG, et al. Tissues in Different Anatomical Sites Can Sculpt and Vary the Tumor Microenvironment to Affect Responses to Therapy. *Mol. Ther.* 2014;22(1):18–27. doi:10.1038/mt.2013.219
270. Nakano K, Nishizawa T, Komura D, Fujii E, Monnai M, Kato A, Funahashi S, Ishikawa S, Suzuki M. Difference in morphology and interactome profiles between orthotopic and subcutaneous gastric cancer xenograft models. *J. Toxicol. Pathol.* 2018;31(4):293–300. doi:10.1293/tox.2018-0020
271. Skovgard MS, Hocine HR, Saini JK, Moroz M, Bellis RY, Banerjee S, Morello A, Ponomarev V, Villena-Vargas J, Adusumilli PS. Imaging CAR T-cell kinetics in solid tumors: Translational implications. *Mol. Ther. - Oncolytics.* 2021;22:355–367. doi:10.1016/j.omto.2021.06.006
272. Murad JP, Tilakawardane D, Park AK, Lopez LS, Young CA, Gibson J, Yamaguchi Y, Lee HJ, Kennewick KT, Gittins BJ, et al. Pre-conditioning modifies the TME to enhance solid tumor CAR T cell efficacy and endogenous protective immunity. *Mol. Ther.* 2021;29(7):2335–2349. doi:10.1016/j.ymthe.2021.02.024
273. Innamarato P, Kodumudi K, Asby S, Schachner B, Hall M, Mackay A, Wiener D, Beatty M,

- Nagle L, Creelan BC, et al. Reactive Myelopoiesis Triggered by Lymphodepleting Chemotherapy Limits the Efficacy of Adoptive T Cell Therapy. *Mol. Ther.* 2020;28(10):2252–2270. doi:10.1016/j.ymthe.2020.06.025
274. Zhang S, Kohli K, Black RG, Yao L, Spadinger SM, He Q, Pillarisetty VG, Cranmer LD, Van Tine BA, Yee C, et al. Systemic Interferon- γ Increases MHC Class I Expression and T-cell Infiltration in Cold Tumors: Results of a Phase 0 Clinical Trial. *Cancer Immunol. Res.* 2019;7(8):1237–1243. doi:10.1158/2326-6066.CIR-18-0940
275. Spitzer MH, Carmi Y, Reticker-Flynn NE, Kwek SS, Madhireddy D, Martins MM, Gherardini PF, Prestwood TR, Chabon J, Bendall SC, et al. Systemic Immunity Is Required for Effective Cancer Immunotherapy. *Cell.* 2017;168(3):487–502.e15. doi:10.1016/j.cell.2016.12.022
276. Frigault MJ, Lee J, Basil MC, Carpenito C, Motohashi S, Scholler J, Kawalekar OU, Guedan S, McGettigan SE, Posey AD, et al. Identification of Chimeric Antigen Receptors That Mediate Constitutive or Inducible Proliferation of T Cells. *Cancer Immunol. Res.* 2015;3(4):356–367. doi:10.1158/2326-6066.CIR-14-0186
277. Pyo KH, Kim JH, Lee JM, Kim SE, Cho JS, Lim SM, Cho BC. Promising preclinical platform for evaluation of immuno-oncology drugs using Hu-PBL-NSG lung cancer models. *Lung Cancer.* 2019;127(November 2018):112–121. doi:10.1016/j.lungcan.2018.11.035
278. Onoe T, Kalscheuer H, Chittenden M, Zhao G, Yang Y-G, Sykes M. Homeostatic Expansion and Phenotypic Conversion of Human T Cells Depend on Peripheral Interactions with APCs. *J. Immunol.* 2010;184(12):6756–6765. doi:10.4049/jimmunol.0901711
279. Siegel JP. Effects of interferon- γ on the activation of human T lymphocytes. *Cell. Immunol.* 1988;111(2):461–472. doi:10.1016/0008-8749(88)90109-8
280. Bhat P, Leggatt G, Waterhouse N, Frazer IH. Interferon- γ derived from cytotoxic lymphocytes directly enhances their motility and cytotoxicity. *Cell Death Dis.* 2017;8(6):e2836–e2836. doi:10.1038/cddis.2017.67
281. Whitmire JK, Tan JT, Whitton JL. Interferon- γ acts directly on CD8+ T cells to increase their abundance during virus infection. *J. Exp. Med.* 2005;201(7):1053–1059. doi:10.1084/jem.20041463
282. Refaeli Y, Van Parijs L, Alexander SI, Abbas AK. Interferon gamma is required for activation-induced death of T lymphocytes. *J. Exp. Med.* 2002;196(7):999–1005. doi:10.1084/jem.20020666
283. Reed JM, Branigan PJ, Bamezai A. Interferon gamma enhances clonal expansion and survival of CD4+ T cells. *J. Interf. Cytokine Res.* 2008;28(10):611–622. doi:10.1089/jir.2007.0145
284. Zhang N, Bevan MJ. TGF- β signaling to T cells inhibits autoimmunity during lymphopenia-driven proliferation. *Nat. Immunol.* 2012;13(7):667–673. doi:10.1038/ni.2319
285. Boulch M, Cazaux M, Loe-Mie Y, Thibaut R, Corre B, Lemaître F, Grandjean CL, Garcia Z, Bousso P. A cross-talk between CAR T cell subsets and the tumor microenvironment is essential for sustained cytotoxic activity. *Sci. Immunol.* 2021;6(57):1–17. doi:10.1126/sciimmunol.abd4344
286. Coughlan AM, Harmon C, Whelan S, O'Brien EC, O'Reilly VP, Crotty P, Kelly P, Ryan M, Hickey FB, O'Farrelly C, et al. Myeloid Engraftment in Humanized Mice: Impact of Granulocyte-Colony Stimulating Factor Treatment and Transgenic Mouse Strain. *Stem Cells Dev.*

2016;25(7):530–541. doi:10.1089/scd.2015.0289

287. Yang Z-Z, Kim HJ, Villasboas JC, Chen Y-P, Price-Troska T, Jalali S, Wilson M, Novak AJ, Ansell SM. Expression of LAG-3 defines exhaustion of intratumoral PD-1+ T cells and correlates with poor outcome in follicular lymphoma. *Oncotarget*. 2017;8(37):61425–61439. doi:10.18632/oncotarget.18251

288. Chou CK, Schietinger A, Liggitt HD, Tan X, Funk S, Freeman GJ, Ratliff TL, Greenberg NM, Greenberg PD. Cell-Intrinsic Abrogation of TGF- β Signaling Delays but Does Not Prevent Dysfunction of Self/Tumor-Specific CD8 T Cells in a Murine Model of Autochthonous Prostate Cancer. *J. Immunol*. 2012;189(8):3936–3946. doi:10.4049/jimmunol.1201415

289. Baitsch L, Baumgaertner P, Devèvre E, Raghav SK, Legat A, Barba L, Wieckowski S, Bouzourene H, Deplancke B, Romero P, et al. Exhaustion of tumor-specific CD8+ T cells in metastases from melanoma patients. *J. Clin. Invest*. 2011;121(6):2350–2360. doi:10.1172/JCI46102

290. Lesch S, Blumenberg V, Stoiber S, Gottschlich A, Ogonek J, Cadilha BL, Dantes Z, Rataj F, Dorman K, Lutz J, et al. T cells armed with C-X-C chemokine receptor type 6 enhance adoptive cell therapy for pancreatic tumours. *Nat. Biomed. Eng*. 2021;5(11). doi:10.1038/s41551-021-00737-6

291. Vasalou C, Helmlinger G, Gomes B. A Mechanistic Tumor Penetration Model to Guide Antibody Drug Conjugate Design Pappalardo F, editor. *PLoS One*. 2015;10(3):e0118977. doi:10.1371/journal.pone.0118977

292. Rudnick SI, Lou J, Shaller CC, Tang Y, Klein-Szanto AJP, Weiner LM, Marks JD, Adams GP. Influence of Affinity and Antigen Internalization on the Uptake and Penetration of Anti-HER2 Antibodies in Solid Tumors. *Cancer Res*. 2011;71(6):2250–2259. doi:10.1158/0008-5472.CAN-10-2277

293. Lu G, Fakurnejad S, Martin BA, van den Berg NS, van Keulen S, Nishio N, Zhu AJ, Chirita SU, Zhou Q, Gao RW, et al. Predicting Therapeutic Antibody Delivery into Human Head and Neck Cancers. *Clin. Cancer Res*. 2020;26(11):2582–2594. doi:10.1158/1078-0432.CCR-19-3717

294. Adams GP, Schier R, McCall AM, Simmons HH, Horak EM, Alpaugh RK, Marks JD, Weiner LM. High affinity restricts the localization and tumor penetration of single-chain Fv antibody molecules. *Cancer Res*. 2001;61(12):4750–4755.

295. Fujimori K, Covell DG, Fletcher JE, Weinstein JN. A modeling analysis of monoclonal antibody percolation through tumors: A binding-site barrier. *J. Nucl. Med*. 1990;31(7):1191–1198.

296. Lu G, Nishio N, van den Berg NS, Martin BA, Fakurnejad S, van Keulen S, Colevas AD, Thurber GM, Rosenthal EL. Co-administered antibody improves penetration of antibody–dye conjugate into human cancers with implications for antibody–drug conjugates. *Nat. Commun*. 2020;11(1):5667. doi:10.1038/s41467-020-19498-y

297. Yokota T, Milenic DE, Whitlow M, Schlom J. Rapid tumor penetration of a single-chain Fv and comparison with other immunoglobulin forms. *Cancer Res*. 1992;52(12):3402–8.

298. Nessler I, Khera E, Vance S, Kopp A, Qiu Q, Keating TA, Abu-Yousif AO, Sandal T, Legg J, Thompson L, et al. Increased Tumor Penetration of Single-Domain Antibody–Drug Conjugates Improves In Vivo Efficacy in Prostate Cancer Models. *Cancer Res*. 2020;80(6):1268–1278. doi:10.1158/0008-5472.CAN-19-2295

299. Dobosz M, Ntziachristos V, Scheuer W, Strobel S. Multispectral Fluorescence Ultramicroscopy: Three-Dimensional Visualization and Automatic Quantification of Tumor Morphology, Drug Penetration, and Antiangiogenic Treatment Response. *Neoplasia*. 2014;16(1):1–13. doi:10.1593/neo.131848
300. Gobert M, Treilleux I, Bendriss-Vermare N, Bachelot T, Goddard-Leon S, Arfi V, Biota C, Doffin AC, Durand I, Olive D, et al. Regulatory T Cells Recruited through CCL22/CCR4 Are Selectively Activated in Lymphoid Infiltrates Surrounding Primary Breast Tumors and Lead to an Adverse Clinical Outcome. *Cancer Res*. 2009;69(5):2000–2009. doi:10.1158/0008-5472.CAN-08-2360
301. Li D, Ji H, Niu X, Yin L, Wang Y, Gu Y, Wang J, Zhou X, Zhang H, Zhang Q. Tumor-associated macrophages secrete CC-chemokine ligand 2 and induce tamoxifen resistance by activating PI3K/Akt/mTOR in breast cancer. *Cancer Sci*. 2020;111(1):47–58. doi:10.1111/cas.14230
302. Zhou S-L, Dai Z, Zhou Z-J, Wang X-Y, Yang G-H, Wang Z, Huang X-W, Fan J, Zhou J. Overexpression of CXCL5 mediates neutrophil infiltration and indicates poor prognosis for hepatocellular carcinoma. *Hepatology*. 2012;56(6):2242–2254. doi:10.1002/hep.25907
303. Zeng Z, Shi F, Zhou L, Zhang M-N, Chen Y, Chang X-J, Lu Y-Y, Bai W-L, Qu J-H, Wang C-P, et al. Upregulation of Circulating PD-L1/PD-1 Is Associated with Poor Post-Cryoablation Prognosis in Patients with HBV-Related Hepatocellular Carcinoma Luk J, editor. *PLoS One*. 2011;6(9):e23621. doi:10.1371/journal.pone.0023621
304. Simone R, Tenca C, Fais F, Luciani M, De Rossi G, Pesce G, Bagnasco M, Saverino D. A Soluble Form of CTLA-4 Is Present in Paediatric Patients with Acute Lymphoblastic Leukaemia and Correlates with CD1d+ Expression Moormann AM, editor. *PLoS One*. 2012;7(9):e44654. doi:10.1371/journal.pone.0044654

8. Table of figures

Figure 1: Structural differences of TCRs and CARs.....	12
Figure 2: Evolution of CAR design.....	14
Figure 3: Structural differences of CARs and AdCARs.....	15
Figure 4: Secretion and activation of latent TGF- β	21
Figure 5: Illustration of AdCAR constructs.....	28
Figure 6: Illustration of the cyclic fluorescent imaging method.....	48
Figure 7: Overcoming the immunosuppressive TME with AdCAR T cells.....	51
Figure 8: LAP expression in presence of tumor cells on human ovarian cancer tissue.....	53
Figure 9: LAP expression in absence of tumor cells on human ovarian cancer tissue.....	54
Figure 10: Activation marker expression of AdCAR1 T cells co-cultured in presence of hLAP and aLAP.....	55
Figure 11: Cytokine secretion of AdCAR1 T cells co-cultured in presence of hLAP and aLAP.....	56
Figure 12: Activation marker expression of AdCAR1 T cells co-cultured in presence of varying concentrations of hLAP or adapter.....	57
Figure 13: Transgene expression in AdCAR1 T cells co-cultured in presence of hLAP and aLAP.....	58
Figure 14: Latent TGF- β secretion of human tumor cell lines <i>in vitro</i>	59
Figure 15: Activation marker expression and cytokine secretion of AdCAR1 T cells co-cultured in presence of AsPC-1-TGF-secreted latent TGF- β and aLAP.....	61
Figure 16: Activation marker expression of AdCAR1 T cells co-cultured in presence of AsPC-1-TGF and aLAP.....	63
Figure 17: Killing of AsPC-1 WT or AsPC-1-TGF in presence of AdCAR T cells at varying ratios of multiple adapter specificities <i>in vitro</i>	65
Figure 18: Activation of AdCAR T cells co-cultured in presence of supernatant of AsPC-1 WT or AsPC-1-TGF at varying ratios of multiple adapter specificities.....	67
Figure 19: Tumor growth kinetic of AsPC-1-TGF in NSG mice.....	69
Figure 20: Localization of latent TGF- β in AsPC-1-TGF tumor-bearing mice.....	70
Figure 21: <i>In vitro</i> functionality of AdCAR1 T cells used for toxicity study.....	71
Figure 22: Concentration of soluble latent TGF- β in human IVIG.....	71
Figure 23: Assessment of aLAP-mediated toxicity in mice treated with AdCAR1 T cells in presence of soluble latent TGF- β	72
Figure 24: IFN- γ levels in mice treated with AdCAR1 T cells and aLAP in presence of soluble latent TGF- β	73
Figure 25: <i>Ex vivo</i> analysis of CD137 expression on mock T cells and AdCAR1 T cells in presence of latent TGF- β and aLAP.....	74
Figure 26: Treatment of AsPC-1-TGF tumor-bearing mice with AdCAR1 T cells and aLAP or CD66c S CAR T cells.....	76

Figure 27: CD8 frequency and tumor infiltration of CAR T cells in AsPC-1-TGF tumor-bearing mice treated with AdCAR1 T cells plus aLAP or CD66c S CAR T cells.	78
Figure 28: Treatment of AsPC-1-TGF- or AsPC-1 WT tumor-bearing mice with AdCAR1 T cells and CD66c xs CAR T cells in presence of aLAP.	80
Figure 29: Concentration of soluble latent TGF- β in sera of AsPC-1-TGF or AsPC-1 WT-bearing mice.	81
Figure 30: Treatment of AsPC-1-TGF tumor-bearing mice with autologous PBMCs and AdCAR2 T cells in presence of aLAP plus aCD66c.	83
Figure 31: Immune cell engraftment and immune cell composition in AsPC-1-TGF tumor-bearing mice treated with AdCAR2 T cells and autologous PBMCs in presence of aLAP plus aCD66c.	85
Figure 32: CD8 frequency and exhaustion marker expression on T cells isolated from AsPC-1-TGF tumor-bearing mice treated with AdCAR2 T cells in presence of aLAP plus aCD66c.	86
Figure 33: T cell infiltration in tumors of AsPC1-TGF tumor-bearing mice treated with AdCAR2 T cells and autologous PBMCs in presence of aLAP plus aCD66c.	87

9. Abbreviation

A

Acc	Acceleration
aCD66c	CD66c-specific antibody
AdCAR	Adapter CAR
ADCC	Antibody-dependent cell-mediated cytotoxicity
aLAP	LAP-specific antibody
ALK	Activin receptor-like kinase
APC	Allophycocyanin
AsPC-1-TGF	latent TGF- β secreting AsPC-1 WT
AsPC-1 WT	AsPC-1 GFP ⁺ luciferase ⁺
ATC	Adoptive cell therapy

B

BCR	B cell receptor
BiTE	Bispecific T cell engager
BLI	Bioluminescent imaging
Br	Break
BSA	Bovine serum albumin

C

CAF	Cancer associated fibroblast
CAR	Chimeric antigen receptor
CRS	Cytokine release syndrome

D

DC	Dendritic cell
DMEM	Dulbecco's Modified Eagle Medium
DMSO	Dimethylsulfoxid

E

ECM	Extra cellular matrix
EMT	Epidermal mesenchymal transition

F

Fab	Fragment-antigen binding
FAP	Fibroblast activation protein
FBS	Fetal bovine serum
FCS	Forward scatter
FDA	U.S. Food and Drug Agency
FITC	Fluorescein isothiocyanate

G

GARP	Glycoprotein A repetitions predominant protein
GFP	Green fluorescent protein
GM-CSF	granulocyte-macrophage colony-stimulating factor
GMP	Good manufacturing practice

H

HEK	Human embryo kidney cells
hLAP	Recombinant human LAP

I

i.v.	Intravenous
IFN	Interferon
IgG	Immunoglobulin G
IL	Interleukin
IVIG	Human intravenous immunoglobulin

L

LAP	Latency associated peptide
LB	Lysogeny broth
LLC	Large latent complex
LLE	Linker label epitope
LP	Leukapheresis
LRRC33	Leucine-Rich Repeat-Containing Protein 33
LTBP	Latent TGF- β binding protein
LVV	Lentiviral vector

M

mAb	Monoclonal antibody
MDSC	Myeloid derived suppressor cells
MFI	Mean fluorescent intensity
MHC	Major histocompatibility complex
MMP	Matrix metalloproteinase
MOI	Multiplicity of integration

N

NSCL	Non-small cell lung cancer
------	----------------------------

P

PBMC	Peripheral blood mononuclear cell
PBS	Phosphate buffered saline
PCC	Pearson correlation coefficient
PDAC	Pancreatic ductal adenocarcinoma
PE	Phycoerythrin
PEB	PBS/EDTA/BSA
PEI	Polyethylenimine

R

ROI	Region of interest
RPMI	Roswell Park Memorial Institute

S

s.c.	Subcutaneous
scFv	Single chain fragment variable
SD	Standard deviation
SEM	Standard error of the mean
SLC	Small latent complex
SSC	Sideward scatter
SP	Signaling peptide
SUP-T1	Stanford University Pediatric T cell line 1

T

TAA	Tumor associated antigen
TAM	Tumor associated macrophages
TCR	T cell receptor
TCT	T cell transduction
TGF- β	Transforming growth factor- β
TIL	Tumor infiltrating lymphocytes
TLS	Tertiary lymphoid structures
TM	Transmembrane domain
TME	Tumor microenvironnement
TNF	Tumor necrosis factor
Treg	Regulatory T cells
T β R	TGF- β receptor

W

w/o	Without
WBC	White blood cell count
WT	Wild type

10. Publications

10.1 Manuscripts

Werchau N, Kotter B, Criado-Moronati E, Gosselink A, Cordes N, Lock D, Lennartz S, Kolbe C, Winter N, Teppert K, et al. Combined targeting of soluble latent TGF- β and a solid tumor-associated antigen with adapter CAR T cells. *Oncoimmunology*. **2022**;11(1):2140534. doi:10.1080/2162402X.2022.2140534

Kotter B, Engert F, Krueger W, Roy A, Rawashdeh W.A, Cordes N, Drees B, Webster B, **Werchau N**, Lock D, Dapa S, Schneider D, Ludwig S, Rossig C, Assenmacher M, Mittelstaet J, Kaiser A.D. Titratable Pharmacological Regulation of CAR T Cells Using Zinc Finger-Based Transcription Factors. *Cancers* **2021**, *13*, 4741. <https://doi.org/10.3390/cancers13194741>

10.2 Poster presentations

International Conference on Lymphocyte Engineering 31 March–2 April 2022 Munich, Germany. *Hum. Gene Ther.* 2022 Mar 30. doi:10.1089/HUM.2022.29200.ABSTRACTS

P038 Topic: ASa03 Engineered T cell therapy for solid tumours

Sensing of soluble antigens with Adapter CAR™ T cells

Werchau N, Teppert K, Kotter B, Abramowski P, Kaiser A.D, Schaser T.

10.3 Patent applications

Werchau N, Kotter B, Mittelstaet J, Kaiser A.D. WO2021156277A1 - Immune cell expressing adapter chimeric antigen receptor for sensing soluble antigens. (2021)

Affidavit



Eidesstattliche Versicherung

Werchau, Niels

Name, Vorname

Ich erkläre hiermit an Eides statt, dass ich die vorliegende Dissertation mit dem Titel:

Sensing of soluble molecules with adapter chimeric antigen receptors for the controllable activation of T cells in an immunosuppressive subcutaneous solid tumor model

selbständig verfasst, mich außer der angegebenen keiner weiteren Hilfsmittel bedient und alle Erkenntnisse, die aus dem Schrifttum ganz oder annähernd übernommen sind, als solche kenntlich gemacht und nach ihrer Herkunft unter Bezeichnung der Fundstelle einzeln nachgewiesen habe.

Ich erkläre des Weiteren, dass die hier vorgelegte Dissertation nicht in gleicher oder in ähnlicher Form bei einer anderen Stelle zur Erlangung eines akademischen Grades eingereicht wurde.

Köln, 28.05.2023

Ort, Datum

Niels Werchau

Unterschrift Doktorandin bzw. Doktorand

Danksagung

Zuallererst gilt mein besonderer Dank meinem Doktorvater, Prof. Dr. Dr. Michael von Bergwelt für das Ermöglichen meiner Promotion. Ich bin sehr dankbar, für sein Engagement und die Betreuung in dieser Zeit. Trotz der großen räumlichen Entfernung und der Pandemie hat er mich herausragend durch die gesamte Promotionsphase hinweg begleitet. Ich bin ihm überaus dankbar für die wissenschaftliche Förderung, die ich dabei erhalten habe.

Weiterhin möchte ich mich recht herzlich bei Dr. Andrew Kaiser für die Möglichkeit bedanken, meine Promotion in seiner Abteilung durchzuführen. Das gemeinsame Entwickeln neuer Ideen und unsere hervorragenden Diskussionen habe ich stets sehr geschätzt. Ich bin überaus dankbar für die wissenschaftliche Förderung und die persönliche Unterstützung, die ich von Andrew erhalten habe. Seine Denkweise und Führungskultur haben mich nachhaltig geprägt.

Großer Dank gilt außerdem meinem Betreuer Dr. Pierre Abramowski für all seine Geduld und sein Verständnis während dieser herausfordernden Zeit. Für seine Unterstützung während meiner Zeit im Labor und speziell in der stressreichen Endphase der Promotion bin ich sehr dankbar.

Außerdem danke ich all meinen Kollegen und Kolleginnen bei Miltenyi, die mich in dieser Zeit unterstützt haben. Die Zusammenarbeit mit euch hat mir immer viel Spaß gemacht. Ohne euch wäre diese Arbeit nicht möglich gewesen.

Ein besonderer Dank gilt meinen Eltern. Ich bin euch unendlich dankbar für die Unterstützung während meiner gesamten Studienzzeit. Euer Rückhalt und eure Zuversicht waren überaus wichtig für mich. Bedanken möchte ich mich auch bei Isabelle. Ich danke dir sehr für dein Verständnis während dieser Zeit. Deine Unterstützung gerade am Ende der Promotion war wunderbar. Ich bin froh, dass du während dieser Zeit an meiner Seite warst.